INSTITUTO POTOSINO DE INVESTIGACIÓN CIENTÍFICA Y TECNOLÓGICA, A.C.

POSGRADO EN CIENCIAS EN BIOLOGIA MOLECULAR

Characterization of *Candida glabrata cis*-acting elements that negatively regulate transcription of *EPA* genes through silencing proteins

Tesis que presenta

Eunice López Fuentes

Para obtener el grado de

Doctora en Ciencias en Biología Molecular

Director de la Tesis:

Dra. Irene Castaño Navarro

San Luis Potosí, S.L.P., Agosto de 2018

IPICYT

Constancia de aprobación de la tesis

La tesis ***"Characterization of Candida glabrata cis-acting elements that negatively regulate transcription of EPA genes through silencing proteins"*** presentada para obtener el Grado de Doctora en Ciencias en Biología Molecular fue elaborada por **Eunice López Fuentes** y aprobada el diecisiete de agosto del dos mil dieciocho por los suscritos, designados por el Colegio de Profesores de la División de Biología Molecular del Instituto Potosino de Investigación Científica y Tecnológica, A.C.

Dra. Irene Beatriz Castaño Navarro
Directora de la tesis

Dr. Gerardo Rafael Argüello Astorga
Miembro del Comité Tutoral

Dra. Lina Raquel Riego Ruiz
Miembro del Comité Tutoral

Dr. Roberto Sánchez Olea
Miembro del Comité Tutoral

Créditos Institucionales

Esta tesis fue elaborada en el Laboratorio de Microbiología Molecular de la División de Biología Molecular del Instituto Potosino de Investigación Científica y Tecnológica, A.C., bajo la dirección del Dra. Irene Castaño Navarro apoyada por el proyecto No. CB-2014-239629.

Durante la realización del trabajo el autor recibió una beca académica del Consejo Nacional de Ciencia y Tecnología 261740 y del Instituto Potosino de Investigación Científica y Tecnológica, A. C.

IPICYT

Instituto Potosino de Investigación Científica y Tecnológica, A.C.

Acta de Examen de Grado

El Secretario Académico del Instituto Potosino de Investigación Científica y Tecnológica, A.C., certifica que en el Acta 101 del Libro Segundo de Actas de Exámenes de Grado del Programa de Doctorado en Ciencias en Biología Molecular está asentado lo siguiente:

En la ciudad de San Luis Potosí a los 17 días del mes de agosto del año 2018, se reunió a las 12:00 horas en las instalaciones del Instituto Potosino de Investigación Científica y Tecnológica, A.C., el Jurado integrado por:

Dra. Lina Raquel Riego Ruiz	**Presidenta**	**IPICYT**
Dr. Gerardo Rafael Argüello Astorga	**Secretario**	**IPICYT**
Dra. Irene Beatriz Castaño Navarro	**Sinodal**	**IPICYT**
Dr. Roberto Sánchez Olea	**Sinodal externo**	**UASLP**

a fin de efectuar el examen, que para obtener el Grado de:

DOCTORA EN CIENCIAS EN BIOLOGÍA MOLECULAR

sustentó la C.

Eunice López Fuentes

sobre la Tesis intitulada:

Characterization of Candida glabrata cis-acting elements that negatively regulate transcription of EPA genes through silencing proteins

que se desarrolló bajo la dirección de

Dra. Irene Beatriz Castaño Navarro

El Jurado, después de deliberar, determinó

APROBARLA

Dándose por terminado el acto a las 13:30 horas, procediendo a la firma del Acta los integrantes del Jurado. Dando fe el Secretario Académico del Instituto.

A petición de la interesada y para los fines que a la misma convengan, se extiende el presente documento en la ciudad de San Luis Potosí, S.L.P., México, a los 17 días del mes de agosto de 2018.

Dr. Horacio Flores Zúñiga
Secretario Académico

Mtra. Ivonne Lizette Cuevas Vélez
Jefa del Departamento del Posgrado

INSTITUTO POTOSINO DE INVESTIGACIÓN CIENTÍFICA Y TECNOLÓGICA, A.C.
IPICYT
SECRETARIA ACADEMICA

A mi madre, *por enseñarme que siempre hay que levantarse, por esa fuerza de voluntad inquebrantable, te amo mamá.*

A Crhistian, *por caminar a mi lado en cada nueva aventura.*

"Un descubrimiento es como enamorarse y llegar a la cima de una montaña después de una dura ascensión, todo en uno, no un éxtasis inducido por las drogas, sino por la revelación de una cara de la naturaleza que nadie ha visto antes y que a menudo resulta ser más sutil y maravillosa de lo que nadie había imaginado."

Max Ferdinand Perutz

AGRADECIMIENTOS

A CONACyT por la beca otorgada (No. 261740) y por el grant No. CB-2014-239629 otorgado a Irene Castaño

Agradezco al IPICYT por abrirme las puertas para realizar mi proyecto de tesis.

Al LANBAMA por la asesoría técnica para llevar a cabo este trabajo.

A **mi madre**, por todo el apoyo incondicional, ese tipo de apoyo que sólo una madre otorga.

Gracias por enseñarme con tu ejemplo.

A **mi padre**, por ayudarme en momentos complicados.

A **mi hermana**, por escucharme y aconsejarme desde lejos.

A mi **familia,** a todos.

A **Irene**, por disfrutar tan jugosamente nuestras pequeñas victorias, por animarme a realizar nuevos experimentos, por brindarme todo su apoyo en cada nuevo proyecto.

Gracias por confiar en mí, fue en verdad una experiencia enriquecedora.

A **Alejandro**, por todas las ideas, críticas constructivas y por todo su apoyo.

A mis sinodales **Lina, Gerardo y Roberto**, por estar presente en cada tutoral y aportar ideas para enriquecer el trabajo.

A **Kasia**, por toda la ayuda para lograr nuestra cereza del pastel.

A **Lupita**, por la asesoría técnica y todos los consejos.

A **Paty, Karen, Norma, Osney, Grecia, Marcela, Gabriel, Alex, Jefté y Blanquita** por todos los momentos que hicieron mucho más divertida la estancia en el laboratorio. Por su amistad.

A **Gloria**, por contarme los secretos de la vida, por siempre estar ahí haciéndome la vida más fácil.

A **Crhistian**, por recorrer este camino juntos, de la mano. Gracias amor por estar para mí en cada paso, por celebrar cada experimento exitoso, por preocuparte con cada tropiezo y sobre todo gracias por ser mi compañero de vida. Te amo.

A **Kyoko,** por sacarme una sonrisa con su sola presencia.

TABLE OF CONTENTS

LIST OF FIGURES

LIST OF TABLES

RESUMEN

Caracterización de los elementos en *cis* que regulan negativamente la transcripción de los genes *EPA* mediante las proteínas del silenciamiento de *Candida glabrata*

La adherencia es un factor importante en la virulencia de distintos patógenos. En *Candida glabrata*, los genes *EPA* (*Epithelial Adhesin*) son responsables de la mayor parte de la adherencia a las células huésped y se localizan en regiones subteloméricas donde se regulan por silenciamiento subtelomérico, el cual depende de Rap1, las proteínas yKu y el complejo SIR. El gen *EPA1*, que codifica la adhesina principal, forma un grupo con *EPA2* y *EPA3* en el telómero derecho del cromosoma E (E_{-R}). Entre *EPA3* y el telómero, se encuentra un elemento que actúa en *cis*, el protosilenciador Sil2126, que requiere el contexto de su telómero para ser funcional. Sil2126 puede silenciar un gen reportero a 32 kb del telómero (donde normalmente no hay silenciamiento). Encontramos que hay elementos situados en la región intergénica entre *EPA2* y *EPA3* que se requieren para la actividad de Sil2126. Estos elementos podrían ser los responsables de la especificidad de Sil2126 por su telómero. El extremo 5' de Sil2126 contiene sitios de unión putativos para Rap1 y Abf1 y estas proteínas se unen al Sil2126 en su posición original y también cuando se coloca a -32 kb (Sil@-32kb). Sil@-32kb también puede reclutar Sir3, lo que sugiere la propagación del silenciamiento hasta esta distancia. Utilizamos el ensayo de 3C (*Chromosome conformation capture*) para determinar las frecuencias de interacciones entre Sil@-32kb y Sil2126 (en su posición original) y varios puntos a lo largo de la región subtelomérica E_{-R}. Los datos revelaron que Sil@-32kb interactúa fuertemente con la región intergénica entre *EPA1* y *EPA2* al formar un *loop* que resulta en la represión de la expresión de *EPA1*. A su vez, Sil2126 puede interactuar con la región intergénica entre *EPA2* y *EPA3*. Proponemos que el mecanismo de acción del protosilenciador Sil2126 es a través del reclutamiento de las proteínas de silenciamiento y la formación de una superestructura que involucra diferentes interacciones entre los elementos que actúan en *cis* y diversas proteínas.

Palabras clave: *Candida glabrata*, silenciamiento subtelomérico, genes *EPA*, protosilenciador, conformación de la cromatina.

ABSTRACT

Characterization of *Candida glabrata cis*-acting elements that negatively regulate transcription of *EPA* genes through silencing proteins

Adherence is an important virulence factor in several pathogens. A higher virulence has been correlated with increased adherence and with an expansion of adhesin-encoding genes. In *Candida glabrata*, the adherence to host cells is mainly mediated by *EPA* (Epithelial Adhesin) genes. Most of *EPA* genes are located in subtelomeric regions regulated by subtelomeric silencing, which depends on Rap1, yKu proteins and the SIR complex. Epa1 mediates most of the adherence to epithelial cells *in vitro*. The *EPA1* gene forms a cluster with *EPA2* and *EPA3* in the right telomere of chromosome E (E_{-R}). Between *EPA3* and the telomere, there is a *cis*-acting element, the protosilencer Sil2126, which requires its own telomere context for its activity. Sil2126 can silence a reporter gene 32 kb away from the telomere (a region where normally there is no silencing). Our results showed that there are *cis*-acting elements located in the *EPA2-EPA3* intergenic region that are required for Sil2126 activity, which perhaps are responsible for the Sil2126 telomere-specificity. The 5' end of Sil2126 contains putative binding sites for Rap1 and Abf1; we found that these proteins bind to Sil2126 in its original position and also when it is placed at -32 kb (Sil@-32kb). Rap1 and Abf1 also bind to other regions in the E_{-R} subtelomeric region. In addition, we detected that Sil@-32kb can recruit Sir3, suggesting the propagation of the silencing up to that distance. We used 3C (Chromosome conformation capture) assays to measure crosslinking frequencies between Sil@-32kb and Sil2126 in its original position across the E_{-R} subtelomeric region. These assays revealed that Sil@-32kb interacts with the *EPA1-EPA2* intergenic region forming a loop that results in the repression of *EPA1*. On the other hand, Sil2126 interacts with the *EPA2-EPA3* intergenic region. We propose that the mechanism of action of Sil2126 is through the recruitment of silencing proteins to form a superstructure involving different interactions between *cis*-acting elements and diverse proteins.

Key words: *Candida glabrata*, subtelomeric silencing, *EPA* genes, protosilencer, chromosome conformation.

1. INTRODUCTION

1.1. Chromosome ends are specialized chromatin structures

The ends of eukaryotic chromosomes are called telomeres which are specialized (Palladino *et al.* 1993), and excluded from the nucleolus (Therizols *et al.* 2010).

In most eukaryotes, the sequence of telomeric DNA consists of a tandem array of short G-rich repeats. Most of the research on telomeres has been done in single-celled organisms. For example in *Saccharomyces cerevisiae*, the telomeres consist of non-coding repeated DNA which is 300 ± 75 bp of simple repeats ($C_{1-3}A/TG_{1-3}$) and at the 3' end there are G-rich sequences, which protrude to form a single-strand overhang (the G-tail) (Teixeira and Gilson 2005; Wellinger and Zakian 2012).

Several proteins involved in diverse functions are bound to telomeres. In budding yeast, telomeric DNA is covered by an array of about 15-20 molecules of Rap1 (Repressor activator protein 1) proteins. The Rap1-binding sites within telomeric DNA are among the highest affinity sites in the cell (Lieb *et al.* 2001). Rap1 interacts either with a set of non-histone proteins called the Silent Information Regulator, or SIR complex, which is involved in the formation of subtelomeric heterochromatin, or with the Rif complex (Rif1 and Rif2), which negatively controls telomere elongation. The G-tail is bound by Cdc13, which forms a heterotrimer with Stn1 and Ten1 involved in capping and telomerase recruitment (Figure 1, Gilson and Géli 2007). In fission yeast (*Schizosaccharomyces pombe*), the DNA-binding protein Taz1 binds to telomeric DNA and can recruit Rap1 which does not bind directly to telomeric repeats (Teixeira and Gilson 2005). Another key telomere binding protein is the yKu complex (yKu70p and yKu80p) involved in nuclear positioning of the telomeres and regulating telomere-repeat addition, which protects telomeres from recombination and degradation (Fisher and Zakian 2005).

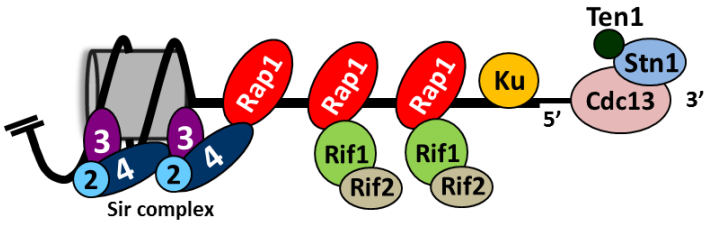

Figure 1. Schematic representation of different proteins bound to the telomeres. The telomere and DNA are represented as a black line wrapped around the nucleosome, represented as a gray cylinder. Proteins are represented by circles or ovals of different colors. (Modified from Gilson and Géli 2007).

1.2. Subtelomeres are dynamic and variable regions near the ends of chromosomes

Subtelomeres are the regions proximal to the telomeres, which exhibit unique characteristics, such as low gene density, epigenetic silencing, high rates of recombination and mutation, high repeat content and extensive sequence similarity (Pryde and Louis 1999; Mefford and Trask 2002; Barton *et al.* 2008; Brown *et al.* 2010).

Subtelomeric regions are variable loci harboring specific and fast-evolving gene families. Subtelomeric gene families are generally composed of 2-4 times more genes than non-subtelomeric families. In yeast, genes involved in biofilm formation and carbohydrate uptake have been found in subtelomeres (Verstrepen and Klis 2006). In pathogenic fungi and parasitic eukaryotes, many virulence genes reside at subtelomeres (Gardner *et al.* 2002b; Domergue *et al.* 2005). Subtelomeric gene families show increased copy number variation due to frequent duplication and deletion events. It is thought that the extraordinary instability of eukaryotic subtelomeres supports fast adaptation to novel niches by promoting gene recombination and duplication favoring functional divergence of the alleles (Brown *et al.* 2010). Thus, subtelomeres provide ideal environments for the rapid evolution of genes upon which selection can then act. Accordingly, a comparison between *S. cerevisiae* isolates showed that strains that produce beer, sherry or champagne

contained increased copy numbers of subtelomeric *MAL*, *SUC*, or *MEL* genes, respectively (Naumov *et al.* 1995; Naumova *et al.* 2005; Dunn *et al.* 2012). Also, given their extensive homology, subtelomeres might promote recombinational processes that allow some cells to regenerate telomeres in the absence of telomerase (Teng and Zakian 1999).

On the other hand, the subtelomeres of diverse species as *S. cerevisiae*, *Plasmodium falciparum*, *Drosophila melanogaster* and humans are structurally similar; they are composed of repeated elements, but the extent of the subtelomeres and the sequence of the elements vary greatly among organisms (Mefford and Trask 2002, Figure 2); One exception is the case of the ends of the chromosomes in *D. melanogaster* that do not have arrays of short telomeric repeats. Instead, the ends in *D. melanogaster* are maintained by retrotransposition of the HeT-A and TART (telomere-associated retrotransposon) elements (Levis *et al.* 1993). The best studied subtelomeres are those of *S. cerevisiae*, they have two classes of elements, X and Y'. X is found in all subtelomeres, but different series of repeats are present in different telomeres. Y' is present only in half of the telomeres (Louis 1995).

1.3. Subtelomeric silencing is a regional transcriptional repression

Silent chromatin involves a specialized chromatin structure, often referred to as heterochromatin. Genes within heterochromatic domains are silenced in many cells of a population but not in all of them and these expression states ("on" or "off") are propagated through successive cell divisions (Bühler and Gasser 2009; Gartenberg and Smith 2016).

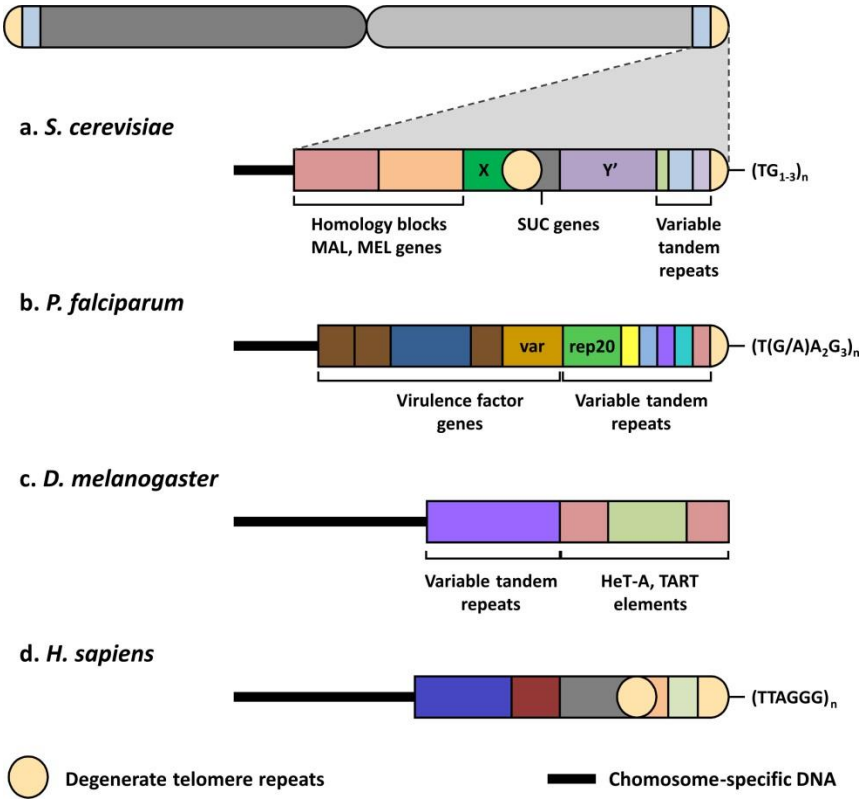

Figure 2. Schematic representation of subtelomeric structures in different organisms. (Modified from Mefford and Trask 2002).

Heterochromatin in *S. cerevisiae* is found at the ribosomal DNA (rDNA) tandem array, the silent mating loci (*HML* and *HMR*) and the telomeres. The transcriptional silencing close to the telomeres is also called telomere position effect (TPE) and is found in many organisms in addition to *S. cerevisiae*, such as fission yeast (*Schizosaccharomyces pombe*), *Drosophila melanogaster*, the sleeping sickness parasite *Trypanosoma brucei*, the malaria parasite *Plasmodium falciparum*, plants, and humans (Gottschling *et al.* 1990; Levis *et al.* 1993; Nimmo *et al.* 1994; Horn and Cross 1995; Scherf *et al.* 1998; Baur *et al.* 2001). Thus, TPE is a widely found and efficient epigenetic layer of negative regulation.

The transcriptional silencing is propagated from the telomere to the centromere, spanning the subtelomeric regions. Genes naturally or heterologously inserted in subtelomeric regions are repressed in a promoter-independent manner. It has

been described that silencing at subtelomeric regions varies from telomere to telomere in some fungi such as *S. cerevisiae* (Pryde and Louis 1999) and in the opportunistic fungal pathogen *Candida glabrata* (Rosas-Hernández *et al.* 2008). In this regard, it is interesting that in some pathogenic organisms several genes encoding known or suspected virulence factors (surface or cell walls proteins) are localized at subtelomeric regions. For example, in the unicellular parasites, the *var* genes of *Plasmodium falciparum* (Gardner *et al.* 2002a) and the single variant-specific surface glycoprotein genes (*VSG*) of *Trypanosoma brucei* are located adjacent to a telomere (Horn and Cross 1995), and the pathogenic fungus *Pneumocystis carinii,* contains the *MSG* (major surface glycoprotein) gene family located near chromosomes ends (Keely *et al.* 2005). Interestingly, in most of these microorganisms, one gene is expressed at a time, suggesting that subtelomeric genes are tightly regulated.

In general, silent chromatin assembly involves a series of molecular steps, starting with a site-specific nucleation step. Next, heterochromatin spreads from the initiation site and, in the case of yeast, silent chromatin is sequestered near the nuclear envelope, generating a sub-nuclear compartment with foci of silencing proteins (Grunstein and Gasser 2013). One of the best understood examples of silencing is the mating loci of *S. cerevisiae*. The heterochromatin assembly begins at the *cis*-acting elements called silencers flanking the mating loci *HML* and *HMR.* These silencers provide binding sites for multifunctional nuclear factors, Rap1, Abf1 and the ORC complex (Origin of Recognition Complex) (Brand *et al.* 1987). Rap1 is able to recruit either Sir4 or Sir3 (Moretti *et al.* 1994; Chen *et al.* 2011), Abf1 can interact with Sir3 and ORC, has high affinity for Sir1, which in turn binds Sir4 (Grunstein and Gasser 2013). Sir1 is unique among the Sir factors, it does not spread with the SIR complex beyond the silencers and it mainly serves in the establishment step of silencing, most likely through its ability to bind the DNA-bound ORC and Sir4 (Rusche *et al.* 2002).

The heterochromatin assembly at telomeres varies in some aspects from the assembly at *HM* loci. Telomeric repeats provide 16 to 20 consensus sites for Rap1

binding (Gotta *et al.* 1996; Marcand *et al.* 1996). Sir4 is recruited by densely-packed Rap1 proteins at telomeres (Moretti and Shore 2001; Luo *et al.* 2002). The telomere end-binding yKu proteins also contribute in the recruitment of Sir4, yKu subunits (yKu70 and yKu80) interact with both ends of Sir4 protein (Roy *et al.* 2004). Sir4 forms a complex with Sir2, a NAD-dependent histone deacetylase that deacetylates lysine 16 (K16) on histone H4. Deacetylation of H4K16 allows Sir3 and Sir4 to bind to the H3 and H4 tails (Rusche *et al.* 2002; Talbert and Henikoff 2006). The sequential-spreading model proposes sequential rounds of Sir2-3-4 complexes binding, histone deacetylation and interactions between new molecules of SIR complexes to deacetylated nucleosomes. This propagates the silent chromatin until a barrier is reached or the pool of free SIR proteins falls below a threshold necessary for efficient binding (Grunstein and Gasser 2013; Gartenberg and Smith 2016) (Figure 3). Recently a nucleosome-free region at the subtelomeric border that blocks heterochromatin spreading into the subtelomere-adjacent euchromatin has been described in *S. pombe* (Tashiro *et al.* 2017).

There are other features in the assembly of heterochromatin in different organisms. Unlike *S. cerevisiae*, in most other eukaryotes the histone H3 K9 methylation that characterizes centromeric heterochromatin, is also present in other heterochromatic regions, as well as the major protein ligand that recognizes this modification (heterochromatin protein 1, or HP1). Also, the RNA interference (RNAi) machinery that facilitates PEV (Position effect variegation) in fission yeast is present at these regions (Talbert and Henikoff 2006; Bühler and Gasser 2009). The PEV is a stochastic and variegated expression of a gene due to juxtaposition to heterochromatic domains and it has been widely described in fission yeast and in *Drosophila*, as well in mammals (Dorer and Henikoff 1994; Allshire and Ekwall 2015; Saksouk *et al.* 2015). In fact, the TPE was termed by analogy to PEV. Thus, silencing is a mechanism to control transcriptional activity in order to achieve cell-specific gene activity.

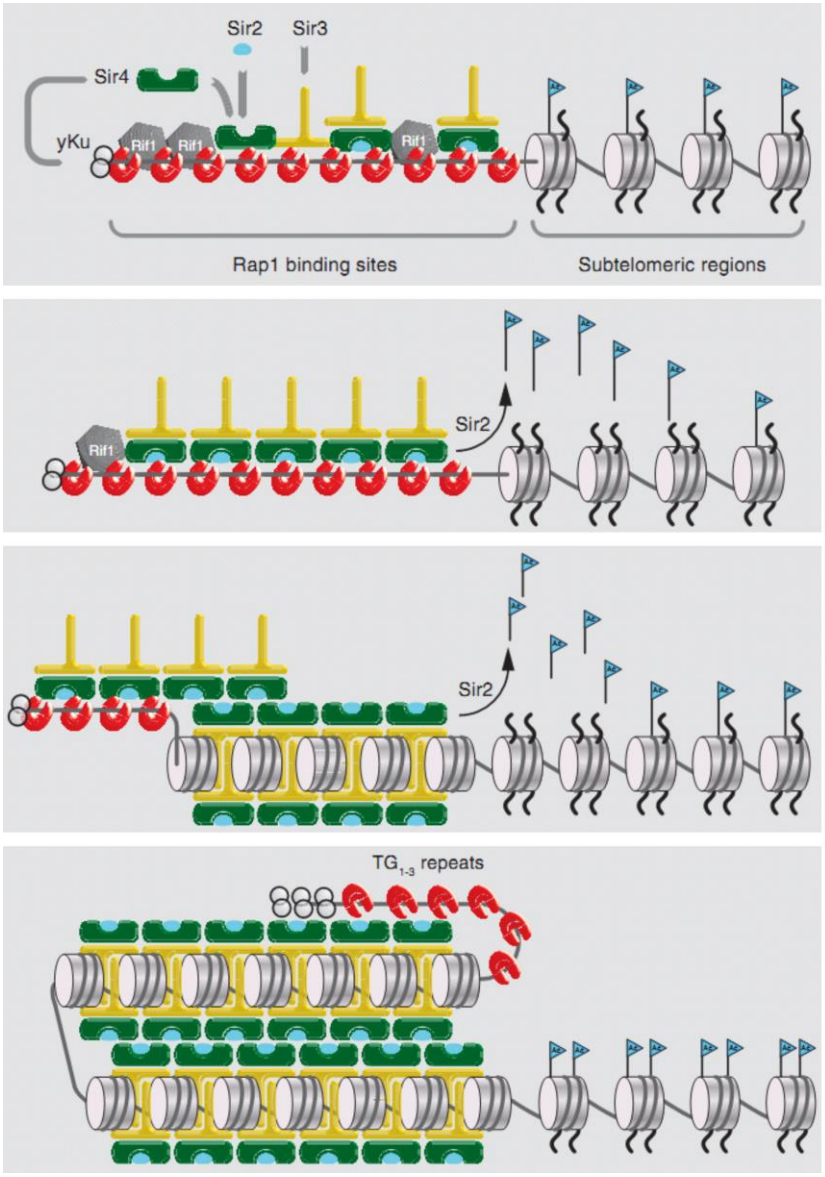

Step 1. Recriutment of Sir4 with bound Sir2, and of Sir3 to TG repeat bound Rap1 and yKu.

Step 2. Sir2-mediated deacetylation of histone H4K16 in nearby nucleosomes.

Step 3. Spreading of the Sir complex along nearby nucleosomes.

Step 4. Folding of a silent telomere into a higher-order structure.

Figure 3. Model of heterochromatin assembly in *S. cerevisiae*. **(Step1)** Rap1 (red C-like figures) binds to the telomeric repeats, as well as yKu, these proteins recruit Sir4, even in the absence of Sir2 or Sir3. **(Step2)** Sir2 is a NAD-dependent histone deacetylase, which deacetylates the acetylaed histone H4K16 residue, thus generating high affinity sites for Sir3 and Sir4. **(Step 3)** Sir3 and Sir4 proteins bind the deacetylated histone H4 tails and SIR complex spread along the nucleosomes. **(Step 4)** The silent chromatin may entail higher-order folding and is sequestered at the nuclear envelope. (Modified from Grunstein and Gasser 2013).

1.4. Proteins involved in subtelomeric silencing

1.4.1. SIR complex

The chromatin binding factors called Silent Information Regulators (SIR complex), Sir2, Sir3 and Sir4, are essential to mediate silencing, whereas Sir1 enhances the efficiency of repression at *HM* loci, but is not found at telomeres. The Sir2-3-4 proteins work as a trimeric complex with 1:1:1 stoichiometry (Cubizolles *et al.* 2006).

Sir2 is the founding member of a protein family of NAD^+-dependent histone/protein deacetylases called sirtuins, which are highly conserved from bacteria to humans (Brachmann CB *et al.* 1995). Yeast Sir2 has a highly conserved catalytic core (aa 237-562) and a binding interface for Sir4 upstream of the catalytic domain (aa 99-150) (Figure 4A; Imai *et al.* 2000).

Sir3 is an Orc1 paralogue that arose through the whole-genome duplication (WGD) of *S. cerevisiae* lineage. Sir3 contains an N-terminal bromo-adjacent domain (BAH, aa 1-214) that binds nucleosomes, a central AAA^+ ATPase-like domain (AAA; aa 532–834) that binds both Sir4 and the nucleosome, and a C-terminal winged helix-turn-helix domain that mediates homodimerization (wH; aa 840–978) (reviewed in Kueng *et al.* 2013) (see Figure 4B). It was proposed that the dimerization of Sir3 through its wH domain mediates interactions between neighboring SIR complexes to facilitate the spread of Sir-mediated silencing (Oppikofer *et al.* 2013).

Sir4 appears to serve as a scaffold for the assembly of the SIR complex given that Sir4 interacts independently with both Sir3 and Sir2, while Sir3 does not interact with Sir2 (reviewed in Oppikofer *et al.* 2013).The scaffold function of Sir4 resides in its C-terminal half (aa 747-1358), which contains the extreme C-terminal coiled-coil domain (aa 1272-1358) that mediates both homodimerization and binding to Sir3, yKu and Rap1, and serves to recruit Sir4 to telomeres. Upstream from this domain are binding sites for both Sir2 and Esc1 (enhancer of silent chromatin), whereas the extreme N-terminus (aa 1–270) binds DNA as well as Sir1 and yKu80 (Figure 4C); (Reviewed in Kueng *et al.* 2013).

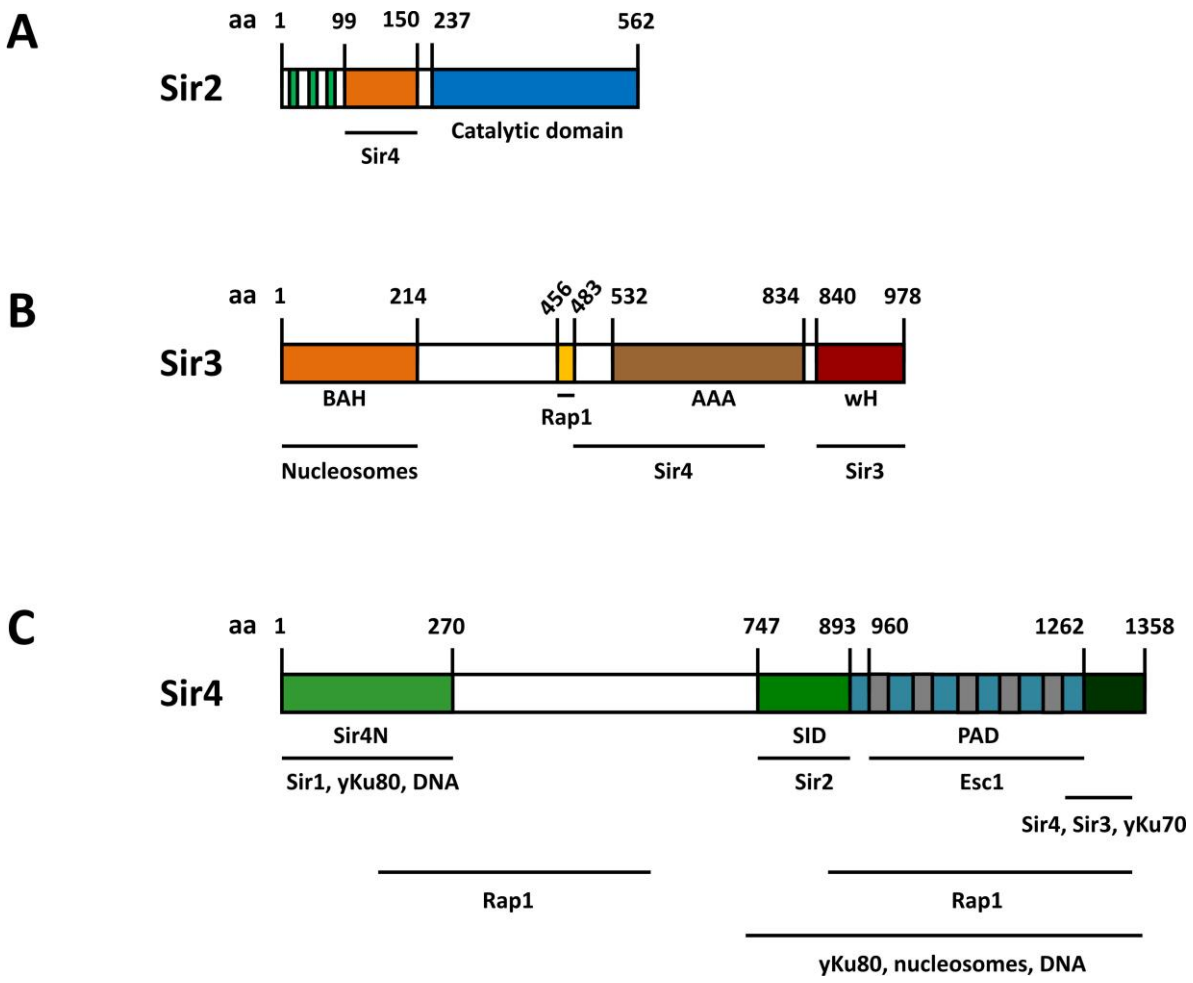

Figure 4. Schematic representation of Sir proteins involved in telomere silencing. **(A)** Representation of important domains of Sir2, the green/white bars represent an apparently unessential N-terminal. **(B)** and **(C)** Representation of the important domains and protein-protein interaction of Sir3 and Sir4. (Modified from Kueng *et al.* 2013).

1.4.2. Rap1 and Abf1

Budding yeast Rap1 (Repressor activator protein 1) is an essential multifunctional protein that works as a key regulator of gene transcription and chromosomal integrity. Rap1 binds directly to telomeric repeats (Conrad *et al.* 1990) and is able to recruit other proteins such as the Rap1 interacting factors (Rif1 and Rif2), Sir3 and Sir4. Together with Rif1 and Rif2, Rap1 forms the core of the yeast shelterin-

like complex, which protects the chromosomal ends from DNA damage response processing (Hardy *et al.* 1992).

The DNA-binding domain (DBD) of Rap1 is centrally located within the 827 aa sequence, from residues 358-601. The DBD consists of two tandem Myb-like motifs, followed by a C-terminal wrapping loop. The Rap1 C-terminal domain (aa 672-827) contains the region required for recruitment of the known Rap1-interacting proteins (Figure 5A, top) (Kyrion *et al.* 1993; Moretti and Shore 2001; Feldmann *et al.* 2015). This C-terminal domain is essential for silencing (Liu *et al.* 1994).

The DBD of Rap1 is conserved in yeast species in which Rap1 is found, suggesting a conserved three-dimensional structure. Accordingly, a 6-bp AC-rich motif resembling the sequence recognized by Rap1 in *S. cerevisiae*, is present at least in *C. glabrata* and *Kluyveromyces lactis* telomeres (Fabre *et al.* 2005). In addition, *Cg*Rap1 has an overall identity of 65% and a similarity of 78% to *Sc*Rap1 (Figure 5A; Haw *et al.* 2001).

Rap1, as well as Abf1 (Autonomously replicating sequence (ARS) binding factor 1), are general regulatory factors (GRFs) that contribute to transcriptional activation of a large number of genes. Rap1 and Abf1 bind ~200-300 promoters each. Genes containing Rap1 or Abf1 binding sites mainly comprise ribosomal protein genes and genes encoding proteins involved in amino acid biosynthesis, regulation of carbon source and sporulation (Lieb *et al.* 2001; Yarragudi *et al.* 2007).

Abf1 is essential for cell growth, binds to several ARSs and stimulates initiation of DNA replication from the origins of replication in yeast. Abf1 has also been implicated in gene silencing within subtelomeric regions (Pryde and Louis 1999) and nucleotide excision repair of silenced chromosomal regions (Reed *et al.* 1999). The DBD of Abf1 comprises the first 500 aa of the protein divided into a zinc finger domain (aa 40-91) and a unique region that determines the sequence specificity of binding (aa 323-496) (Cho *et al.* 1995). The C-terminus of Abf1 (aa 604-731) is divided in two domains, CS1 (C-terminal sequence 1, aa 624-628) and CS2 (aa

639-662). CS1 has a role in transcriptional silencing and/or repression in a context-dependent manner, whereas CS2 is universally required for transcriptional activation, stimulation of DNA replication, and gene silencing (Miyake *et al.* 2002) (Figure 5B, top). In *C. glabrata*, Abf1 is 80 and 77% identical in each of the bipartite DNA binding domain of *Sc*Abf1. In addition, *Cg*Abf1 does not contain the CS1 domain, it only has the silencing domain CS2, which is highly conserved (87% identity and 96% of similarity) with respect to *Sc*Abf1 (Figure 5B, bottom; Castanedo-Ibarra and Castaño 2015).

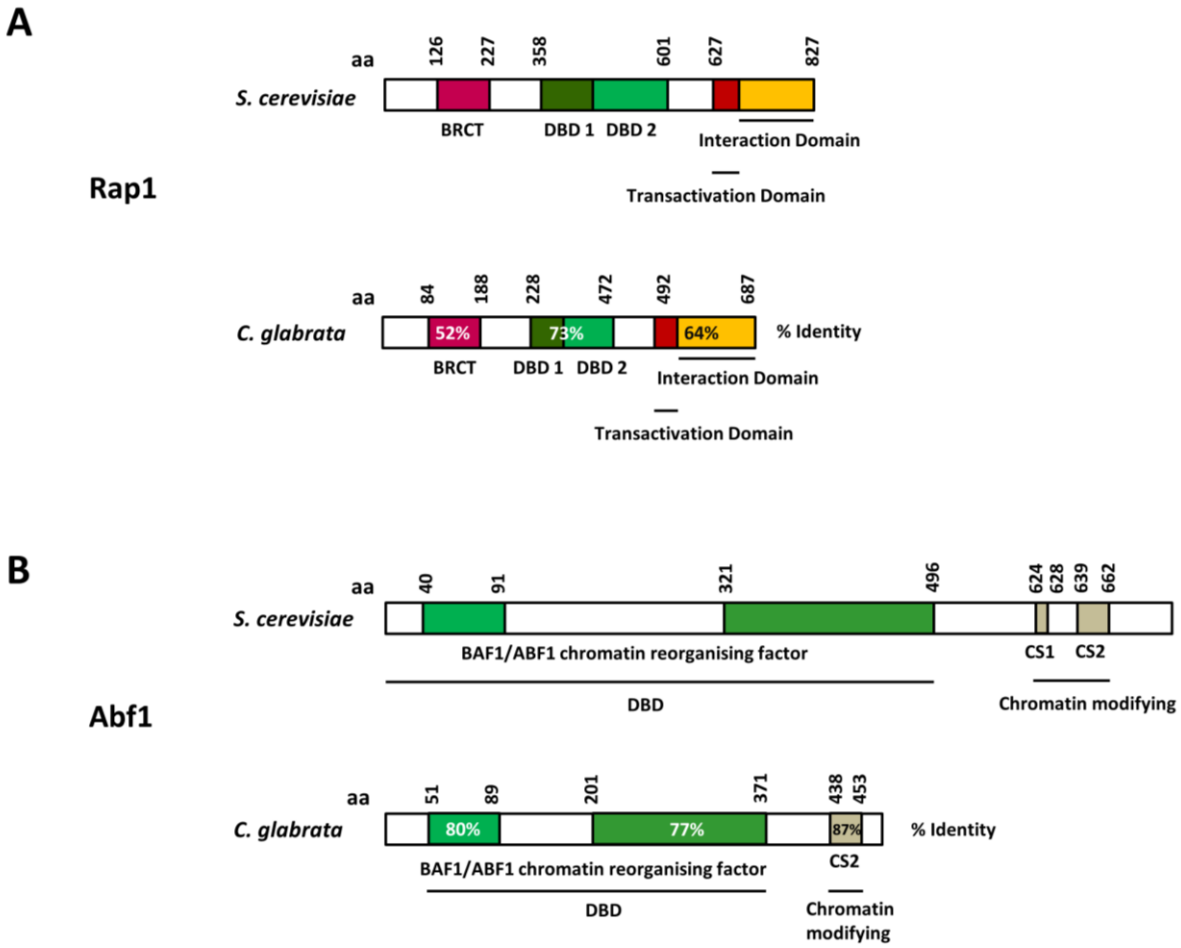

Figure 5. Schematic representation of Rap1 and Abf1 proteins. **(A)** Representation of relevant domains of Rap1 in *S. cerevisiae* (top) and in *C. glabrata* (bottom). BRCT domain (BRCA1 C-terminus), DBD (DNA binding domain). **(B)** Representation of important domains of Abf1 in *S. cerevisiae* (top) and in *C. glabrata* (bottom). The percentages of identity of each domain with respect to *S. cerevisiae* are indicated inside each box.

1.5. *Cis*-acting elements form an intricate silencing network

In addition to the proteins involved in silencing, there are also other elements involved known as *cis*-acting elements, such as silencers, protosilencers and barrier elements (Figure 6).

Silencers are negative regulatory *cis*-acting elements composed of binding sites for various factors that act collectively in the establishment and stable inheritance of a repressed state (Figure 6A). In the telomeres of budding yeast, the terminal repeated TG1-3 sequences serve as silencers. The silencers of the *HM* loci (E and I) are compact elements spanning <150 bp, that contain different combinations of binding sites for factors essential for silencing (Rap1, ORC, Abf1) (Boscheron *et al.* 1996), and are necessary for silencing of *HM* loci. Flanking the silencers, there are other *cis*-acting elements called “barrier elements”, which limit the silencing activity to the *HM* loci (Donze *et al.* 1999). The activity of this barrier was found to require the transcriptional potential of $tRNA^{Thr}$ gene (Donze and Kamakaka 2001), suggesting that the barrier elements or boundaries may determine the polarity of the silencers (West *et al.* 2002). Barrier elements (STAR, subtelomeric antisilencing regions) have also been located between the X and Y’ repeats of budding yeast, that constrain telomeric silencing to limited areas (Figure 6E; Fourel *et al.* 1999). Silencers act in a continuous manner to maintain the structure and function of silent chromatin (Cheng and Gartenberg 2000).

In addition, a single binding site for any of the silencer-binding proteins can enhance the activity of a distant silencer without acting as a silencer *per se*; these elements are referred to as protosilencers (Boscheron *et al.* 1996). Protosilencers, like silencers, act by binding sequence-specific factors that lead to the recruitment of Sir proteins. Protosilencers play essential roles in the propagation of silencing in heterochromatin regions (Figure 6B and 6C; Fourel *et al.* 2002) and can prevent loss of silencing in G1 phase at *HML*α locus in the absence of E and I silencers.

Silencer-protosilencer arrangements involved in silencing have been found in different organisms besides *S. cerevisiae*. Protosilencers flanking mating cassettes

in *S. pombe* facilitate the bidirectional spreading of silencing. In vertebrates, the *HoxD* complex of homebox genes is globally maintained in a repressed state through a master silencer-protosilencer array. In *Drosophila*, the repression mediated by the Polycomb-group complex depends not only on silencers called Polycomb responsive elements (PRE) but also on the cooperative extension of the complex involving additional weak targets (reviewed in Fourel *et al.* 2002). In the silencer–protosilencer interactions, silencing of genes located in the region flanked by the silencer and protosilencer was found to be increased compared to genes silenced only by one silencer (Boscheron *et al.* 1996; Cheng and Gartenberg 2000; Lebrun *et al.* 2001). The interactions of combinations of *cis*-acting elements form an intricate silencing network.

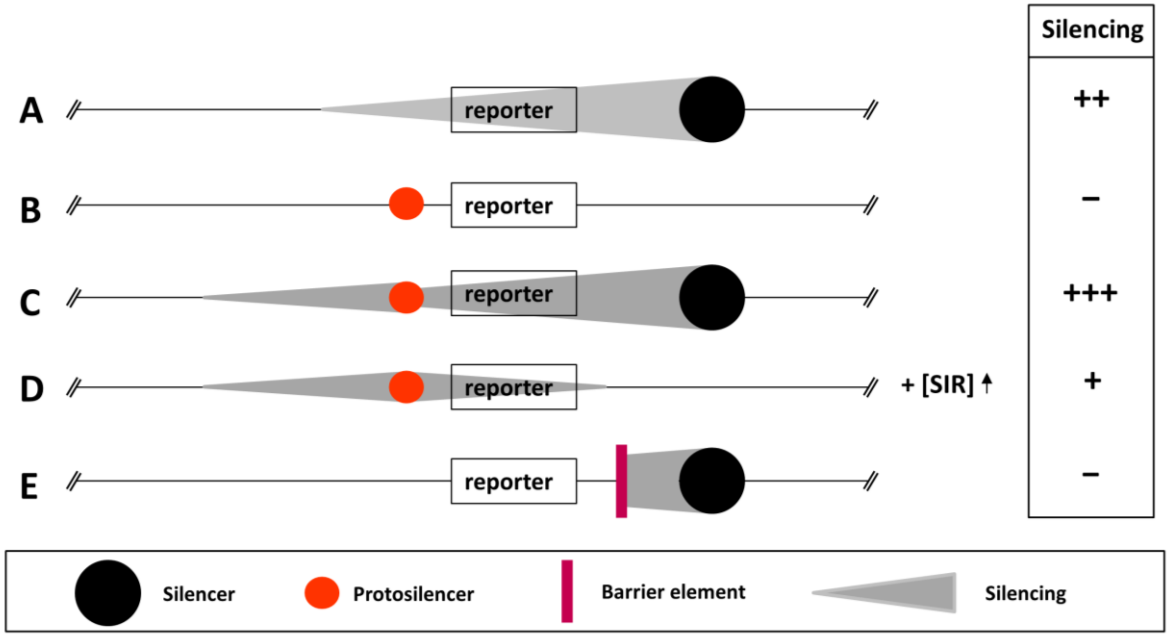

Figure 6. Operational definition of *cis*-acting elements. The elements shown are described at the bottom of the figure and the relative silencing level of the different arrangements is show to the right. A silencer can silence the adjacent reporter **(A)**. In contrast, a protosilencer cannot silence the reporter by itself **(B)**. However, a protosilencer can cooperate with a silencer to reinforce silencing and extending its influence **(C)**. Of note, a protosilencer can be functional in a silencing conductive context, such as overexpression of Sir3 or Sir4 **(D)**. Propagation of silencing can be interrupted by barrier elements, such as STAR (subtelomeric antisilencing region) sequence **(E)**. (Modified from Fourel *et al.* 2002).

1.6. Gene regulation involves long-range communication between silencers, enhancers, and promoters.

Long-range communication between distantly located elements in chromosomes is achieved through chromatin looping, which is involved in many chromatin related processes ranging from transcriptional activation, repression, enhancer blocking, recombination events, to structural organization of the genome (Li *et al.* 2006; Talbert and Henikoff 2006; Palstra 2009). Chromatin loops are not only found between distal regulatory elements and promoters but also between promoters and the untranslated terminator regions of genes. This interaction between the promoter with the terminator of the same gene through a loop is termed intragenic looping, which is transcription dependent (reviewed in Randise-Hinchliff and Brickner 2012). 3C experiments have revealed intragenic looping in yeast genes such as *GAL10* and *FMP27* genes (Sullivan *et al.* 2004) (Figure 7A).

Several studies in yeast provide evidence that SIR complex is able to fold chromatin into a higher-order structure. One piece of evidence came from studies where Rap1 binds to the telomeric repeats, and is also found at subtelomeric sites, suggesting that telomere folding allows Rap1-Sir interactions within subtelomeric chromatin (Strahl-Bolsinger *et al.* 1997). Also, genetic evidence supports telomere looping, the enhancer-like, *UAS* (Upstream activating sequence) activates transcription only when it is positioned upstream of a gene. In yeast, UAS_G (containing four Gal4 binding sites) inserted adjacent to the telomere and downstream of the reporter gene, is able to activate the reporter when it is linked to a telomere, but not if it is inserted at internal chromosomal locus. This is thought to be due to telomere folding, which places the UAS_G close to the promoter of the telomere-linked gene (Figure 7B) (de Bruin *et al.* 2001). Telomere loops have also been detected in mammals (Griffith *et al.* 1999), ciliates (Murti and Prescott 1999), and trypanosomes (Muñoz-Jordán *et al.* 2001).

Another example of the formation of a loop in silent chromatin has been described in the mating loci in *S. cerevisiae*, the silencer elements flanking *HMR* communicate with one another to mediate repression via the recruitment of Sir

proteins along the DNA forming a chromatin fiber and stable repression (Figure 7C) (Valenzuela *et al.* 2008).

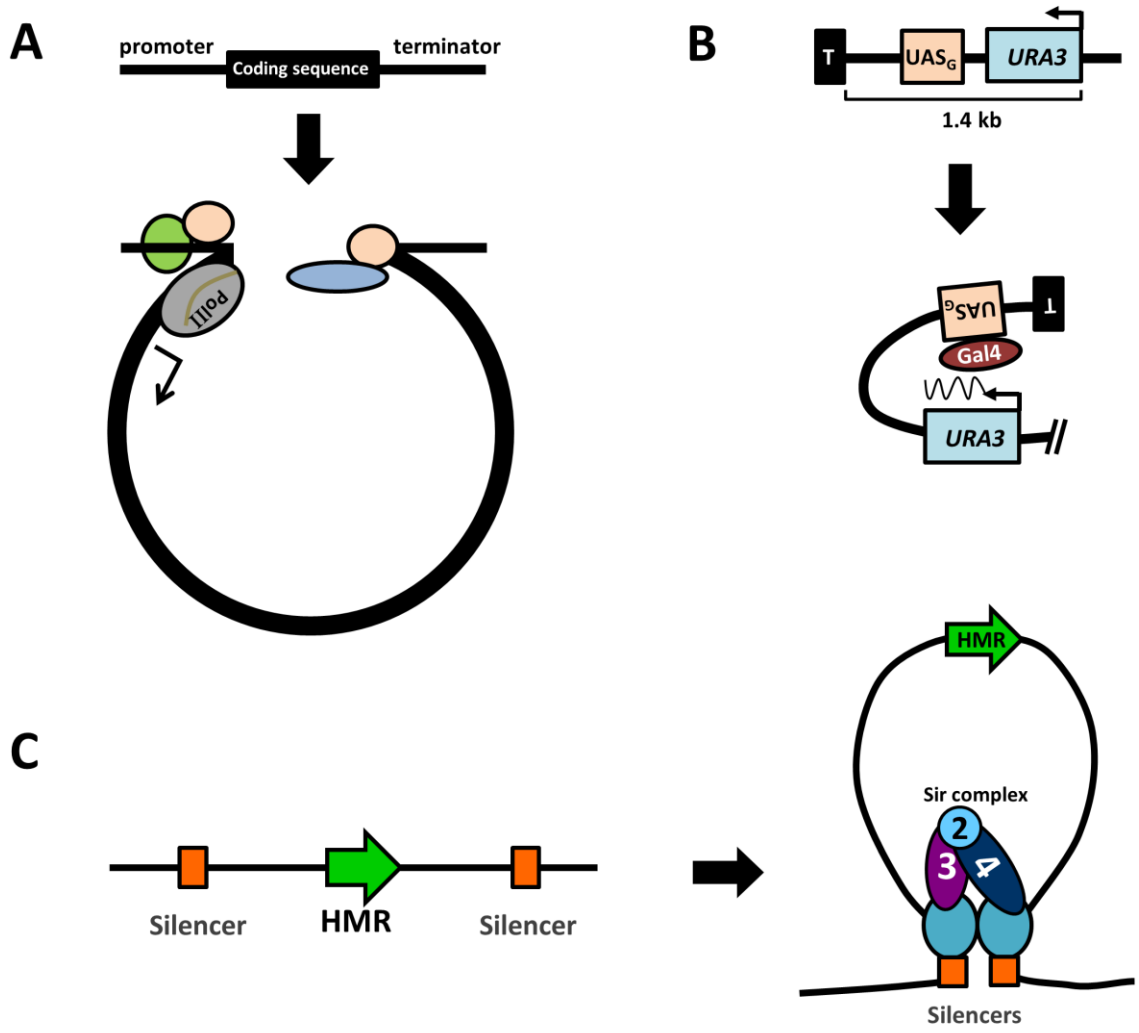

Figure 7. Chromosome and gene loops are implicated in diverse processes. (**A**) Intragenic looping is transcription-dependent. The promoter and the terminator are indicated (black line). (**B**) Telomere looping in reporter gene activation. The *UAS*$_G$ was inserted adjacent to the telomere and immediately 3' of the *URA3* gene. (**C**) Silencing model at *S. cerevisiae HMR*. The flanking silencers (orange squares) interact to silence the *HMR* loci in a SIR complex dependent manner.

1.7. *Candida glabrata* as a model organism to study the subtelomeric silencing

Candida glabrata is a haploid budding yeast, which has emerged as an important nosocomial fungal pathogen associated with an attributable mortality of ~30% (Klevay *et al.* 2009). It normally resides as a commensal in the flora of healthy human mucosal tissues to which it adheres tightly, but can cause infections in immunocompromised patients (Pfaller and Diekema 2007).

In *C. glabrata*, subtelomeric silencing requires the SIR complex, as well as the Rif1, Rap1 and the yKu proteins, and can extend >20 kb toward the centromere (De las Peñas *et al.* 2003; Domergue *et al.* 2005; Rosas-Hernández *et al.* 2008). Interestingly, different telomeres in *C. glabrata* have different protein requirements for silencing. For instance, the proteins yKu70 and yKu80 are not required in the right telomere of the chromosome E (E_R) where *EPA1* forms a cluster with *EPA2* and *EPA3* genes. This independence of yKu proteins is due to a *cis*-acting element, the protosilencer Sil2126, which has overlapping functions with the yKu proteins (Juárez-Reyes *et al.* 2012).

In addition to the Chr E_{-R}, silencing has been tested in other telomeres of *C. glabrata*. *EPA4* and *EPA5* genes (which form an almost perfect inverted repeat) are located at the right telomere of chromosome I (Chr I_{-R}) and here, the silencing can propagate at least 24 kb and depends on Rap1, Sir complex, Rif1 and yKu proteins (De las Peñas *et al.* 2003; Rosas-Hernández *et al.* 2008). Also, the silencing at both ends of chromosome C, where *EPA6* and *EPA7* are located, depends on SIR complex and yKu proteins (Castaño *et al.* 2005; Rosas-Hernández *et al.* 2008). Therefore, in *C. glabrata*, TPE plays an important role in regulation of expression of virulence genes such as adhesins.

1.7.1. Epa family members are highly glycosylated mannoproteins

C. glabrata can differentially express glycosylphosphatidylinositol-cell wall proteins (GPI-CWPs) on its cell surface, which allows for its adaptation to different environmental conditions. The largest family of CWPs is the Epa (Epithelial

adhesin) family. Most of the *EPA* genes encoding adhesins, are located in subtelomeric regions. The Epa family contains at least 17 and up to 23 paralogues, depending on the strain. Epa1 mediates most of the adherence to epithelial cells *in vitro* (Cormack *et al.* 1999), and Epa6 and Epa7 have been shown to be functional adhesins involved in kidney colonization (Castaño *et al.* 2005).

Additionally, Epa family is involved in biofilm formation, which can increase infection probability because this life form is more tolerant or resistant to host defense machinery and antifungal drugs. *EPA3* is upregulated during biofilm formation in rich and semi-defined media, whereas *EPA1*, *EPA3*, *EPA22* and *EPA7* are induced only in biofilms grown in semi-defined media (Kraneveld *et al.* 2011). Epa6 expression is also associated with the ability of *C. glabrata* to form biofilm on plastic surfaces (Iraqui *et al.* 2005). In a high-throughput analysis, *EPA3* was found to be highly induced by osmotic stress and glucose starvation (Roetzer *et al.* 2008).

2. BACKGROUND

A cluster of *EPA* genes containing *EPA1*, *EPA2* and *EPA3* is localized at the right telomere of chromosome E (Chr E_{-R}) (De las Peñas *et al.* 2003). *EPA1* expression is negatively regulated by two distinct mechanisms. One of them is the silencing propagating from the telomere that depends on the SIR complex, Rap1 and Rif1. *EPA1* transcription is also repressed by a *cis*-acting element, the negative element (NE), a repression that depends on yKu proteins but is independent from the silencing from the telomere (Figure 8; Gallegos-García *et al.* 2012).

EPA2 is repressed by subtelomeric silencing; however, it is induced in the presence of oxidative stress *in vitro.* This induction is mediated by transcription factors such as Yap1 and Skn7 (Juárez-Cepeda *et al.* 2015).

Due to the subtelomeric localization of the *EPA* genes, these are normally silenced; however, various *EPA* genes (*EPA4-7*) can be derepressed upon loss of subtelomeric silencing by the deletion of Sir3, Sir4 or Rap1 (De las Peñas *et al.* 2003; Domergue *et al.* 2005). *EPA2* and *EPA3* are not expressed *in vitro* in a *sir3*Δ, *rif1*Δ or *rap1-21* strain, suggesting additional layers in their regulation (Castaño *et al.* 2005). In addition to the *cis*-acting element, the NE, there is another *cis*-acting element in this subtelomeric region, a protosilencer called Sil2126. Sil2126 performs overlapping functions with yKu proteins since removing both the yKu proteins and Sil2126, results in higher derepression of *EPA3* (Juárez-Reyes *et al.* 2012). This *cis*-acting element might be an extra layer of regulation for the *EPA1-3* cluster of genes.

Sil2126 has two essential regions for its activity, namely R1 and R2. R1 contains a putative binding site for Abf1 (ARS binding factor), and adjacent to R1 on the 5' side, there is a putative binding site for Rap1 (Figure 8, bottom). Sil2126 can silence a reporter when both are inserted 32 kb away from the right telomere of the chromosome E (Sil@-32kb). However, it requires its own telomere context because when we placed Sil2126 and the reporter (Sil-reporter system) at similar

distances in other telomeres, Sil2126 is not able to silence the adjacent reporter (Juárez-Reyes *et al.* 2012).

Sil2126 activity at its native position could have an impact in the regulation of the main adhesin, Epa1. Furthermore, determining the silencing mechanism in this telomere will allow us to gain insights on the mechanisms of regulation of adhesin expression.

In this work, we wanted to understand the mechanism of action by which Sil2126 extends silencing in the subtelomeric region of telomere E_R. We also decided to determine what elements in this region are required for its activity.

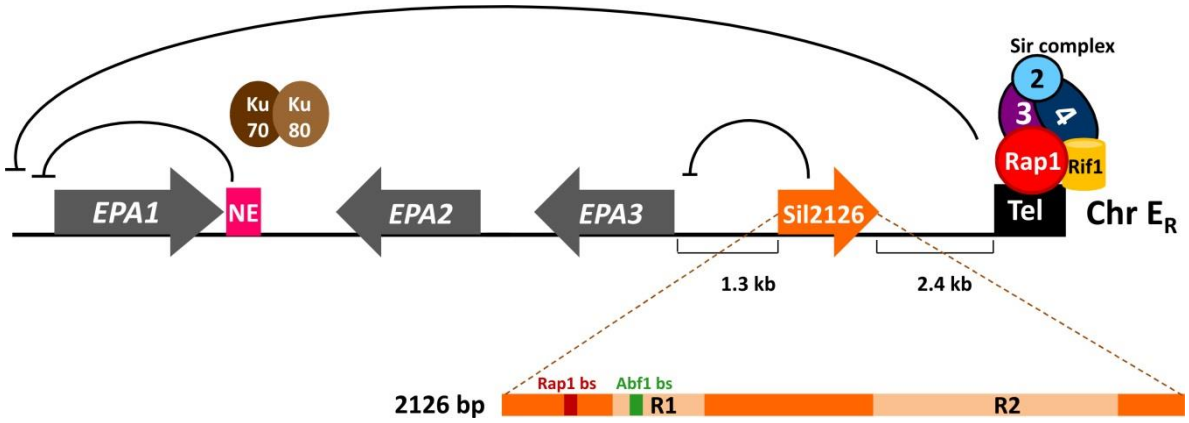

Figure 8. Map of the subtelomeric region of Chr E_{-R}, where *EPA1*, *EPA2* and *EPA3* are located. *EPA1* expression is negatively regulated by two mechanisms, the Ku-dependent (brown circles) *cis*-acting element called Negative Element (NE, pink square) and silencing from the telomere (see above). *EPA3* is negatively regulated by the protosilencer Sil2126 (orange arrow), which has two essential regions for its activity. The putative binding sites for Rap1 and Abf1 are shown in red and green rectangles, respectively (zoom in, bottom). The distances from Sil2126 to *EPA3* and to the telomere are indicated.

3. AIMS

To determine the silencing mechanism by which the protosilencer Sil2126 extends silencing in the right telomere of chromosome E and to uncover the *trans* and *cis*-acting elements that are required for its activity.

3.1. Specific aims

- To uncover the *cis*-acting elements located in the Chr E_{-R} required for Sil@-32kb activity.
- To determine whether the silencing proteins Rap1 and Abf1 are recruited by Sil2126.
- To test if Sil2126 can interact with other regions in the Chr E_{-R} to propagate silencing.
- To determine whether the putative binding sites for Rap1 and Abf1 are functional.

4. MATERIALS AND METHODS

4.1. Strains

All strains and plasmids used are listed in Table S1 and S2, respectively.

4.2. Media

Candida glabrata strains were grown at 30°C in plates with YPD medium which contains 10 g/L of yeast extract and 20 g/L of peptone, supplemented with 2% glucose and 2% agar. If necessary, culture plates were supplemented with Hygromycin (Invitrogen®) 440 µg/mL or Nourseothricin 100 µg/mL (Streptothricin Sulfate, NTC, clonNAT, CAT#N-500-1). In order to test silencing level, we performed growth plate assays in SC medium supplemented with casaminoacids or with 5-fluoroorotic acid (5-FOA; Toronto Research Chemicals). This medium contains 1.7 g/L yeast nutrient base (without $(NH_4)_2SO_4$ and amino acids), 5 g/L $(NH_4)_2SO_4$ and is supplemented with 0.6% casaminoacids and 2% glucose. SC+5-FOA medium is supplemented with 0.9 g/L 5-FOA and 25 mg/L uracil. Minimal medium was used for the ChIP and 3C assays. This medium contains 1.7 g/L yeast nutrient base, 5 g/L $(NH_4)_2SO_4$ and is supplemented with 2% glucose and 25 mg/L uracil.

Bacteria were grown at 30°C in LB medium as described previously by (Ausubel *et al.* 2001). LB medium contains 5 g/L yeast extract, 10 g/L tryptone and 5 g/L NaCl. If necessary, 1.5% agar was added. All plasmid constructs were introduced via electroporation into the DH10 strain. 50 mg/mL carbenicillin (Invitrogen®) was added for plasmid selection.

4.3. Yeast transformation

Yeast transformation was performed using the lithium acetate protocol as described previously by Castano *et al.* (2003).

4.4. Plate growth assays

The level of silencing or expression of the *URA3* reporter was assessed using a plate growth assay as described previously (De las Peñas *et al.* 2003; Castaño *et al.* 2005). Briefly, strains containing the different *URA3* insertions were grown at 30°C in YPD for 48 hr to stationary phase. The cultures were adjusted to an optical density of 1 at 600 nm with sterile water. 10-fold serial dilutions were made in 96-well plates. A total of 5 µL of each dilution was spotted onto YPD, SC-Ura and SC +5-FOA plates, and plates were incubated for 48 hrs at 30°C and photographed.

4.5. Western blot assay

We constructed epitope-tagged versions of each protein tested. Rap1 and Sir3 were tagged with FLAG epitope at the C-terminus and integrated in their native loci, respectively. To test Abf1, we constructed a plasmid containing an N-terminal fusion of cMyc with Abf1 and under the inducible promoter P_{MT1}. The strains were grown in YPD and harvested in stationary phase. The protein extraction and western blot assays were done as described with minor modifications (Orta-Zavalza *et al.* 2013; Robledo-Márquez *et al.* 2016). Briefly, cells were resuspended in lysis buffer (45 mM HEPES, 400 mM Potassium acetate, 0.5% Nonidet P-40, 1 mM EDTA, 1 mM DTT, 1 mM PMSF, 1X Complete protease inhibitors cocktail ROCHE®), 100 µL of zirconia beads were added and cells were broken using a FastPrep®-24 (MP Biomedicals®) equipment, with three times for 60 s at 6 m/s. The cells were centrifuged at 15000 rpm for 40 min at 4°C, the supernatant was recovered and the protein content was determined by Bradford assay. 50 µg of total protein mixed with 2X SDS loading buffer were preheated (95°C for 8 min) and then loaded in a 10% SDS-polyacrylamide gel. After electrophoresis, the proteins were blotted onto PVDF membranes (BIO-RAD®) and probed with anti-Flag (Sigma®) at a final concentration of 3 µg/mL overnight. After washing, the membrane was probed with a goat-mouse horseradish peroxidase-conjugated secondary antibody (MERCK®). Signal was detected by ECL chemiluminiscence reagents (Pierce®) and recorded using a BioRad ChemiDoc MP System equipped with chemiluminiscence.

4.6. GFP expression by flow cytometry

Strains were grown for 48 hr at 30°C in SC medium supplemented with uracil when it was necessary. Culture cells were diluted into fresh media to induce *EPA1* expression. We measured the activity of *EPA1* promoter using the GFP reporter every 2 hr. Fluorescence was assessed by FACS analysis using a BD FACSCalibur flow cytometer with Cell Quest Pro software. The data analysis was done using FlowJo® software.

4.7. Chromatin immunoprecipitation (ChIP) assay

Yeast cultures (150 mL) were grown in minimal medium to an OD_{600} of 1 at 30°C with shaking. The grown cultures were put on ice for 15 min. Cells were fixed with 1% formaldehyde for 15 min at 25°C at 180 rpm. Cross-linking was quenched by the addition of glycine to 125 mM and incubated for 5 min. The cells were harvested, washed twice with TBS buffer (20 mM Tris-HCl [pH 7.5], 150 mM NaCl) and transferred to 1.5 mL centrifuge tubes; yeast pellets were frozen at -80°C. The cells were lysed with 500 µL lysis buffer (10 mM EDTA [pH 8], 50 mM Tris-HCl [pH 8], 1% SDS and, 1 mM PMSF and protease inhibitor ULTRA Tablet Mini/10 mL (EASYpack [ROCHE®]) added just before use, 500 µL glass beads were added and cells were disrupted by vortexing for 30 s and placed on ice for 1 minute (repeated ten times). The chromatin in the lysates was sheared by sonication with 30 cycles (effective sonication time: 3 min 45 s) at 20% amplitude in Episonic multi-functional bioprocessor Model Oasis 180. The DNA was sheared to an average size ~ 500 bp. Tagged proteins were immunoprecipitated with 5µg mouse anti-FLAG (Sigma®) or anti-cMyc (Millipore®) bound to Dynabeads® Protein G for immunoprecipitation (Invitrogen). Dynabeads with the immunoprecipitates were washed with Dilution buffer (2 mM EDTA [pH 8], 20 mM Tris-HCl [pH 8], 150 mM NaCl, 1% Triton) twice and washed with Wash buffer (2 mM EDTA [pH 8], 20 mM Tris-HCl [pH 8], 150 mM NaCl, 1% Triton, 0.1% SDS) four times. Protein and cross-linked DNA were eluted in 100 µL of Elution buffer (1% SDS, 0.1M $NaHCO_3$) at 65°C for 10 min. To reverse the crosslinking, the mixture was incubated at 65°C overnight with 50µg/mL proteinase K. DNA was extracted with

phenol:chloroform:isoamyl alcohol 25:24:1 and precipitated with 5M NaCl, glycogen and ethanol. The IPs were resuspended in 30 µL of TE (10 mM Tris-Cl [pH 8], 1 mM EDTA) containing 2µg/mL RNase cocktail (Ambion). Input DNA was prepared by mixing 20% of the starting lysate (after sonication) with 200 µL TE. The lysate was processed in the same way as the immunoprecipitates, proteinase K was added, the crosslinking was reversed and the DNA was extracted. The immunoprecipitated DNA and the input were used as templates for qPCR reactions conducted with ABI 7500 instrumentation (Applied Biosystems®) and SYBR Green PCR Master Mix (Life Technologies®). The primers used are listed in Table S3. The results shown represent the average of duplicate biological samples and three technical replicates. The ChIP assays are presented as % Input relative to the target where there is no binding. For Rap1 and Sir3, the ChIP assays are presented as % Input relative to ISC1 binding and for Abf1 relative to binding to the telomere (Genetics' paper, Figures 5, 6, S1, S5, S6 and S7).

4.8. Chromosome conformation capture (3C) assay

Chromosome Conformation Capture (3C) in budding yeast was performed as described in Hagège *et al.* (2007) and Belton and Dekker (2015b). Briefly, cells were grown in SC medium to an OD_{600} of 1. Cells were fixed with 3% formaldehyde for 20 min at 25°C. The crosslinking was quenched by adding 2.5 M glycine at 2X the volume of formaldehyde used in the previous step and the culture was shaken for 5 min at 25°C. Cross-linked cells were washed with cold water and resuspended in the appropriate 1X restriction enzyme buffer (*Hind*III buffer prepared as NEB *Hind*III buffer). The sample was frozen and ground with liquid nitrogen for 10 min adding it as necessary. The ground sample was resuspended in 1X restriction enzyme buffer and adjusted to OD_{600} of 10. Cells (38 µL) were distributed into a 96-well PCR plate. Chromatin was solubilized by the addition of SDS (0.1% final) and incubated for 10 minutes at 65°C. Triton X-100 was added to a final concentration of 1% to sequester the SDS. Chromatin was digested with 100U of *Hind*III and incubated overnight at 37°C. The restriction enzyme was denatured by adding SDS (1.67% final) and incubating for 20 min at 65°C.

Chromatin fragments were ligated in dilute (12X) conditions assembling the ligation reaction (1% Triton X-100, 1X Ligation buffer, 0.1 mg/mL BSA, 1mM ATP, 4.8 U/mL T4 DNA ligase and water) and incubating 4 h at 16°C. Cross-links were reversed by incubating the samples for 4 h at 65°C in the presence of 0.0625 mg/mL proteinase K, followed by adding again 0.0625 mg/mL proteinase K and incubating overnight at 65°C. DNA was purified by a series of phenol-chloroform extractions followed by ethanol precipitation. The resulting template was then treated with RNase cocktail (Ambion) and incubated 1 h at 37°C yielding the "3C template". The chromatin digestion was evaluated as reported in (Hagège *et al.* 2007) and is shown in the Figure S1. In addition to the 3C template, a randomized ligation control template was also generated (Belton and Dekker 2015a) which was used to determine the PCR amplification efficiency of specific ligation products. This template was generated by digesting naked, non-crosslinked yeast genomic DNA with *Hind*III and ligating it in concentrated conditions to maximize the formation of random inter-molecular combinations of chimeric ligation products. The resulting template was purified by a series of phenol-chloroform extractions and ethanol precipitations and treated with RNase cocktail (Ambion).

Once the 3C samples were generated, DNA concentration was determined by SybrGreen quantitative PCR (qPCR) using an internal primer set (*ISC1* primers 2503 and 2504 showed in Table S3). 3C samples were adjusted to 50 ng/µL and the concentrations were verified once again by qPCR. Quantification of ligation products was performed with qPCR using Applied Biosystems™ TaqMan® MGB probes and PerfeCTa FastMix II Low ROX (Quanta Biosciences Inc.). The qPCR reactions contain an anchor primer (anchor H), a TaqMan probe (probe H) and one of the test primers (primers H1 through H8). The probe and primers used are listed in Table S3. A standard curve was performed with each pair of primers using serial dilutions of randomized ligation control. The parameters of each standard curve are shown in the Table S4. The conditions used for qPCR were: 15 min at 95°C (cycle 1) and 10 s at 95°C, 1 min at 60°C (cycles 2-40) conducted with ABI 7500 instrumentation (Applied Biosystems®). Experiments were performed in technical triplicates.

5. RESULTS

Most of the results generated in this project were published in the following paper:

5.1. *Candida glabrata cis*-element Sil2126 negatively regulates the expression of *EPA* genes through chromatin loop formation.

Eunice López-Fuentes[1], Grecia Hernández-Hernández[1], Leonardo Castanedo-Ibarra[1], Guadalupe Gutiérrez-Escobedo[1], Katarzyna Oktaba[2], Alejandro De Las Peñas[1], and Irene Castaño[1]*. **2018**. *GENETICS Early online July 12, 2018; https://doi.org/10.1534/genetics.118.301202*

5.2. Collaborations

In addition, I participated as co-author in the following publications:

Reviews:

5.2.1. Local and Regional Chromatin Silencing in *Candida glabrata*: consequences for adhesion and the response to stress

Alejandro De Las Peñas, Jacqueline Juárez-Cepeda, Eunice López-Fuentes, Marcela Briones-Martín-del-Campo, Guadalupe Gutiérrez-Escobedo and Irene Castaño*. **2015**. *FEMS Yeast Res.* 15.

5.2.2. *Candida glabrata*'s genome plasticity confers a unique pattern of expressed cell wall proteins

Eunice López-Fuentes[1], Guadalupe Gutiérrez-Escobedo[1], Bea Timmermans[2, 3], Patrick Van Dijck[2,3], Alejandro De Las Peñas[1] and Irene Castaño[1, *]. *J. Fungi* **2018**, 4, 67; doi:10.3390/jof4020067

Research paper:

5.2.3. Molecular characterization of the Silencing complex SIR in *Candida glabrata* hyperadherent clinical isolates

Osney Leiva-Peláez, Guadalupe Gutiérrez-Escobedo, Eunice López-Fuentes, José Cruz-Mora, Alejandro De Las Peñas, Irene Castaño*. *Fungal Genet. Biol*. 118 (**2018**) 21-31. https://doi.org/10.3390/jof4020067

6. ADDITIONAL RESULTS

6.1. Activity of *EPA1* promoter is not affected by the absence of Sil2126

EPA1 gene encodes the Epa1 adhesin, which mediates most of the adherence *in vitro* (Cormack *et al.* 1999). *EPA1* is located in the Chr E_{-R}, where forms a cluster with *EPA2* and *EPA3*. The activity of *EPA1* promoter is negatively regulated by a *cis*-acting element, the NE (Gallegos-García *et al.* 2012). In addition to the NE, there is another *cis*-acting element, the protosilencer Sil2126, which is telomere specific. *EPA2* and *EPA3* are expressed when both Sil2126 and yKu proteins are removed (Juárez-Reyes *et al.* 2012). Thus, we wondered whether *EPA1* expression is regulated by Sil2126.

We measured the activity of *EPA1* promoter in the absence of the *cis*-acting elements using two different reporters. *EPA1* replaced by *URA3* and *EPA1* replaced by *GFP* in its native position near the Chr E_{-R} telomere.

6.1.1. Activity of *EPA1* promoter using *URA3* as a reporter gene in the absence of *cis*-acting elements

The *URA3* expression was assayed by the ability of the strains to grow on plates without uracil (SC-ura) and the silencing level was tested by the ability to grow on plates containing 5-FOA. We measured the activity of *EPA1* promoter in the single mutants (*sil*Δ and *ne*Δ) and in the double mutant (*sil*Δ *ne*Δ).

We have previously shown that the *ne*Δ strain grows better than the parental strain in SC-ura, but there is no difference in the growth on 5-FOA plates (Figure 9 bottom, compare line 1 with 2 and Figure S2). Thus, the NE negatively regulates *EPA1* expression and this regulation is an independent mechanism from the telomeric silencing (Gallegos-García *et al.* 2012). In a strain with Sil2126 deletion (*sil*Δ), we observed the same extent of growth in SC-ura than the parental strain (Figure 9 bottom, compare line 1 with line 3). However, we observed a subtle effect in the double mutant (*sil*Δ and *ne*Δ) with respect to the *ne*Δ strain in SC-ura plates, where double mutant grew to a lesser extent than the *ne*Δ strain (Figure 9,

compare line 2 with 4). These results suggest that Sil2126 can affect the *EPA1* expression when the NE is absent.

In addition, we decided to test the activity of *EPA1* promoter when a barrier element, such as a strong promoter, is present instead of Sil2126 (Figure 9B). When the barrier element (P_{PGK1}::*hph*) is adjacent to the telomere, the *sil*Δ::(P_{PGK1}::*hph*) strain and in the double mutant without NE [*ne*Δ *sil*Δ::(P_{PGK1}::*hph*)], the cells of both strains grew better in the absence of uracil than the *sil*Δ and neΔ *sil*Δ strains respectively (Figure 9 bottom, compare line 3 with 5 and line 4 with 6), suggesting that a barrier element can decrease the silencing of *EPA1* coming from the telomere. However, the effect of the NE can still be appreciated as judged by the larger colony size of the strains with the deletion of NE (Figure 9 bottom, compare lines 3 with 4 and lines 5 with 6).

We have previously observed that in the presence of a barrier element, the silencing of the insertions throughout the right telomere of chromosome E is abrogated in almost all the reporter insertions, except the one adjacent to the telomere (before the barrier element) (Juárez-Reyes *et al.* 2012). However, when we tested the *EPA1* expression, we observed that the silencing of *EPA1* promoter is not eliminated in presence of the barrier element (note the robust growth on 5-FOA lines 5 and 6), but we could detect a higher expression in SC-ura plates (Figure 9 bottom, compare colony size on SC-ura between line 3 and 5).

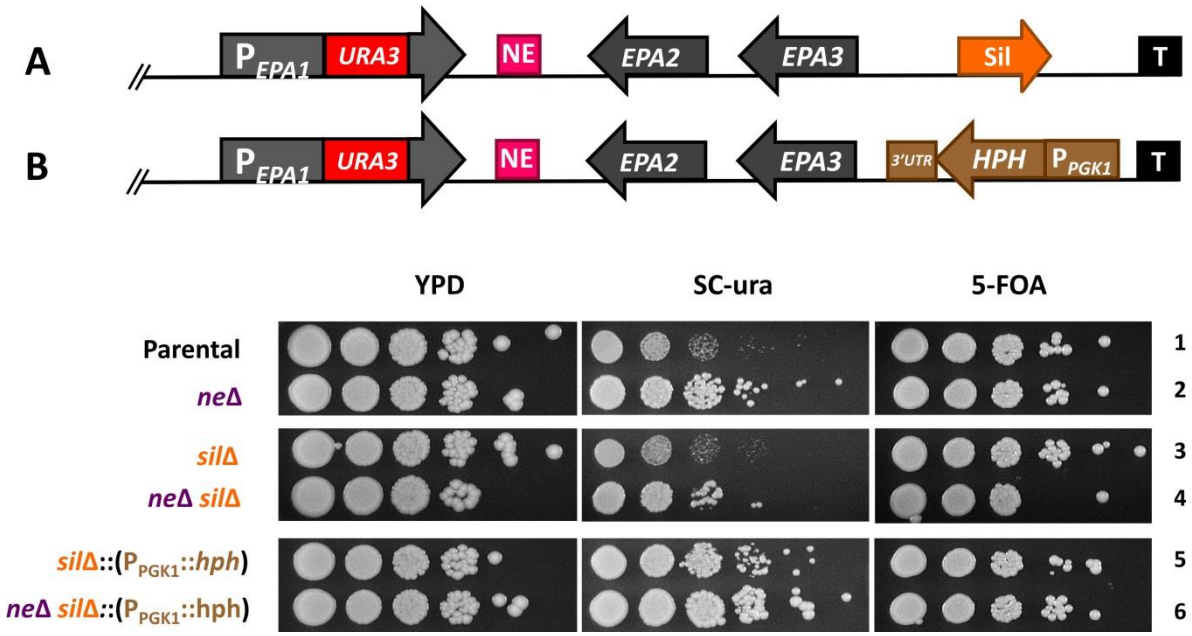

Figure 9. Assessment of the level of silencing of *EPA1* promoter in the absence of *cis*-acting elements. (**A**) *URA3* under the control of *EPA1* promoter in its chromosomal location. (**B**) Insertion of a barrier element between *EPA3* and the telomere. Strains were grown in YPD for 48 hr at 30°. Cells were washed and adjusted to OD = 1. Ten-fold dilutions were spotted on the different media. The plates were incubated at 30° for 48hrs and photographed.

The regulation of *EPA1* by the NE depends on yKu proteins (Gallegos-García *et al.* 2012). In addition, this particular telomere is not dependent on yKu proteins for subtelomeric silencing due to the presence of Sil2126. We only observed that *EPA3* transcription is strongly derepressed in the absence of both Sil2126 and yKu proteins. Thus, we wondered whether the *EPA1* expression might be affected in the absence of these three elements, the two *cis*-acting elements (NE and Sil2126) and the yKu proteins. We evaluated the activity of *EPA1* promoter in the different combinations of deletions using a growth plate assay (Figure 10). We observed the same extent of growth on the SC-ura plates in all deletions of *cis*-acting elements in combination with the mutants of yKu proteins (*HDF1* and *HDF2* encoding yKu70 and yKu80, respectively) (Figure 10, line 5 to 12). This result reinforces the conclusion that the NE requires the yKu proteins to exert repression of P_{EPA1} since the presence or absence of the NE has no effect on *hdf1*Δ or *hdf2*Δ strains. The

subtle effect of Sil2126 in the activity of *EPA1* promoter is masked by the regulation exerted by the NE, which in turn depends on yKu proteins.

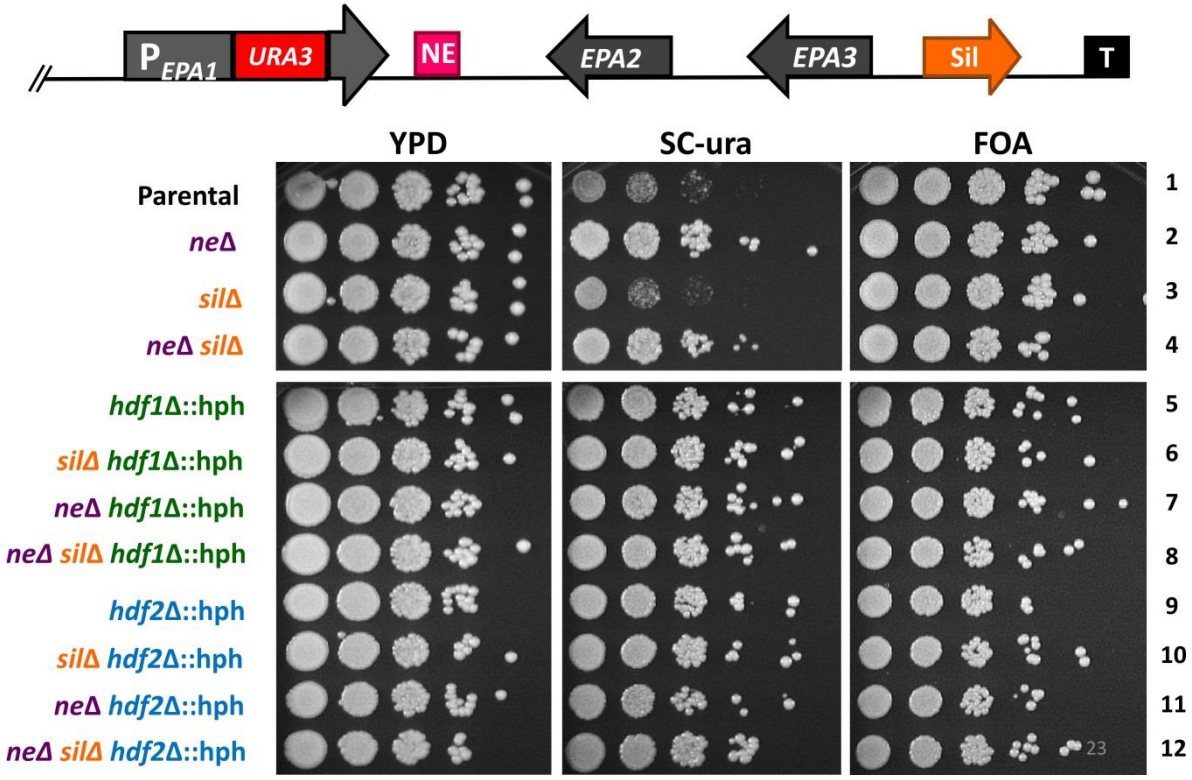

Figure 10. The yKu proteins are required for the negative effect by the NE on the *EPA1* promoter. (**Top**) Schematic representation of the *URA3* gene under control of *EPA1* promoter in the Chr E_{-R}. (**Bottom**) Assessment of the silencing level of the *URA3* reporter in the absence of *cis*-acting elements and/or yKu proteins. The growth plate assay was done as described in Figure 8.

6.1.2. Activity of *EPA1* promoter using *GFP* as a reporter gene in the absence of *cis*-acting elements

Because we tested the activity of *EPA1* promoter using the *URA3* reporter with a qualitative assay, we decided to test the activity of *EPA1* promoter using *GFP* as a reporter and determined the activity by fluorescence activated cell sorting (FACS). We used two control strains, BG198 (P_{EPA1}::*GFP*-NE) and BG201 (P_{EPA1}::*GFP*::pYIplac211-NE), in this last strain the NE is moved away from *EPA1* promoter by 3.7 kb and as a consequence, GFP reporter activity remains high (Gallegos-García *et al.* 2012) (Figure 11, purple and blue line). We generated a different strain containing a 6 kb insertion between the 3'UTR_{EPA1} (300 bp from

TAA of *EPA1*) and the NE. We found a similar induction pattern of GFP in the strains with the 6 kb and the 3.7 kb insertions (Figure 11, compare the blue line with the orange line). We wondered whether Sil2126 has an effect on the *EPA1* expression when the NE is moved away from *EPA1*. We observed that the presence or absence of Sil2126 does not change the induction pattern of GFP (Figure 11, compare the pink with the blue line, and the brown with the orange line).

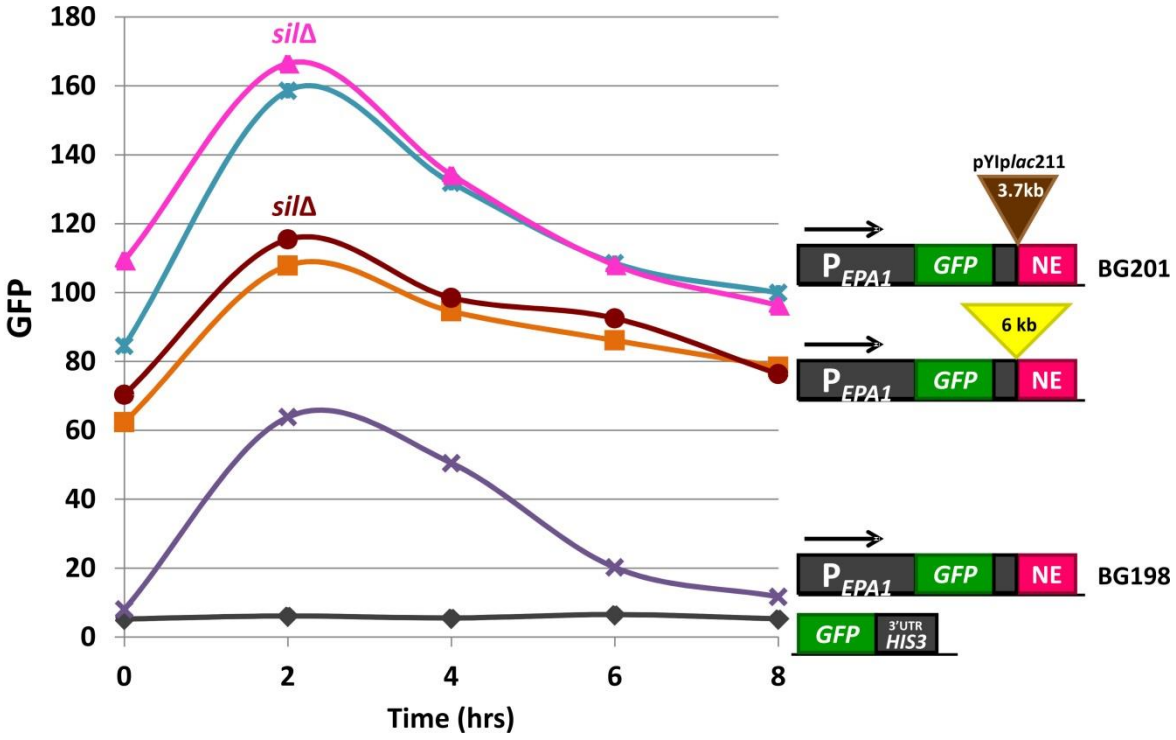

Figure 11. Activity of *EPA1* promoter measured by FACS. A schematic representation of the genotype for each strain is shown to the right. GFP was used as a reporter. Strains were grown in SC with or without uracil for 48 hrs, then we diluted the cells (1:500) into fresh media and samples were taken every two hours.

6.2. *EPA6* and *EPA7* are tightly regulated by *cis*-acting elements

As mentioned above, the negative regulation of *EPA1* by the NE is telomere independent and depends on yKu proteins. We have found nine additional copies of this *cis*-acting element in the *C. glabrata* genome, some of them are associated with *EPA* genes (Gallegos-García *et al.* 2012). In particular, we are interested in

the regulation of the best characterized adhesins, *EPA6* and *EPA7*, which are 94% identical to each other and they are both subject to subtelomeric silencing (Castaño *et al.* 2005).

We tested whether the NEs associated to *EPA6* and *EPA7* are functional by measuring the activity of each promoter using transcriptional fusions of two different fragment sizes containing each promoter with YFP cloned into replicative plasmids. Our data show that in the shortest versions of the promoters (P_{EPA6} 975 bp and P_{EPA7} 1767 bp), the NE located in the 3'UTR is active and does not allow the induction of YFP (Figure 12, middle). Instead, in the longest version of *EPA6* promoter (P_{EPA6L} 3075 bp), we do not observe an effect when the NE is present (Figure 12, bottom, left), but we do observe a subtle regulation of the longest version of the *EPA7* promoter (P_{EPA7L} 2552 bp) by its NE (Figure 12, bottom, right). These data indicate that the NEs adjacent to *EPA6* and *EPA7* are functional and its repression mechanism is telomere independent. These results illustrate another example of the tight regulation that the subtelomeric adhesins are subjected to.

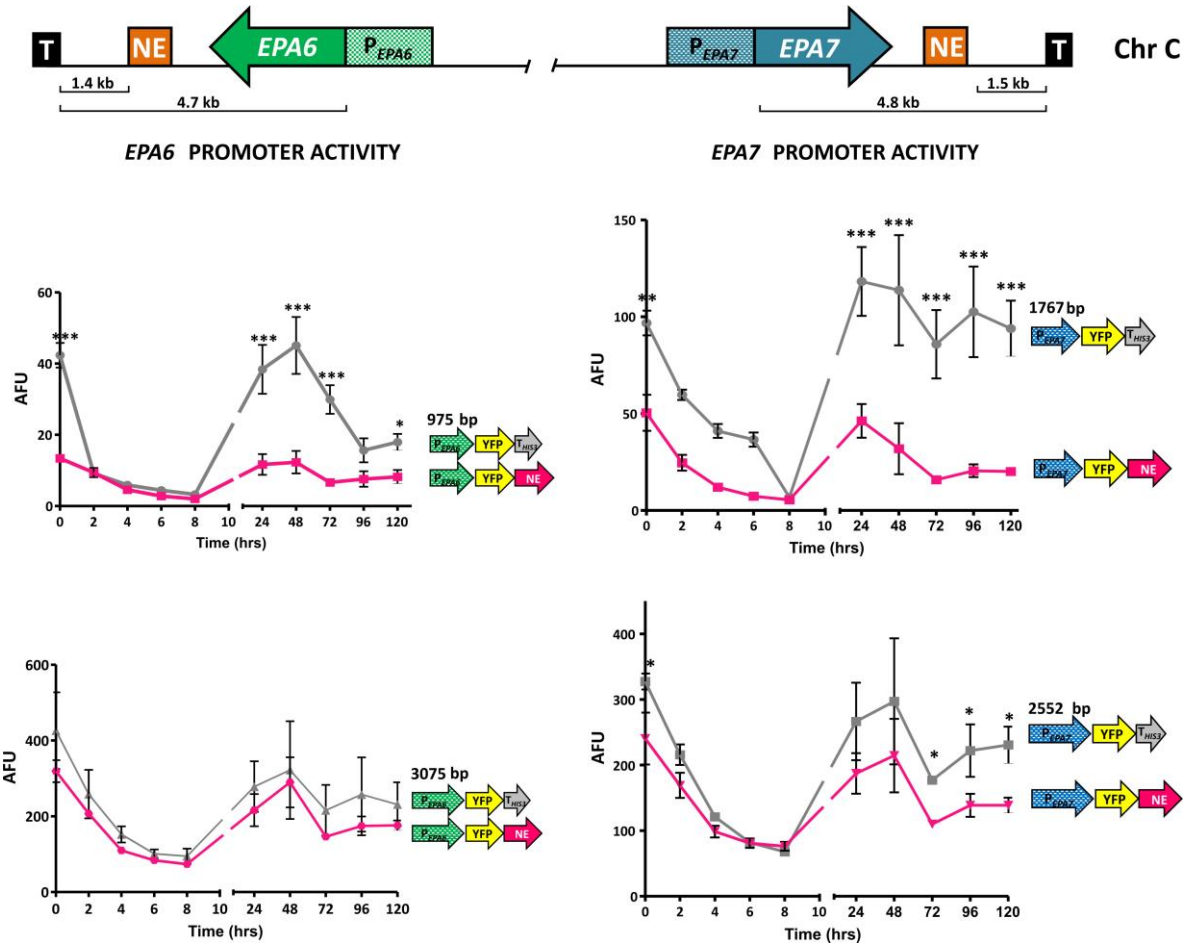

Figure 12. Activity of *EPA6* and *EPA7* promoters measured by FACS. (**Top**) Map of the ends of the chromosome C where *EPA6* and *EPA7* are located. The relevant distances are indicated. (**Middle and bottom**) Measurement of the *EPA6* promoter activity (left) and *EPA7* promoter activity (right) using YFP as reporter. All the constructs are in plasmids and they are indicated in each graph. The protocol was done as described in Figure 10. AFU: Arbitrary fluorescence units.

6.3. Rap1-Flag fusion protein is compromised for silencing activity of some Sil@-32kb deletions

In order to determine the functionality of the epitope-tagged version of Rap1 at the C-terminus, we tested the silencing level of the *URA3* reporter that is part of Sil@-32kb insertion, in a growth plate assay in different media. These experiments were done in the absence of the original copy of Sil2126 (*sil*Δ). First, we tested the silencing level of the full length and functional Sil2126 in the parental strain

containing Rap1-Flag. We observed that the silencing level decreases slightly in the background where Rap1 is tagged (Figure 13, compare line 2 with line1), it is possible that the epitope at the C-terminus interferes slightly with its silencing activity. We then decided to determine the silencing activity of the different deletions of Sil2126 in the Rap1-Flag tagged strain. We found that the deletion of the first 262 bp (*sil* 1-262Δ), displayed an increased level of silencing in the strain containing Rap1-Flag compared to the untagged version, as judged by growth on 5-FOA, and even the size of the colonies on SC-ura is smaller (Figure 13, compare line 4 with line 2). However, the silencing level in the rest of the deletions in Sil2126 does not change in the strain carrying the epitope tagged Rap1-Flag (Figure 13, line 5 to line 8). This data suggests that the silencing activity of Rap1-Flag is somewhat modified, but only in one of the versions of Sil where we observed a higher level of silencing than the previously observed data reported by Juárez-Reyes *et al.* (2012).

Since we observed that only the deletion of the first 262 bp had a different phenotype in the Rap1-Flag strain, we decided to repeat the growth assay including the parental and the previously reported strains. All strains were harvested at the same time and spotted on the same plates. We found that the results we obtained with the *sil* 1-262Δ Rap1-Flag strain were reproducible: increased silencing in this strain compared to a Rap1 background or in the presence of Sil2126 (Figure 14, compare line 5 and 6 with line 4 and line 5 and 6 with line 2). In addition, we tested the Rap1-Flag::*NAT* strain, in which we saw the unaffected silencing level, because in this background the mRNA has a higher stability given by 3'UTR$_{CTA1}$ present in the construct (Figure 14, compare line 3 with 4).

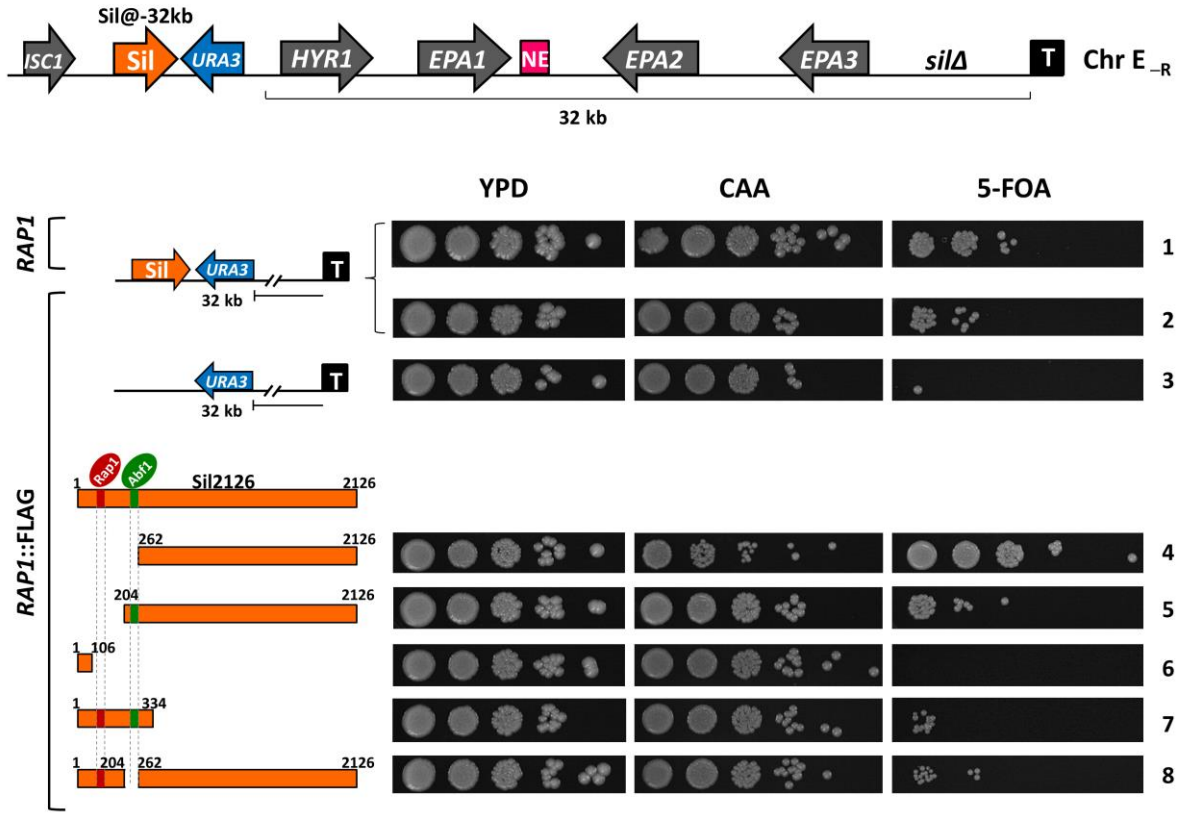

Figure 13. Assessment of silencing activity in Sil@-32kb deletions. (**Top**) Map of the Chr E_{-R} with the insertion of both Sil2126 and *URA3* reporter at 32 kb from the telomere in a *sil*Δ background. (**Bottom**) Plate growth assay for testing silencing activity of the Sil@-32kb deletions in the Rap1-Flag background. The genotype of each strain is indicated to the left. Cells were spotted in the indicated media as described in Figure 8.

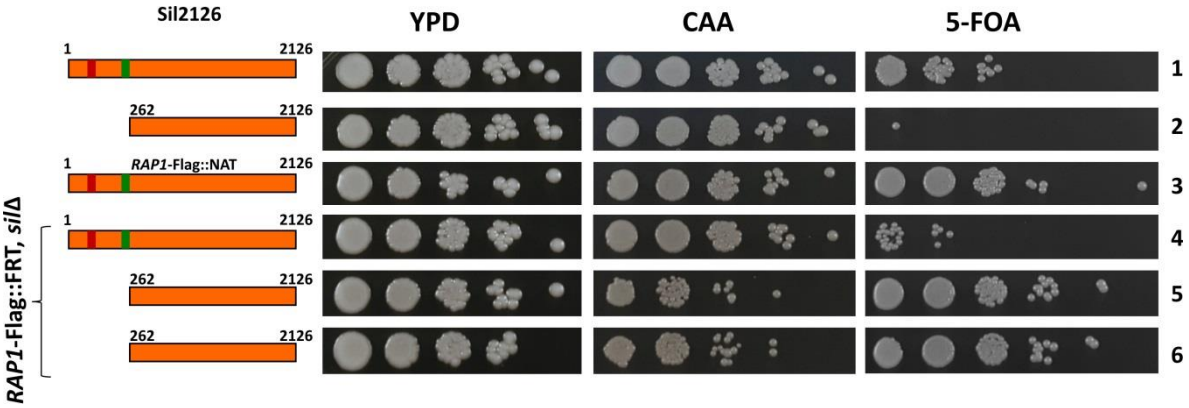

Figure 14. Assessment of the silencing level in different backgrounds. Sil2126 is integrated 32 kb from the telomere adjacent to the *URA3* reporter (not shown). The genotype of the each strain is indicated to the left. Lines 5 and 6 are two independent colonies from the same integration.

6.4. Strains carrying tagged versions of both Rap1 and Abf1 result in loss of silencing

Given that we already know that Rap1 and Abf1 are required for Sil@-32kb activity, we are interested in testing the interaction of these proteins with each other. We constructed a strain with both proteins tagged, each one with a different epitope. *RAP1* was tagged at the C-terminal end with Flag and integrated at its native chromosomal location. An extra copy of *ABF1* was tagged at the N-terminal end and provided on a plasmid under the regulation of *MT1* promoter, inducible with copper (Figure 15, top). In order to evaluate the functionality of silencing of these tagged proteins, we performed a spot assay with both Sil@-32 kb and *sil*Δ. We found that the silencing is abrogated when both of these proteins are tagged in the same background (Figure 15, compare line 2 and 4 with line 5). This could reflect and additive effect due to two partly functional silencing proteins.

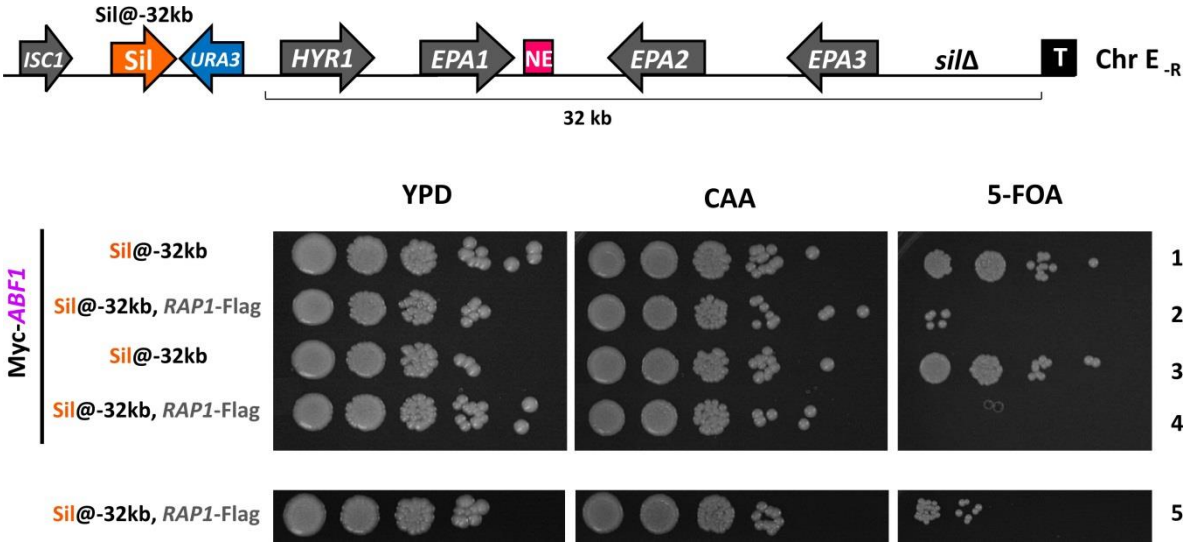

Figure 15. Assessment of silencing activity in strains carrying tagged versions of Rap1 and Abf1. Rap1 and Abf1 were tagged in a Sil@-32kb and *sil*Δ background indicated at the top. The genotype for each strain is indicated to the left. The biological duplicates (lines 1 and 3 and lines 2 and 4) are shown in the plate growth assay.

6.5. Analysis of silencing by spot assay of strains used in 3C assay

From the 3C experiments described in the paper, we found an interaction between Sil@-32kb and *EPA1-EPA2* intergenic region (Genetics' paper, Figure 7A). We also tested whether this interaction depends on the silencing proteins. To answer this question, we constructed a strain carrying an allele deficient in silencing, *rap1-21* in the strain containing Sil@-32kb and *sil*Δ. We also generated a similar strain but carrying a deletion in *SIR3* (*sir3*Δ) in the Sil@-32kb, *sil*Δ background. As expected, silencing of the reporter @-32kb is lost in the silencing mutants (Figure 16, compare line 3 and 5 with line 1).

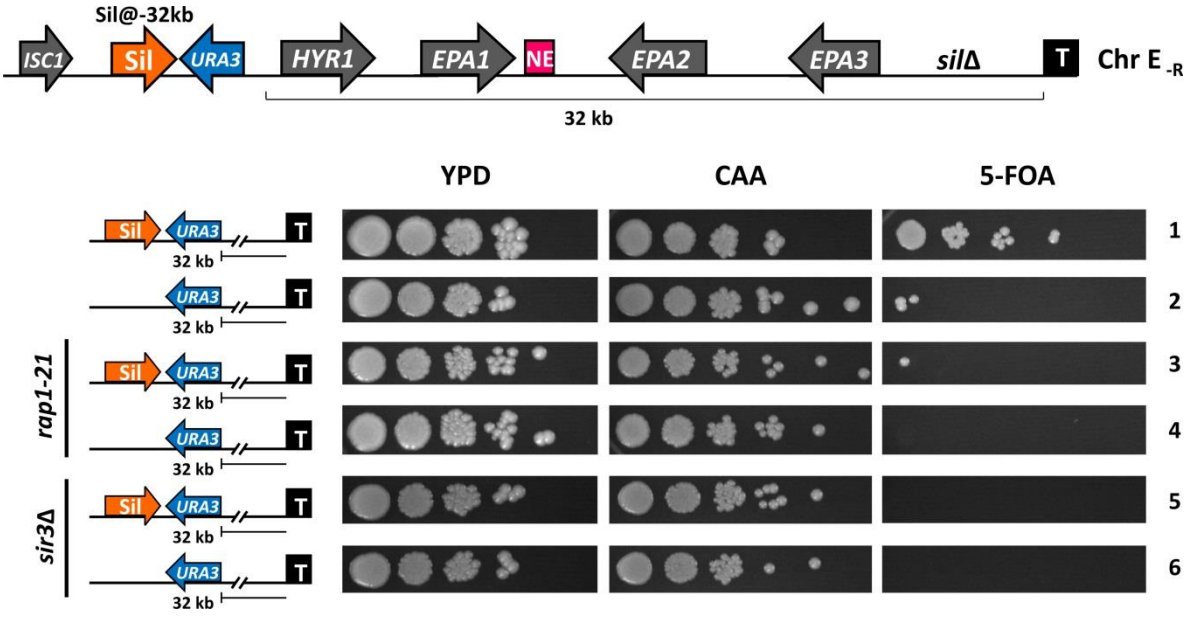

Figure 16. Assessment of Sil2126 activity in silencing mutants (*rap1-21* and *sir3*Δ alleles). (**Top**) Map of the Chr E$_{-R}$ of the parental strain analyzed indicating its genotype (Sil@-32kb and *sil*Δ). (**Bottom**) Plate growth assay of the different strains indicated to the left. This assay was done as described in Figure 8.

6.6. The interaction between Sil2126 and *EPA2-EPA3* intergenic region is not dependent on silencing proteins Rap1 and Sir3

We described the interaction between Sil2126 located in its original position with the *EPA2-EPA3* intergenic region (Figure 17 pink line, and Genetics' paper, Figure 7B). We then decided to analyze whether this interaction depends on silencing

proteins, we tested two strains, the strain carrying the *rap1-21* allele, and the *sir3*Δ containing strain, both proteins have an important role in subtelomeric silencing.

We designed the assay with the anchor primer (Anchor_H) and the Taqman probe (probe_H) aligning in Sil2126 in its original location (Figure 17, bottom). The crosslinking frequencies in a 3C assay showed that the strains where there is no silencing display a similar behavior to the wt strain (Figure 17). The *rap1-21* strain has crosslinking frequencies even higher than the wt (Figure 17, compare red line with pink line). In the three strains tested, we observed that Sil2126 interacts with the *EPA2-EPA3* intergenic region even when there is no silencing (*rap1-21* and *sir3*Δ strains).

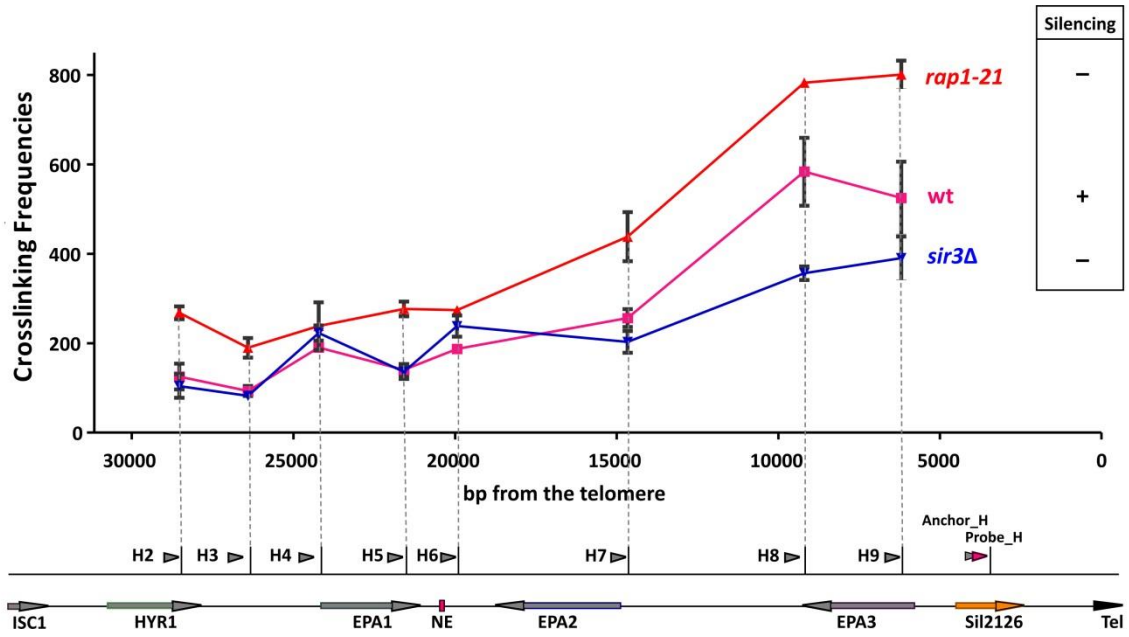

Figure 17. Chromatin interactions close to the telomere are maintained even in the absence of silencing. (**Top**) 3C analysis represented by crosslinking frequencies throughout the Chr E_{-R} with Sil2126 in its original position. The silencing phenotype is indicated to the right as measured by silencing of a *URA3* reporter inserted between *EPA3* and the telomere. The crosslinking frequency indicates the abundance of each ligation product. Each point in the graph represents the crosslinking frequency between each fragment tested and Sil2126 at its original position. (**Bottom**) Schematic representation of the telomere E_{-R} drawn to scale. The positions of the primers and the probe are indicated. The primers are numbered to H2 to H9 and were designed 150 bp before the *Hind*III recognition site.

7. DISCUSSION

Subtelomeric silencing is a regional transcriptional repression that depends on different proteins, as well as several *cis*-acting elements (De Las Peñas *et al.* 2015). In *C. glabrata*, subtelomeric silencing negatively regulates the expression of genes located close to different telomeres, such as the *EPA* genes. These genes encode for adhesins involved in the adherence to host cells and are located within 25 kb from the telomeres. In the right telomere of chromosome E there is a cluster of *EPA* genes, *EPA1*, *EPA2* and *EPA3;* in addition to the regulation by subtelomeric silencing, these genes are also negatively regulated by *cis*-acting elements, such as NE and the protosilencer Sil2126. Besides, these genes are expressed under particular conditions (De las Peñas *et al.* 2003; Rosas-Hernández *et al.* 2008; Juárez-Reyes *et al.* 2012; Gallegos-García *et al.* 2012; Juárez-Cepeda *et al.* 2015).

In this work, we showed that the telomere-specific activity of Sil2126, is probably due to the presence of other *cis*-acting elements in the *EPA2-EPA3* intergenic region. Furthermore, we showed that when the protosilencer is placed 32 kb away from the telomere, a position where normally there is no silencing, it recruits the silencing proteins Rap1, Abf1 and Sir3. We propose that Sil@-32kb can induce the formation of a DNA loop in the Chr E_{-R} by interacting with *EPA1-EPA2* intergenic region probably through protein-protein interactions. When Sil2126 is located in its native position, it can efficiently interact with *EPA2-EPA3* intergenic region, the same region required for Sil@-32kb activity. These alternative interactions seem to be formed according to the presence of *cis*-acting elements and the proteins recruited to establish the heterochromatin structure (Genetics' paper).

7.1. Sil2126 interacts with intergenic regions in Chr E_{-R} to propagate silencing

We found that Sil@-32kb interacts with *EPA1-EPA2* intergenic region by 3C assay. This interaction depends on the presence of a full length and functional Sil@-32kb as well as on the presence of silencing proteins, such as Rap1 and Sir3. We also determined the Sir3 binding profile in this background (Sil@-32kb) and found that

this protein is bound at Sil@-32kb (Paper Genetics, Figure S5). These data suggest that silencing can be propagated when Sil2126 is ectopically inserted 32 kb away from the telomere. This hypothesis is supported by the repression of *EPA1* promoter when Sil2126 is at -32 kb, at this position the protosilencer can reinforce silencing from the telomere and silence the genes located in between (like *EPA1*, Paper Genetics, Figure 8).

Under native conditions, *i.e*. Sil2126 located between *EPA3* and the telomere, it interacts with *EPA2-EPA3* intergenic region. Probably, when Sil2126 is in its original location, the silencing in this telomere is discontinuous. This is in agreement with the previous data where the silencing level gradually decreases over the 20 kb adjacent to the telomere, as measured by silencing of a reporter inserted at increasing distances from the telomere (De Las Peñas *et al.* 2003). Silencing in this subtelomeric region can be detected up to the 3'UTR region of *EPA1*. However, the *EPA1* promoter is also subject to subtelomeric silencing (Gallegos-García *et al.* 2012).

The silencing mechanism of the protosilencer is by recruiting silencing proteins, like Rap1 and Abf1; which in turn can recruit other proteins, such as the SIR complex. This allows the establishment of subtelomeric silencing probably through the formation of a chromatin superstructure that allows propagation of the silent chromatin. A higher-order structure for silenced chromatin has been previously described (Dekker 2002; Valenzuela *et al.* 2008; Miele *et al.* 2009). In *S. cerevisiae*, the flanking silencers of *HMR* locus physically interact with each other to form a loop that depends on the SIR complex (Valenzuela *et al.* 2008; Thurtle and Rine 2014). Furthermore, it has been shown that the telomere can fold (de Bruin *et al.* 2001) helping in this way the formation of these structures. The 3C method has been used to describe interactions between distant *cis*-elements. For example interactions between promoter-enhancer, enhancer-enhancer, and enhancer-boundary in the mouse globin (Tolhuis *et al.* 2002; Liu and Garrard 2005), and *Hox* genes (Noordermeer *et al.* 2014); as well as the mechanisms of

repression in *Drosophila* (Chopra *et al.* 2012). These studies have allowed gaining insights on the organization of chromatin and its role in the gene regulation.

7.2. The interaction between Sil2126 and *EPA2-EPA3* intergenic region is independent of silencing proteins

We found that Sil2126 in its original position clearly interacts with *EPA2-EPA3* intergenic region (Figure 17). Interestingly, this interaction does not depend on at least two silencing proteins (Figure 17). We tested the *rap1-21* and *sir3*Δ mutants where there is no detectable silencing (measured by silencing of the *URA3* reporter inserted at different subtelomeric regions) and we observed that the crosslinking frequencies remain at high levels, indicating the formation of a chromatin loop. This might suggest that the interactions between elements very close to the telomere may not need to be in a heterochromatin state induced by these silencing proteins. This could be related to the degree of peripheral anchoring of the subtelomeric regions, or the contacts with the nuclear structure such as the lamina. This observation was also found in another study using 3C data, where the interaction between *HMR* and the telomere is not reduced upon deletion of *SIR2* and *SIR3* (Miele *et al.* 2009).

7.3. Sil2126 in its native position does not regulate the *EPA1* expression

We have previously shown that the negatively regulation of *EPA1* expression by the NE is independent of the silencing spreading from the telomere (Gallegos-García *et al.* 2012). In this work, we found that in the double mutant (*sil*Δ *ne*Δ), the *EPA1* expression assessed by expression of the *URA3* reporter fused to the P_{EPA1} was slightly decreased compared to the *ne*Δ single mutant. This subtle effect may be due to the fact that in the double mutant, the P_{EPA1} is 1 kb closer to the telomere. At this telomere, we have shown that silencing is stronger when the reporter gene is closer to the telomere (De las Peñas *et al.* 2003), in a similar way to what is observed in *S. cerevisiae* (Gottschling *et al.* 1990; Renauld *et al.* 1993). Another possibility is that the chromatin conformation is likely to be modified in the absence of the *cis*-acting elements. This is the case in *S. cerevisiae* where large

differences in silencing level are observed when the X and Y' elements from some telomeres are deleted (Fourel *et al.* 1999).

7.4. Chromatin 3-D conformations are dynamic

The 3C method is widely used to document proximity between regions of chromatin. It takes advantage of the formaldehyde fixation, which creates a genome-wide snapshot of interactions between any pair of genomic loci (Dekker 2006).

We described different interactions between Sil2126 with intergenic regions at the Chr E_{-R}. In particular, Sil2126 in its original position can interact with *EPA2-EPA3* intergenic region. Also, it is possible that Sil2126 can interact with other *cis*-elements located in other intergenic regions (*EPA1-EPA2* or *HYR1-EPA1*). These interactions were detected only as weak interactions, probably because they were only observed after prolonged cross-linking.

Furthermore, 3C is performed on large numbers of pooled cells, and thus it yields an average of interactions across all cells that might not take place simultaneously in one cell. Therefore, transient and dynamic interactions might be underrepresented (Dean 2011). In addition, some loops can change depending on the growth phase or the stage of development (Lanzuolo *et al.* 2007; Rutledge *et al.* 2015). Thus, the spatial organization of the genome is highly variable between cells, two nuclei will not display the exact same set of interactions in a particular time point (Gibcus and Dekker 2013).

8. CONCLUSIONS

The right telomere of chromosome E is a unique telomere where three *EPA* genes are located. It contains large intergenic regions between these *EPA* genes where several regulatory elements reside. This telomere is a good model to gain insight on the negative regulation by subtelomeric silencing of genes involved in virulence factors.

Subtelomeric silencing involves several layers of regulation; silencing proteins, *cis*-acting elements and chromatin structure. The combination of all these elements results in regulatory networks for which interactions between proteins and between *cis*-elements are required. In the Chr E_{-R}, the protosilencer Sil2126 is required to propagate silencing, which is achieved by recruiting silencing proteins such as Rap1, Abf1 and SIR complex. This element can modify the chromatin structure by interacting with different intergenic regions depending on where it is located.

8.1. Particular conclusions

- Sil2126 requires its telomere context probably because of the presence of *cis*-acting elements in the *EPA2-EPA3* intergenic region.
- The first binding sites for Rap1 and Abf1 (at the 5' end of the element) are functional and are required for Sil@-32kb activity.
- Sil2126 can recruit Rap1, Abf1 and Sir3 in its original position and at a distant position from the telomere in an environment where there is not silencing (-32 kb from the telomere).
- The binding profile of Rap1 and Abf1 is modified depending on the presence of the different *cis*-acting elements.
- Sil2126 inserted 32 kb away from the telomere interacts with the *EPA1-EPA2* intergenic region forming a loop to propagate silencing. This interaction depends on silencing proteins.
- Sil2126 in its original position interacts with *EPA2-EPA3* intergenic region and this interaction is independent on silencing proteins.

- Sil2126 inserted 32 kb away from the telomere, but not in its original position, negatively regulates *EPA1* expression.

9. PERSPECTIVES

- Characterize the putative *cis*-acting elements located in the *EPA2-EPA3* intergenic region required for Sil@-32kb activity. This large intergenic region contains 5.6 kb. We will generate systematic deletions and we will test the Sil@-32kb activity in a ***sil***Δ background.
- Determine the Sir3 binding profile in the backgrounds where there is no silencing. We found that Rap1 and Abf1 are bound at Sil@-32kb where there is no silencing, we will test whether Sir3 is bound too.
- Measure the level of adherence to HeLa cells in the backgrounds where *EPA1* is repressed by Sil@-32kb.
- Determine the binding profile of Rap1, Abf1 and Sir3 proteins in other telomeres by ChIP assay.
- Evaluate the activity of the additional copies of Sil2126 in the other telomeres in *C. glabrata*. There are two additional copies of Sil2126, one in the Chr A and a small fragment of Sil at the Chr I. We will place these copies in their respective telomeres at a position where there is no silencing and we will test silencing of the reporter.
- Characterize the 3' end of Sil2126. There are several putative binding sites for Rap1 and Abf1 in the 3' end of Sil216. We will test the binding profile of these proteins by ChIP-qPCR assay.
- Determine whether the interactions found require the nuclear periphery attachment. We will tag the two fragments involved in the interaction and we will capture 3D images by microscopy.
- Elucidate the chromatin conformation of the subtelomeres in the absence of silencing. First, we will test mutants of proteins involved in chromatin remodeling or envelope anchor and we will perform a 3C assay.

10. REFERENCES

Allshire R. C., Ekwall K., 2015 Epigenetics regulation of chromatin states in *Schizosaccharomyces pombe*. Cold Spring Harb Perspect. Biol. **7**: 1–25.

Ausubel F. M., Brent R., Kingston R. E., Moore D. D., Seidman J. G., Smith J. A., Struhl K. (Eds.), 2001 *Current Protocols in Molecular Biology*. John Wiley & Sons, Inc., Hoboken, NJ, USA.

Barton A. B., Pekosz M. R., Kurvathi R. S., Kaback D. B., 2008 Meiotic recombination at the ends of chromosomes in Saccharomyces cerevisiae. Genetics **179**: 1221–1235.

Baur J. A., Zou Y., Shay J. W., Wright W. E., 2001 Telomere position effect in human cells. Science **292**: 2075–7.

Belton J.-M., Dekker J., 2015a Randomized ligation control for chromosome conformation capture. Cold Spring Harb. Protoc. **2015**: 587–592.

Belton J.-M., Dekker J., 2015b Chromosome Conformation Capture (3C) in Budding Yeast. Cold Spring Harb. Protoc. **2015**: 580–6.

Boscheron C., Maillet L., Marcand S., Tsai-Pflugfelder M., Gasser S. M., Gilson E., 1996 Cooperation at a distance between silencers and proto-silencers at the yeast HML locus. EMBO J. **15**: 2184–95.

Brachmann CB, Sherman JM, Devine SE, Cameron EE, Pillus L, Boeke JD, 1995 The SIR2 gene family, conserved \nfrom bacteria to humans, functions in \nsilencing, cell cycle progiression, and \nchromosome stability . Genes Dev. **9**: 2888–2902.

Brand A. H., Micklem G., Nasmyth K., 1987 A yeast silencer contains sequences that can promote autonomous plasmid replication and transcriptional activation. Cell **51**: 709–719.

Brown C. a, Murray A. W., Verstrepen K. J., 2010 Rapid expansion and functional divergence of subtelomeric gene families in yeasts. Curr. Biol. **20**: 895–903.

Bruin D. de, Zaman Z., Liberatore R. a, Ptashne M., 2001 Telomere looping permits gene activation by a downstream UAS in yeast. Nature **409**: 109–113.

Bühler M., Gasser S. M., 2009 Silent chromatin at the middle and ends: lessons from yeasts. EMBO

J. **28**: 2149–61.

Castanedo-Ibarra L., Castaño I., 2015 Análisis de la interacción entre las proteínas Abf1 y Rap1 de Candida glabrata con los elementos de regulación en cis del telómero E derecho.

Castano I., Kaur R., Pan S., Cregg R., Penas A. D. Las, Guo N., Biery M. C., Craig N. L., Cormack B. P., 2003 Tn7-based genome-wide random insertional mutagenesis of Candida glabrata. Genome Res. **13**: 905–15.

Castaño I., Pan S.-J., Zupancic M., Hennequin C., Dujon B., Cormack B. P., 2005 Telomere length control and transcriptional regulation of subtelomeric adhesins in Candida glabrata. Mol. Microbiol. **55**: 1246–58.

Chen Y., Rai R., Zhou Z.-R., Kanoh J., Ribeyre C., Yang Y., Zheng H., Damay P., Wang F., Tsujii H., Hiraoka Y., Shore D., Hu H.-Y., Chang S., Lei M., 2011 A conserved motif within RAP1 has diversified roles in telomere protection and regulation in different organisms. Nat. Struct. Mol. Biol. **18**: 213–221.

Cheng T. H., Gartenberg M. R., 2000 Yeast heterochromatin is a dynamic structure that requires silencers continuously. Genes Dev. **14**: 452–463.

Cho G., Kim J., Rho H. M., Jung G., 1995 Structure-function analysis of the DNA binding domain of. Nucleic Acids Res. **23**: 2980–2987.

Chopra V. S., Kong N., Levine M., 2012 Transcriptional repression via antilooping in the Drosophila embryo. Proc. Natl. Acad. Sci. **109**: 9460–9464.

Conrad M. N., Wright J. H., Wolf a J., Zakian V. a, 1990 RAP1 protein interacts with yeast telomeres in vivo: overproduction alters telomere structure and decreases chromosome stability. Cell **63**: 739–50.

Cormack B. P., Ghori N., Falkow S., 1999 An adhesin of the yeast pathogen Candida glabrata mediating adherence to human epithelial cells. Science **285**: 578–82.

Cubizolles F., Martino F., Perrod S., Gasser S. M., 2006 A homotrimer-heterotrimer switch in Sir2 structure differentiates rDNA and telomeric silencing. Mol. Cell **21**: 825–836.

De Las Peñas A., Pan S., Castaño I., Alder J., Cregg R., Cormack B. P., 2003 Virulence-related surface

glycoproteins in the yeast pathogen Candida glabrata are encoded in subtelomeric clusters and subject to RAP1- and SIR-dependent transcriptional silencing. Genes Dev. **17**: 2245–2258.

De Las Peñas A., Juárez-Cepeda J., López-Fuentes E., Briones-Martín-del-Campo M., Gutiérrez-Escobedo G., Castaño I., 2015 Local and regional chromatin silencing in Candida glabrata: consequences for adhesion and the response to stress (M Bolotin-Fukuhara, Ed.). FEMS Yeast Res. **15**.

Dean A., 2011 In the loop: Long range chromatin interactions and gene regulation. Brief. Funct. Genomics **10**: 3–10.

Dekker J., 2002 Capturing Chromosome Conformation. Science (80-.). **295**: 1306–1311.

Dekker J., 2006 The three “C” s of chromosome conformation capture: controls, controls, controls. Nat. Methods **3**: 17–21.

Domergue R., Castaño I., Las Peñas A. De, Zupancic M., Lockatell V., Hebel J. R., Johnson D., Cormack B. P., 2005 Nicotinic acid limitation regulates silencing of Candida adhesins during UTI. Science **308**: 866–70.

Donze D., Adams C. R., Rine J., Kamakaka R. T., 1999 The boundaries of the silenced HMR doamin in Saccharomyces cerevisiae. Genes Dev. **13**: 698–708.

Donze D., Kamakaka R. T., 2001 RNA polymerase III and RNA polymerase II promoter complexes are heterochromatin barriers in <i>Saccharomyces cerevisiae. EMBO J. **20**: 520–31.

Dorer D. R., Henikoff S., 1994 Expansions of transgene repeats cause heterochromatin formation and gene silencing in Drosophila. Cell **77**: 993–1002.

Dunn B., Richter C., Kvitek D. J., Pugh T., Sherlock G., 2012 Analysis of the Saccharomyces cerevisiae Pan genome reveals a pool of copy number variants distributed in diverse yeast strains from differing industrial enviroments.pdf. Genome Res. **22**: 908–924.

Fabre E., Muller H., Therizols P., Lafontaine I., Dujon B., Fairhead C., 2005 Comparative genomics in hemiascomycete yeasts: Evolution of sex, silencing, and subtelomeres. Mol. Biol. Evol. **22**: 856–873.

Feldmann E. A., Bona P. De, Galletto R., 2015 The wrapping loop and Rap1 C-terminal (RCT)

domain of yeast Rap1 modulate access to different DNA binding modes. J. Biol. Chem. **290**: 11455–11466.

Fisher T. S., Zakian V. A., 2005 Ku: A multifunctional protein involved in telomere maintenance. DNA Repair (Amst). **4**: 1215–1226.

Fourel G., Revardel E., Catherine Elaine K., Gilson E., 1999 Cohabitation of insulators and silencing elements in yeast subtelomeric regions. Embo J **18**: 2522–2537.

Fourel G., Lebrun E., Gilson E., 2002 Protosilencers as building blocks for heterochromatin. Bioessays **24**: 828–35.

Gallegos-García V., Pan S.-J., Juárez-Cepeda J., Ramírez-Zavaleta C. Y., Martin-del-Campo M. B., Martínez-Jiménez V., Castaño I., Cormack B., Las Peñas A. De, 2012 A novel downstream regulatory element cooperates with the silencing machinery to repress EPA1 expression in Candida glabrata. Genetics **190**: 1285–97.

Gardner M. J., Hall N., Fung E., White O., Berriman M., Richard W., Carlton J. M., Pain A., Nelson K. E., Bowman S., Ian T., James K., Eisen J. A., Rutherford K., Salzberg S. L., Kyes S., Chan M., Nene V., Shallom S. J., Peterson J., Angiuoli S., Pertea M., Allen J., Haft D., Mather M. W., Vaidya A. B., Martin D. M. A., Alan H., 2002a Genome sequence of the human malaria parasite Plasmodium falciparum. Nature **419**: 3–9.

Gardner M. J., Hall N., Fung E., White O., Berriman M., Hyman R. W., Carlton J. M., Pain A., Nelson K. E., Bowman S., Paulsen I. T., James K., Eisen J. A., Rutherford K., Salzberg S. L., Craig A., Kyes S., Chan M.-S., Nene V., Shallom S. J., Suh B., Peterson J., Angiuoli S., Pertea M., Allen J., Selengut J., Haft D., Mather M. W., Vaidya A. B., Martin D. M. A., Fairlamb A. H., Fraunholz M. J., Roos D. S., Ralph S. A., McFadden G. I., Cummings L. M., Subramanian G. M., Mungall C., Venter J. C., Carucci D. J., Hoffman S. L., Newbold C., Davis R. W., Fraser C. M., Barrell B., 2002b Genome sequence of the human malaria parasite Plasmodium falciparum. Nature **419**: 498–511.

Gartenberg M. R., Smith J. S., 2016 The nuts and bolts of transcriptionally silent chromatin in Saccharomyces cerevisiae. Genetics **203**: 1563–1599.

Gibcus J. H., Dekker J., 2013 The Hierarchy of the 3D Genome. Mol. Cell **49**: 773–782.

Gilson E., Géli V., 2007 How telomeres are replicated. Nat. Rev. Mol. Cell Biol. **8**: 825–38.

Gotta M., Laroche T., Formenton A., Maillet L., Scherthan H., Gasser S. M., 1996 The clustering of telomeres and colocalization with Rap1, Sir3, and Sir4 proteins in wild-type Saccharomyces cerevisiae. J. Cell Biol. **134**: 1349–1363.

Gottschling D. E., Aparicio O. M., Billington B. L., Zakian V. A., 1990 Position Effect at S . cerevisiae Telomeres : Reversible Repression of Pol II Transcription. Cell **63**: 751–762.

Griffith J. D., Comeau L., Rosenfield S., Stansel R. M., Bianchi A., Moss H., Lange T. De, 1999 Mammalian telomeres end in a large duplex loop. Cell **97**: 503–514.

Grunstein M., Gasser S. M., 2013 Epigenetics in Saccharomyces cerevisiae. Cold Spring Harb. Perspect. Biol. **5**.

Hagège H., Klous P., Braem C., Splinter E., Dekker J., Cathala G., Laat W. de, Forné T., 2007 Quantitative analysis of chromosome conformation capture assays (3C-qPCR). Nat. Protoc. **2**: 1722–1733.

Hardy C., Sussel L., Shore D., 1992 A RAP 1-interacting protein involved in transcriptional silencing and telomere length regulation. Genes Dev **6**: 801–814.

Haw R., Yarragudi a D., Uemura H., 2001 Isolation of a Candida glabrata homologue of RAP1, a regulator of transcription and telomere function in Saccharomyces cerevisiae. Yeast **18**: 1277–84.

Horn D., Cross A. M., 1995 A Developmentally Regulated Position Effect at a Telomeric Locus in Trypanosoma brucei. Cell **83**: 555–561.

Imai S., Armstrong C. M., Kaeberlein M., Guarente L., 2000 Transcriptional silencing and longevity protein Sir2 is an NAD-dependent histone deacetylase. Nature **403**: 795–800.

Iraqui I., Garcia-Sanchez S., Aubert S., Dromer F., Ghigo J. M., D'Enfert C., Janbon G., 2005 The Yak1p kinase controls expression of adhesins and biofilm formation in Candida glabrata in a Sir4p-dependent pathway. Mol. Microbiol. **55**: 1259–1271.

Juárez-Cepeda J., Orta-Zavalza E., Cañas-Villamar I., Arreola-Gómez J., Pérez-Cornejo G. P., Hernández-Carballo C. Y., Gutiérrez-Escobedo G., Castaño I., Las Peñas A. De, 2015 The EPA2

adhesin encoding gene is responsive to oxidative stress in the opportunistic fungal pathogen Candida glabrata. Curr. Genet. **61**: 529–544.

Juárez-Reyes A., Ramírez-Zavaleta C. Y., Medina-Sánchez L., Las Peñas A. De, Castaño I., 2012 A protosilencer of subtelomeric gene expression in Candida glabrata with unique properties. Genetics **190**: 101–11.

Keely S. P., Renauld H., Wakefield A. E., Cushion M. T., Smulian A. G., Fosker N., Fraser A., Harris D., Murphy L., Price C., Quail M. A., Seeger K., Sharp S., Tindal C. J., Warren T., Zuiderwijk E., Barrell B. G., Stringer J. R., Hall N., 2005 Gene Arrays at Pneumocystis carinii Telomeres. Genetics **170**: 1589–1600.

Klevay M. J., Horn D. L., Neofytos D., Pfaller M. A., Diekema D. J., PATH Alliance M. B., Edwards J. E., America I. D. S. of, Webster K. M., Neofytos D., Kontoyiannis D. P., 2009 Initial treatment and outcome of Candida glabrata versus Candida albicans bloodstream infection. Diagn. Microbiol. Infect. Dis. **64**: 152–7.

Kraneveld E. a, Soet J. J. de, Deng D. M., Dekker H. L., Koster C. G. de, Klis F. M., Crielaard W., Groot P. W. J. de, 2011 Identification and differential gene expression of adhesin-like wall proteins in Candida glabrata biofilms. Mycopathologia **172**: 415–27.

Kueng S., Oppikofer M., Gasser S. M., 2013 SIR proteins and the assembly of silent chromatin in budding yeast. Annu. Rev. Genet. **47**: 275–306.

Kyrion G., Liu K., Liu C., Lustig A. J., 1993 RAP1 and telomere structure regulate telomere position effects in Saccharomyces cerevisiae. Genes Dev. **7**: 1146–1159.

Lanzuolo C., Roure V., Dekker J., Bantignies F., Orlando V., 2007 Polycomb response elements mediate the formation of chromosome higher-order structures in the bithorax complex. Nat. Cell Biol. **9**: 1167–1174.

Lebrun E., Revardel E., Li R., Gilson E., 2001 Protosilencers in Saccharomyces cerevisiae subtelomeric regions. Genetics **158**: 167–176.

Levis R. W., Ganesan R., Houtchens K., Tolar L. A., Sheen F. miin, 1993 Transposons in place of telomeric repeats at a Drosophila telomere. Cell **75**: 1083–1093.

Li Q., Barkess G., Qian H., 2006 Chromatin looping and the probability of transcription. Trends Genet. **22**: 197–202.

Lieb J. D., Liu X., Botstein D., Brown P. O., 2001 Promoter-specific binding of Rap1 revealed by genome-wide maps of protein-DNA association. Nat. Genet. **28**: 327–334.

Liu C., Mao X., Lustig A. J., 1994 Mutational analysis defines a C-terminal tail domain of RAP1 essential for telomeric silencing in Saccharomyces cerevisiae. Genetics **138**: 1025–1040.

Liu Z., Garrard W. T., 2005 Long-Range Interactions between Three Transcriptional Enhancers, Active V Gene Promoters, and a 3J Boundary Sequence Spanning 46 Kilobases. Mol. Cell. Biol. **25**: 3220–3231.

Louis E. J., 1995 The chromosome ends of Saccharomyces cerevisiae. Yeast **11**: 1553–1573.

Luo K., Vega-Palas M. a, Grunstein M., 2002 Rap1-Sir4 binding independent of other Sir, yKu, or histone interactions initiates the assembly of telomeric heterochromatin in yeast. Genes Dev. **16**: 1528–39.

Marcand S., Buck S. W., Moretti P., Gilson ??ric, Shore D., 1996 Silencing of genes at nontelomeric sites in yeast is controlled by sequestration of silencing factors at telomeres by Rap1 protein. Genes Dev. **10**: 1297–1309.

Mefford H. C., Trask B. J., 2002 The complex structure and dynamic evolution of human subtelomeres. Nat. Rev. Genet. **3**: 91–102.

Miele A., Bystricky K., Dekker J., 2009 Yeast silent mating type loci form heterochromatic clusters through silencer protein-dependent long-range interactions. PLoS Genet. **5**: e1000478.

Miyake T., Loch C. M., Li R., 2002 Identification of a Multifunctional Domain in Autonomously Replicating Sequence-Binding Factor 1 Required for Transcriptional Activation , DNA Replication , and Gene Silencing. Mol. Cell. Biol. **22**: 505–516.

Moretti P., Freeman K., Coodly L., Shore D., 1994 Evidence that a complex of SIR proteins interacts with the silencer and telomere-binding protein RAP1. Genes Dev. **8**: 2257–2269.

Moretti P., Shore D., 2001 Multiple Interactions in Sir Protein Recruitment by Rap1p at Silencers and Telomeres in Yeast. Mol. Cell. Biol. **21**: 8082–8094.

Muñoz-Jordán J. L., Cross G. A. M., Lange T. De, Griffith J. D., 2001 T-Loops At Trypanosome Telomeres. EMBO J. **20**: 579–588.

Murti K. G., Prescott D. M., 1999 Telomeres of polytene chromosomes in a ciliated protozoan terminate in duplex DNA loops. Proc. Natl. Acad. Sci. U. S. A. **96**: 14436–9.

Naumov G. I., Naumova E. S., Korhola M. P., 1995 of Saccharomyces cerevisiae. FEMS Microbiol. Lett. **127**: 41–45.

Naumova E. S., Ivannikova Y. V., Naumov G. I., 2005 Genetic differentiation of the sherry yeasts Saccharomyces cerevisiae. Appl. Biochem. Microbiol. **41**: 578–582.

Nimmo E. R., Cranston G., Allshire R. C., 1994 Telomere-associated chromosome breakage in fission yeast results in variegated expression of adjacent genes. EMBO J **13**: 3801–3811.

Noordermeer D., Leleu M., Schorderet P., Joye E., Chabaud F., Duboule D., 2014 Temporal dynamics and developmental memory of 3D chromatin architecture at Hox gene loci. Elife **2014**: 1–21.

Oppikofer M., Kueng S., Gasser S. M., 2013 SIR-nucleosome interactions: structure-function relationships in yeast silent chromatin. Gene **527**: 10–25.

Orta-Zavalza E., Guerrero-Serrano G., Gutiérrez-Escobedo G., Cañas-Villamar I., Juárez-Cepeda J., Castaño I., Las Peñas A. De, 2013 Local silencing controls the oxidative stress response and the multidrug resistance in Candida glabrata. Mol. Microbiol. **88**: 1135–1148.

Palladino F., Laroche T., Gilson E., Axelrod A., Pillus L., Gasser S. M., 1993 SIR3 and SIR4 proteins are required for the positioning and integrity of yeast telomeres. Cell **75**: 543–555.

Palstra R.-J. T. S., 2009 Close encounters of the 3C kind: long-range chromatin interactions and transcriptional regulation. Brief. Funct. Genomic. Proteomic. **8**: 297–309.

Pfaller M. A., Diekema D. J., 2007 Epidemiology of invasive candidiasis: a persistent public health problem. Clin. Microbiol. Rev. **20**: 133–63.

Pryde F. E., Louis E. J., 1999 Limitations of silencing at native yeast telomeres. EMBO J. **18**: 2538–50.

Randise-Hinchliff C. E., Brickner J. H., 2012 A New Direction for Gene Looping. Dev. Cell **23**: 919–921.

Reed S. H., Akiyama M., Stillman B., Friedberg E. C., 1999 Yeast autonomously replicating sequence binding factor is involved in nucleotide excision repair. Genes Dev. **13**: 3052–3058.

Renauld H., Aparicio O. M., Zierath P. D., Billington B. L., Chhablani S. K., Gottschling D. E., 1993 Silent domains are assembled continuously from the telomere and are defined by promoter distance and strength, and by SIR3 dosage. Genes Dev. **7**: 1133–45.

Robledo-Márquez K., Gutiérrez-Escobedo G., Yáñez-Carrillo P., Vidal-Aguiar Y., Briones-Martín-del-Campo M., Orta-Zavalza E., Las Peñas A. De, Castaño I., 2016 Candida glabrata encodes a longer variant of the mating type (MAT) alpha2 gene in the mating type-like MTL3 locus, which can form homodimers. FEMS Yeast Res. **16**: 1–12.

Roetzer A., Gregori C., Jennings A. M., Quintin J., Ferrandon D., Butler G., Kuchler K., Ammerer G., Schüller C., 2008 Candida glabrata environmental stress response involves Saccharomyces cerevisiae Msn2/4 orthologous transcription factors. Mol. Microbiol. **69**: 603–620.

Rosas-Hernández L. L., Juárez-Reyes A., Arroyo-Helguera O. E., Las Peñas A. De, Pan S.-J., Cormack B. P., Castaño I., 2008 yKu70/yKu80 and Rif1 regulate silencing differentially at telomeres in Candida glabrata. Eukaryot. Cell **7**: 2168–78.

Roy R., Meier B., McAinsh A. D., Feldmann H. M., Jackson S. P., 2004 Separation-of-function Mutants of Yeast Ku80 Reveal a Yku80p-Sir4p Interaction Involved in Telomeric Silencing. J. Biol. Chem. **279**: 86–94.

Rusche L. N., Kirchmaier A. L., Rine J., 2002 Ordered Nucleation and Spreading of Silenced Chromatin in Saccharomyces cerevisiae. Mol. Biol. Cell **13**: 2207–2222.

Rutledge M. T., Russo M., Belton J.-M., Dekker J., Broach J. R., 2015 The yeast genome undergoes significant topological reorganization in quiescence. Nucleic Acids Res. **43**: 8299–313.

Saksouk N., Simboeck E., Déjardin J., 2015 Constitutive heterochromatin formation and transcription in mammals. Epigenetics Chromatin **8**: 3.

Scherf A., Hernandez-Rivas R., Buffet P., Bottius E., Benatar C., Pouvelle B., Gysin J., Lanzer M.,

1998 Antigenic variation in malaria: In situ switching, relaxed and mutually exclusive transcription of var genes during intra-erythrocytic development in Plasmodium falciparum. EMBO J. **17**: 5418–5426.

Strahl-Bolsinger S., Hecht A., Luo K., Grunstein M., 1997 SIR2 and SIR4 interactions differ in core and extended telomeric heterochromatin in yeast. Genes Dev. **11**: 83–93.

Sullivan J. M. O., Tan-wong S. M., Morillon A., Lee B., Coles J., Mellor J., Proudfoot N. J., 2004 Gene loops juxtapose promoters and terminators in yeast. **36**: 1014–1018.

Talbert P. B., Henikoff S., 2006 Spreading of silent chromatin: inaction at a distance. Nat. Rev. Genet. **7**: 793–803.

Tashiro S., Nishihara Y., Kugou K., Ohta K., Kanoh J., 2017 Subtelomeres constitute a safeguard for gene expression and chromosome homeostasis. Nucleic Acids Res.: 1–17.

Teixeira M. T., Gilson E., 2005 Telomere maintenance, function and evolution: The yeast paradigm. Chromosom. Res. **13**: 535–548.

Teng S. C., Zakian V. A., 1999 Telomere-telomere recombination is an efficient bypass pathway for telomere maintenance in Saccharomyces cerevisiae. Mol. Cell. Biol. **19**: 8083–93.

Therizols P., Duong T., Dujon B., Zimmer C., Fabre E., 2010 Chromosome arm length and nuclear constraints determine the dynamic relationship of yeast subtelomeres. Proc. Natl. Acad. Sci. **107**: 2025–2030.

Thurtle D. M., Rine J., 2014 The molecular topography of silenced chromatin in Saccharomyces cerevisiae. Genes Dev. **28**: 245–58.

Tolhuis B., Palstra R. J., Splinter E., Grosveld F., Laat W. De, 2002 Looping and interaction between hypersensitive sites in the active β-globin locus. Mol. Cell **10**: 1453–1465.

Valenzuela L., Dhillon N., Dubey R. N., Gartenberg M. R., Kamakaka R. T., 2008 Long-range communication between the silencers of HMR. Mol. Cell. Biol. **28**: 1924–35.

Verstrepen K. J., Klis F. M., 2006 Flocculation, adhesion and biofilm formation in yeasts. Mol. Microbiol. **60**: 5–15.

Wellinger R. J., Zakian V. a, 2012 Everything you ever wanted to know about Saccharomyces cerevisiae telomeres: beginning to end. Genetics **191**: 1073–105.

West A. G., Gaszner M., Felsenfeld G., West A. G., Gaszner M., Felsenfeld G., 2002 Insulators : many functions , many mechanisms Insulators : many functions , many mechanisms. : 271–288.

Yarragudi A., Parfrey L. W., Morse R. H., 2007 Genome-wide analysis of transcriptional dependence and probable target sites for Abf1 and Rap1 in Saccharomyces cerevisiae. Nucleic Acids Res. **35**: 193–202.

11. SUPPLEMENTARY INFORMATION

11.1. Papers published

- De Las Peñas A., J. Juárez-Cepeda, **E. López-Fuentes**, M. Briones-Martín-del-Campo, G. Gutiérrez-Escobedo, *et al.*, 2015 Local and regional chromatin silencing in *Candida glabrata*: consequences for adhesion and the response to stress, (M. Bolotin-Fukuhara, Ed.). *FEMS* Yeast Res. 15. doi: 10.1093/femsyr/fov056
  DOI: https://doi.org/10.1093/femsyr/fov056
- **López-Fuentes E**., G. Gutiérrez-Escobedo, B. Timmermans, P. Van Dijck, A. De Las Peñas, *et al.*, 2018 *Candida glabrata*'s Genome Plasticity Confers a Unique Pattern of Expressed Cell Wall Proteins. J. Fungi 4. doi: 0.3390/jof4020067
  DOI: https://doi.org/10.3390/jof4020067
- Leiva-Peláez O., G. Gutiérrez-Escobedo, **E. López-Fuentes**, J. Cruz-Mora, A. De Las Peñas, *et al.*, 2018 Molecular characterization of the Silencing complex SIR in Candida glabrata hyperadherent clinical isolates. Fungal Genet. Biol. 118: 21–31. doi:10.1016/j.fgb.2018.05.005
  DOI: https://doi.org/10.1016/j.fgb.2018.05.005
- **Eunice López-Fuentes**[1], Grecia Hernández-Hernández[1], Leonardo Castanedo-Ibarra[1], Guadalupe Gutiérrez-Escobedo[1], Katarzyna Oktaba[2], Alejandro De Las Peñas[1], and Irene Castaño[1]*. **2018**. ***Candida glabrata cis*-element Sil2126 negatively regulates the expression of *EPA* genes through chromatin loop formation.** *GENETICS Early online July 12, 2018; https://doi.org/10.1534/genetics.118.301202*

11.2. Table S1. *Escherichia coli* and *Candida glabrata* strains used in this study

***E. coli* strains**	**Genotype**	**Reference**
DH10B	F⁻ *mcrA* Δ(*mrr-hsdRMS-mcrBC*) f80d*lacZ*Δ*M15* Δ*lacX74 deoR recA1 endA1 araD139*Δ(*ara,leu*)7697 *galU galK* l⁻ *rpsL nupG*	(Calvin and Hanawalt 1988)

***Candida glabrata* strains**			
Strain	**Parent**	**Genotype**	**Reference**
BG2		Clinical isolate	(Fidel *et al.* 1996)
BG14	BG2	*ura3*Δ::Tn*903* G418^R	(Cormack *et al.* 1999)
Sil2126-*URA3* integration at different genomic loci			
CGM397	BG14	*ura3*Δ::Tn*903* G418^R pAP430-*Spe*I integrated between *ISC1* and *HYR1*	(Rosas-Hernández *et al.* 2008)
CGM399	BG14	*ura3*Δ::Tn*903* G418^R pAP509-*Spe*I integrated between *ISC1* and *HYR1*	(Rosas-Hernández *et al.* 2008)
CGM1414	BG14	*ura3*Δ::Tn*903* G418^R pAJ51-*Bst*XI integrated at -26 kb of telomere C_{-L}	(Juárez-Reyes *et al.* 2012)
CGM1417	BG14	*ura3*Δ::Tn*903* G418^R pAJ53-*Bst*XI integrated at -23 kb of telomere I_{-L}	(Juárez-Reyes *et al.* 2012)
CGM1421	BG14	*ura3*Δ::Tn*903* G418^R pAJ55-*Mfe*I integrated at -19 kb of telomere K_{-R}	(Juárez-Reyes *et al.* 2012)
Sil2126-*URA3* at -31.9 kb of telomere in the absence of the NE			
CGM685	BG14	*ura3*Δ::Tn*903* G418^R *sil*Δ::(P_{PGK1}::hph::3'UTR_{HIS3}::FRT) (pAJ25-*Bcg*I)	(Juárez-Reyes *et al.* 2012)
CGM742	CGM685	*ura3*Δ::Tn*903* G418^R *sil*Δ::FRT	(Juárez-Reyes *et al.* 2012)
CGM817	CGM742	*ura3*Δ::Tn*903* G418^R *sil*Δ pAP430/*Spe*I integrated between *ISC1* and *HYR1*	(Juárez-Reyes *et al.* 2012)
CGM2476	BG14	*ura3*Δ::Tn*903* G418^R *ne*Δ::NAT (pLF11-*Bsg*I)	This work
CGM2502	CGM742	*ura3*Δ::Tn*903* G418^R *sil*Δ *ne*Δ::NAT (pLF11-*Bsg*I)	This work
CGM2575	CGM2476	*ura3*Δ::Tn*903* G418^R	This work

		*ne*Δ::FRT	
CGM2590	CGM2502	*ura3*Δ::Tn*903* G418^R *sil*Δ *ne*Δ::FRT	This work
CGM2592	CGM2575	*ura3*Δ::Tn*903* G418^R *ne*Δ::FRT pAP509-*Spe*I integrated between *ISC1* and *HYR1*	This work
CGM2594	CGM2575	*ura3*Δ::Tn*903* G418^R *ne*Δ::FRT pAP430-*Spe*I integrated between *ISC1* and *HYR1*	This work
CGM2596	CGM2590	*ura3*Δ::Tn*903* G418^R *sil*Δ *ne*Δ pAP509-*Spe*I integrated between *ISC1* and *HYR1*	This work
CGM2598	CGM2590	*ura3*Δ::Tn*903* G418^R *sil*Δ *ne*Δ pAP430-*Spe*I integrated between *ISC1* and *HYR1*	This work
Sil2126-*URA3* at -31.9 kb of telomere in the absence of the intergenics			
CGM3223	BG14	*ura3*Δ::Tn*903* G418^R *EPA1-EPA2* intergenic replacement::pLF60/*Bsg*I Nat^R	This work
CGM3225	CGM742	*ura3*Δ::Tn*903* G418^R *sil*Δ::FRT *EPA1-EPA2* intergenic replacement::pLF60/*Bsg*I Nat^R	This work
CGM3248	CGM3223	*ura3*Δ::Tn*903* G418^R *EPA1-EPA2* intergenic replacement::pLF60/*Bsg*I Nat^S	This work
CGM3263	CGM3248	*ura3*Δ::Tn*903* G418^R *EPA1-EPA2* intergenic replacement::pLF60/*Bsg*I Nat^S pAP430-*Spe*I integrated between *ISC1* and *HYR1*	This work
CGM3265	CGM3248	*ura3*Δ::Tn*903* G418^R *EPA1-EPA2* intergenic replacement::pLF60/*Bsg*I Nat^S pAP509-*Spe*I integrated between *ISC1* and *HYR1*	This work
CGM3267	CGM3225	*ura3*Δ::Tn*903* G418^R *sil*Δ::FRT *EPA1-EPA2* intergenic replacement::pLF60/*Bsg*I Nat^S	This work
CGM3413	CGM3267	*ura3*Δ::Tn*903* G418^R *sil*Δ::FRT *EPA1-EPA2* intergenic replacement::pLF60/*Bsg*I Nat^S pAP509-*Spe*I integrated between *ISC1* and *HYR1*	This work
CGM3415	CGM3267	*ura3*Δ::Tn*903* G418^R *sil*Δ::FRT *EPA1-EPA2* intergenic replacement::pLF60/*Bsg*I Nat^S pAP430-*Spe*I integrated between *ISC1* and *HYR1*	This work
CGM3445	BG14	*ura3*Δ::Tn*903* G418^R *EPA2-EPA3* intergenic replacement::pLF70/*Bsg*I Nat^R	This work
CGM3448	CGM742	*ura3*Δ::Tn*903* G418^R *sil*Δ::FRT *EPA2-EPA3* intergenic replacement::pLF70/*Bsg*I Nat^R	This work
CGM3449	CGM3248	*ura3*Δ::Tn*903* G418^R *EPA1-EPA2* intergenic replacement::pLF60/*Bsg*I Nat^S *EPA2-EPA3* intergenic replacement::pLF70/*Bsg*I Nat^R	This work
CGM3452	CGM3267	*ura3*Δ::Tn*903* G418^R *sil*Δ::FRT *EPA1-EPA2* intergenic replacement::pLF60/*Bsg*I Nat^S *EPA2-EPA3* intergenic replacement::pLF70/*Bsg*I Nat^R	This work
CGM3478	CGM3445	*ura3*Δ::Tn*903* G418^R *EPA2-EPA3* intergenic replacement::pLF70/*Bsg*I Nat^S	This work
CGM3480	CGM3448	*ura3*Δ::Tn*903* G418^R *sil*Δ::FRT *EPA2-EPA3* intergenic replacement::pLF70/*Bsg*I Nat^S	This work
CGM3482	CGM3449	*ura3*Δ::Tn*903* G418^R *EPA1-EPA2* intergenic replacement::pLF60/*Bsg*I Nat^S *EPA2-EPA3* intergenic replacement::pLF70/*Bsg*I Nat^S	This work
CGM3484	CGM3452	*ura3*Δ::Tn*903* G418^R *sil*Δ::FRT *EPA1-EPA2* intergenic replacement::pLF60/*Bsg*I Nat^S	This work

		EPA2-EPA3 intergenic replacement::pLF70/*Bsg*I Nat^S	
CGM3514	CGM3478	*ura3*Δ::Tn*903* G418^R *EPA2-EPA3* intergenic replacement::pLF70/*Bsg*I Nat^S pAP430-*Spe* I integrated between *ISC1* and *HYR1*	This work
CGM3516	CGM3478	*ura3*Δ::Tn*903* G418^R *EPA2-EPA3* intergenic replacement::pLF70/*Bsg*I Nat^S pAP509-*Spe*I integrated between *ISC1* and *HYR1*	This work
CGM3518	CGM3480	*ura3*Δ::Tn*903* G418^R *sil*Δ::FRT *EPA2-EPA3* intergenic replacement::pLF70/*Bsg*I Nat^S pAP430-*Spe*I integrated between *ISC1* and *HYR1*	This work
CGM3520	CGM3480	*ura3*Δ::Tn*903* G418^R *sil*Δ::FRT *EPA2-EPA3* intergenic replacement::pLF70/*Bsg*I Nat^S pAP509-*Spe*I integrated between *ISC1* and *HYR1*	This work
CGM3522	CGM3482	*ura3*Δ::Tn*903* G418^R *EPA1-EPA2* intergenic replacement::pLF60/*Bsg*I Nat^S *EPA2-EPA3* intergenic replacement::pLF70/*Bsg*I Nat^S pAP430-*Spe*I integrated between *ISC1* and *HYR1*	This work
CGM3524	CGM3482	*ura3*Δ::Tn*903* G418^R *EPA1-EPA2* intergenic replacement::pLF60/*Bsg*I Nat^S *EPA2-EPA3* intergenic replacement::pLF70/*Bsg*I Nat^S pAP509-*Spe*I integrated between *ISC1* and *HYR1*	This work
CGM3526	CGM3484	*ura3*Δ::Tn*903* G418^R *sil*Δ::FRT *EPA1-EPA2* intergenic replacement::pLF60/*Bsg*I Nat^S *EPA2-EPA3* intergenic replacement::pLF70/*Bsg*I Nat^S pAP430-*Spe*I integrated between *ISC1* and *HYR1*	This work
CGM3528	CGM3484	*ura3*Δ::Tn*903* G418^R *sil*Δ::FRT *EPA1-EPA2* intergenic replacement::pLF60/*Bsg*I Nat^S *EPA2-EPA3* intergenic replacement::pLF70/*Bsg*I Nat^S pAP509-*Spe*I integrated between *ISC1* and *HYR1*	This work
Deletion analysis of Sil2126-*URA3* reporter system at -31.9 kb in the absence of Sil2126 in its original position			
CGM3554	CGM742	*ura3*Δ::Tn*903* G418^R *sil*Δ::FRT pAP509-*Spe*I integrated between *ISC1* and *HYR1*	This work
CGM3557	CGM742	*ura3*Δ::Tn*903* G418^R *sil*Δ::FRT pAP571-*Spe*I integrated between *ISC1* and *HYR1*	This work
CGM3559	CGM742	*ura3*Δ::Tn*903* G418^R *sil*Δ::FRT pAJ7-*Spe*I integrated between *ISC1* and *HYR1*	This work
CGM3561	CGM742	*ura3*Δ::Tn*903* G418^R *sil*Δ::FRT pAJ33-*Spe*I integrated between *ISC1* and *HYR1*	This work
CGM3563	CGM742	*ura3*Δ::Tn*903* G418^R *sil*Δ::FRT pAJ59-*Spe*I integrated between *ISC1* and *HYR1*	This work
***RAP1*-Flag ChIP assay**			
CGM2415	BG14	*ura3*Δ::Tn*903* G418^R *RAP1*-Flag::NAT (pCI24-*Bsg*I/*Sal*I)	(Castanedo-Ibarra and Castaño 2015)
CGM2875	CGM2416	*ura3*Δ::Tn*903* G418^R *RAP1*-myc::NAT pAP430-*Spe*I integrated between *ISC1* and *HYR1*	This work
CGM2879	CGM2415	*ura3*Δ::Tn*903* G418^R *RAP1*-Flag::NAT pAP430-*Spe*I integrated between *ISC1* and *HYR1*	This work
CGM3111	CGM2415	*ura3*Δ::Tn*903* G418^R *RAP1*-Flag	This work

CGM3153	CGM3111	*ura3*Δ::Tn*903* G418^R *RAP1*-Flag *sil*Δ::hph (pAJ25-*Bcg*I)	This work
CGM3170	CGM3153	*ura3*Δ::Tn*903* G418^R *RAP1*-Flag *sil*Δ::FRT	This work
CGM3228	CGM3170	*ura3*Δ::Tn*903* G418^R *RAP1*-Flag *sil*Δ::FRT pAP430-*Spe*I integrated between *ISC1* and *HYR1*	This work
CGM3230	CGM3170	*ura3*Δ::Tn*903* G418^R *RAP1*-Flag *sil*Δ::FRT pAP509-*Spe*I integrated between *ISC1* and *HYR1*	This work
CGM3231	CGM3170	*ura3*Δ::Tn*903* G418^R *RAP1*-Flag *sil*Δ::FRT pAP572-*Spe*I integrated between *ISC1* and *HYR1*	This work
CGM3234	CGM3170	*ura3*Δ::Tn*903* G418^R *RAP1*-Flag *sil*Δ::FRT pAP571-*Spe*I integrated between *ISC1* and *HYR1*	This work
CGM3245	CGM3170	*ura3*Δ::Tn*903* G418^R *RAP1*-Flag *sil*Δ::FRT pAJ33-*Spe*I integrated between *ISC1* and *HYR1*	This work
CGM3247	CGM3170	*ura3*Δ::Tn*903* G418^R *RAP1*-Flag *sil*Δ::FRT pAJ59-*Spe*I integrated between *ISC1* and *HYR1*	This work
CGM3257	CGM3170	*ura3*Δ::Tn*903* G418^R *RAP1*-Flag *sil*Δ::FRT pAJ7-*Spe*I integrated between *ISC1* and *HYR1*	This work
CGM3602	CGM3518	*ura3*Δ::Tn*903* G418^R *sil*Δ::FRT *EPA2-EPA3* intergenic replacement::pLF70/*Bsg*I Nat^S pAP430-*Spe*I integrated between *ISC1* and *HYR1* *RAP1*-Flag::NAT (pCI24-*Bsg*I/*Sal*I)	This work
CGM3650	CGM3514	*ura3*Δ::Tn*903* G418^R *EPA2-EPA3* intergenic replacement::pLF70/*Bsg*I Nat^S pAP430-*Spe* I integrated between *ISC1* and *HYR1* *RAP1*-Flag::NAT (pCI24-*Bsg*I/*Sal*I)	This work
CGM3652	CGM3478	*ura3*Δ::Tn*903* G418^R *EPA2-EPA3* intergenic replacement::pLF70/*Bsg*I Nat^S *RAP1*-Flag::NAT (pCI24-*Bsg*I/*Sal*I)	This work
CGM3654	CGM3480	*ura3*Δ::Tn*903* G418^R *sil*Δ::FRT *EPA2-EPA3* intergenic replacement::pLF70/*Bsg*I Nat^S *RAP1*-Flag::NAT (pCI24-*Bsg*I/*Sal*I)	This work
***Myc-ABF1* ChIP assay**			
CGM3431	CGM817	*ura3*Δ::Tn*903* G418^R *sil*Δ pAP430/SpeI integrated between *ISC1* and *HYR1* Replicative plasmid pGH8 (P_{MT1}-Myc-*ABF1*)	This work
CGM3433	CGM3228	*ura3*Δ::Tn*903* G418^R *RAP1*-Flag *sil*Δ::FRT pAP430-*Spe*I integrated between *ISC1* and *HYR1* Replicative plasmid pGH8 (P_{MT1}-Myc-*ABF1*)	This work
CGM3435	CGM3230	*ura3*Δ::Tn*903* G418^R *RAP1*-Flag *sil*Δ::FRT pAP509-*Spe*I integrated between *ISC1* and *HYR1* Replicative plasmid pGH8 (P_{MT1}-Myc-*ABF1*)	This work
CGM3437	CGM3234	*ura3*Δ::Tn*903* G418^R *RAP1*-Flag *sil*Δ::FRT pAP571-*Spe*I integrated between *ISC1* and *HYR1* Replicative plasmid pGH8 (P_{MT1}-Myc-*ABF1*)	This work
CGM3439	CGM3245	*ura3*Δ::Tn*903* G418^R *RAP1*-Flag *sil*Δ::FRT pAJ33-*Spe*I integrated between *ISC1* and *HYR1* Replicative plasmid pGH8 (P_{MT1}-Myc-*ABF1*)	This work
CGM3441	CGM3247	*ura3*Δ::Tn*903* G418^R *RAP1*-Flag *sil*Δ::FRT pAJ59-*Spe*I integrated between *ISC1* and *HYR1* Replicative plasmid pGH8 (P_{MT1}-Myc-*ABF1*)	This work
CGM3443	CGM3257	*ura3*Δ::Tn*903* G418^R *RAP1*-Flag *sil*Δ::FRT	This work

		pAJ7-*Spe*I integrated between *ISC1* and *HYR1* Replicative plasmid pGH8 (P_{MT1}-Myc-*ABF1*)	
CGM3453	BG14	*ura3*Δ::Tn*903* G418^R Replicative plasmid pGH8 (P_{MT1}-Myc-*ABF1*)	(Hernandez-Hernandez and Castano 2017)
CGM3534	BG14	*ura3*Δ::Tn*903* G418^R Replicative plasmid pGH3 (P_{MT1}-Myc)	(Hernandez-Hernandez and Castano 2017)
CGM3564	CGM3554	*ura3*Δ::Tn*903* G418^R *sil*Δ::FRT pAP509-*Spe*I integrated between *ISC1* and *HYR1* Replicative plasmid pGH8 (P_{MT1}-Myc-*ABF1*)	This work
CGM3566	CGM3557	*ura3*Δ::Tn*903* G418^R *sil*Δ::FRT pAP571-*Spe*I integrated between *ISC1* and *HYR1* Replicative plasmid pGH8 (P_{MT1}-Myc-*ABF1*)	This work
CGM3596	CGM742	*ura3*Δ::Tn*903* G418^R *sil*Δ::FRT Replicative plasmid pGH8 (P_{MT1}-Myc-*ABF1*)	This work
CGM3598	CGM3514	*ura3*Δ::Tn*903* G418^R *EPA2-EPA3* intergenic replacement::pLF70/*Bsg*I Nat^S pAP430-*Spe* I integrated between *ISC1* and *HYR1* Replicative plasmid pGH8 (P_{MT1}-Myc-*ABF1*)	This work
CGM3600	CGM3518	*ura3*Δ::Tn*903* G418^R *sil*Δ::FRT *EPA2-EPA3* intergenic replacement::pLF70/*Bsg*I Nat^S pAP430-*Spe*I integrated between *ISC1* and *HYR1* Replicative plasmid pGH8 (P_{MT1}-Myc-*ABF1*)	This work
CGM3655	CGM397	*ura3*Δ::Tn*903* G418^R pAP430-*Spe*I integrated between *ISC1* and *HYR1* Replicative plasmid pGH8 (P_{MT1}-Myc-*ABF1*)	This work
CGM3657	CGM3478	*ura3*Δ::Tn*903* G418^R *EPA2-EPA3* intergenic replacement::pLF70/*Bsg*I Nat^S Replicative plasmid pGH8 (P_{MT1}-Myc-*ABF1*)	This work
CGM3659	CGM3480	*ura3*Δ::Tn*903* G418^R *sil*Δ::FRT *EPA2-EPA3* intergenic replacement::pLF70/*Bsg*I Nat^S Replicative plasmid pGH8 (P_{MT1}-Myc-*ABF1*)	This work
Sir3-Flag and Sir4-Flag ChIP assay			
CGM921	BG14	*ura3*Δ::Tn*903* G418^R *SIR4*-Flag::hph (pJV13/*Bgl*II-*Bcg*I)	(Juárez-Vega and Castaño 2010)
CGM957	BG14	*ura3*Δ::Tn*903* G418^R *SIR3*-Flag::hph (pJV22/*Bsr*G1-*Hpa*I)	(Juárez-Vega and Castaño 2010)
CGM1107	CGM957	*ura3*Δ::Tn*903* G418^R *SIR3*-Flag	(Juárez-Vega and Castaño 2010)
CGM1113	CGM921	*ura3*Δ::Tn*903* G418^R *SIR4*-Flag	(Juárez-Vega and Castaño

			2010)
CGM3568	CGM1107	*ura3*Δ::Tn*903* G418^R *SIR3*-Flag pAP430-*Spe*I integrated between *ISC1* and *HYR1*	This work
CGM3570	CGM1107	*ura3*Δ::Tn*903* G418^R *SIR3*-Flag pAP509-*Spe*I integrated between *ISC1* and *HYR1*	This work
CGM3572	CGM1107	*ura3*Δ::Tn*903* G418^R *SIR3*-Flag pAP571-*Spe*I integrated between *ISC1* and *HYR1*	This work
CGM3574	CGM1113	*ura3*Δ::Tn*903* G418^R *SIR4*-Flag pAP430-*Spe*I integrated between *ISC1* and *HYR1*	This work
CGM3576	CGM1113	*ura3*Δ::Tn*903* G418^R *SIR4*-Flag pAP509-*Spe*I integrated between *ISC1* and *HYR1*	This work
CGM3578	CGM1113	*ura3*Δ::Tn*903* G418^R *SIR4*-Flag pAP571-*Spe*I integrated between *ISC1* and *HYR1*	This work
CGM3717	CGM1107	*ura3*Δ::Tn*903* G418^R *SIR3*-Flag *sil*Δ::hph (pAJ25-*Bcg*I)	This work
CGM3725	CGM3717	*ura3*Δ::Tn*903* G418^R *SIR3*-Flag *sil*Δ::FRT	This work
CGM3735	CGM3725	*ura3*Δ::Tn*903* G418^R *SIR3*-Flag *sil*Δ::FRT pAP430-*Spe*I integrated between *ISC1* and *HYR1*	This work
CGM3737	CGM3725	*ura3*Δ::Tn*903* G418^R *SIR3*-Flag *sil*Δ::FRT pAP509-*Spe*I integrated between *ISC1* and *HYR1*	This work
3C assay			
BG592	BG14	*ura3*Δ::Tn*903* G418^R *rap1-21*	(De las Peñas *et al.* 2003)
BG676	BG14	*ura3*Δ::Tn*903* G418^R *sir3*Δ	(De las Peñas *et al.* 2003)
CGM817	CGM742	*ura3*Δ::Tn*903* G418^R *sil*Δ pAP430/*Spe*I integrated between *ISC1* and *HYR1*	(Juárez-Reyes *et al.* 2012)
CGM3559	CGM742	*ura3*Δ::Tn*903* G418^R *sil*Δ::FRT pAJ7-*Spe*I integrated between *ISC1* and *HYR1*	This work
CGM3715	BG592	*ura3*Δ::Tn*903* G418^R *rap1-21* *sil*Δ::hph (pAJ25-*Bcg*I)	This work
CGM3721	BG676	*ura3*Δ::Tn*903* G418^R *sir3*Δ *sil*Δ::hph (pAJ25-*Bcg*I)	This work
CGM3723	CGM3715	*ura3*Δ::Tn*903* G418^R *rap1-21* *sil*Δ::FRT	This work
CGM3727	CGM3721	*ura3*Δ::Tn*903* G418^R *sir3*Δ *sil*Δ::FRT	This work
CGM3732	CGM3723	*ura3*Δ::Tn*903* G418^R *rap1-21 sil*Δ::FRT pAP430/*Spe*I integrated between *ISC1* and *HYR1*	This work
CGM3739	CGM3727	*ura3*Δ::Tn*903* G418^R *sir3*Δ *sil*Δ::FRT pAP430/*Spe*I integrated between *ISC1* and *HYR1*	This work
abf1-43			
CGM3068	BG14	*abf1-43*::NAT (pCI32/BsgI)	(Hernandez-Hernandez

			and Castano 2017)
CGM3113	CGM3068	*abf1-43*::FRT	(Hernandez-Hernandez and Castano 2017)
***EPA1* promoter activity assays using *GFP* as reporter**			
BG198 (CGM1936)	BG14	*ura3*Δ::Tn*903* G418^R *epa1*Δ*::GFP* under the control of the *EPA1* promoter	(De las Peñas *et al.* 2003)
BG201 (CGM1937)	BG14	*ura3*Δ::Tn*903* G418^R *epa1*Δ*::GFP* pYIp*lac*211 integrated 300bp from TAA of *EPA1. GFP* under the control of the *EPA1* promoter	(Gallegos-García *et al.* 2012)
CGM514	BG14	*ura3*Δ::Tn*903* G418^R pMC14 replicative plasmid	(Juárez-Cepeda *et al.* 2015)
CGM1950	BG198	*ura3*Δ::Tn*903* G418^R pLF1-AvrII integrated 210pb from TAA of EPA1	This work
CGM2005	CGM1950	*ura3*Δ::Tn*903* G418^R *ne*Δ Segregant_1	This work
CGM2024	CGM1950	*ura3*Δ::Tn*903* G418^R *ne*Δ Segregant_2	This work
CGM2187	BG201	*ura3*Δ::Tn*903* G418^R *epa1*Δ*::GFP* pYIp*lac*211 integrated 300bp from TAA of *EPA1. GFP* under the 64control of the *EPA1* promoter *sil*Δ::hph (pAJ25-*Bcg*I)	This work
CGM2189	CGM2005	*ura3*Δ::Tn*903* G418^R *ne*Δ *sil*Δ::hph (pAJ25-*Bcg*I)	This work
CGM2263	CGM2187	*ura3*Δ::Tn*903* G418^R *epa1*Δ*::GFP* pYIp*lac*211 integrated 300bp from TAA of *EPA1. GFP* under the 64ontrolo f the *EPA1* promoter *sil*Δ::FRT	This work
CGM2265	CGM2189	*ura3*Δ::Tn*903* G418^R *ne*Δ *sil*Δ::FRT	This work
CGM2287	BG14	*ura3*Δ::Tn*903* G418^R pAP385 Replicative plasmid	This work
CGM2307	CGM1950	*ura3*Δ::Tn*903* G418^R pLF1-AvrII integrated 210pb from TAA of EPA1 *sil*Δ::hph (pAJ25-*Bcg*I)	This work
CGM2343	CGM2307	*ura3*Δ::Tn*903* G418^R pLF1-AvrII integrated 210pb from TAA of EPA1 *sil*Δ::FRT	This work
CGM2927	BG198	*ura3*Δ::Tn*903* G418^R *epa1*Δ*::GFP* under the control of the *EPA1* promoter *ne*Δ::NAT (pLF11 *Bsg*I)	This work
CGM2933	CGM2927	*ura3*Δ::Tn*903* G418^R *epa1*Δ*::GFP* under the control of the *EPA1* promoter *ne*Δ::FRT	This work
CGM3701	BG198	*ura3*Δ::Tn*903* G418^R *epa1*Δ*::GFP* under the control of the	This work

		EPA1 promoter *sil*Δ::hph (pAJ25-*Bcg*I)	
CGM3703	CGM3701	*ura3*Δ::Tn*903* G418^R *epa1*Δ*::GFP* under the control of the *EPA1* promoter *sil*Δ::FRT	This work
CGM3705	CGM3703	*ura3*Δ::Tn*903* G418^R *epa1*Δ*::GFP* under the control of the *EPA1* promoter. *sil*Δ::FRT pAP430-*Spe*I integrated between *ISC1* and *HYR1*	This work
CGM3707	CGM3703	*ura3*Δ::Tn*903* G418^R *epa1*Δ*::GFP* under the control of the *EPA1* promoter. *sil*Δ::FRT pAP509-*Spe*I integrated between *ISC1* and *HYR1*	This work
CGM3709	CGM3703	*ura3*Δ::Tn*903* G418^R *epa1*Δ*::GFP* under the control of the *EPA1* promoter. *sil*Δ::FRT pAJ7-*Spe*I integrated between *ISC1* and *HYR1*	This work
***EPA1* promoter activity assays using *URA3* as reporter**			
BG1124 (CGM88)	BG1212	*ura3*Δ::Tn*903* G418^R *epa1*Δ::*URA3* *URA3* under the control of the *EPA1* promoter	(Gallegos-García *et al.* 2012)
BG1132 (CGM95)	BG14	*ura3*Δ::Tn*903* G418^R *epa1*Δ::*URA3 ne*Δ::*cat* *EPA1* replaced by *URA3* and NE (negative element) replaced by the bacterial cat gene, chloramphenicol acetyl transferase from pACYC184. *URA3* under the control of the *EPA1* promoter	(Gallegos-García *et al.* 2012)
CGM1907	BG1124	*ura3*Δ::Tn*903* G418^R *epa1*Δ::*URA3* *sil*Δ::(P_{PGK1}::hph::3'UTR$_{HIS3}$::FRT) (pAJ25-*Bcg*I)	This work
CGM1909	BG1132	*ura3*Δ::Tn*903* G418^R *epa1*Δ::*URA3 ne*Δ::*cat* *sil*Δ::(P_{PGK1}::hph::3'UTR$_{HIS3}$::FRT) (*pAJ25-Bcg*I)	This work
CGM1915	CGM1907	*ura3*Δ::Tn*903* G418^R *epa1*Δ::*URA3* *sil*Δ::FRT (pAJ25-*Bcg*I)	This work
CGM1917	CGM1909	*ura3*Δ::Tn*903* G418^R *epa1*Δ::*URA3 ne*Δ::*cat* *sil*Δ::FRT (pAJ25-*Bcg*I)	This work
CGM2179	CGM1915	*ura3*Δ::Tn*903* G418^R *epa1*Δ::*URA3 sil*Δ::FRT *hdf1*Δ::hph (pAJ27-*Bcg*I)	This work
CGM2181	CGM1917	*ura3*Δ::Tn*903* G418^R *epa1*Δ::*URA3 ne*Δ::*cat sil*Δ::FRT *hdf1*Δ::hph (pAJ27-*Bcg*I)	This work
CGM2183	CGM1915	*ura3*Δ::Tn*903* G418^R *epa1*Δ::*URA3 sil*Δ::FRT *hdf2*Δ::hph (pAJ28-*Bcg*I)	This work
CGM2185	CGM1917	*ura3*Δ::Tn*903* G418^R *epa1*Δ::*URA3 ne*Δ::*cat sil*Δ::FRT *hdf2*Δ::hph (pAJ28-*Bcg*I)	This work
CGM2255	CGM2179	*ura3*Δ::Tn*903* G418^R *epa1*Δ::*URA3 sil*Δ::FRT *hdf1*Δ::FRT	This work
CGM2257	CGM2181	*ura3*Δ::Tn*903* G418^R *epa1*Δ::*URA3 ne*Δ::*cat sil*Δ::FRT *hdf1*Δ::FRT	This work
CGM2259	CGM2183	*ura3*Δ::Tn*903* G418^R *epa1*Δ::*URA3 sil*Δ::FRT *hdf2*Δ::FRT	This work

CGM2261	CGM2185	*ura3*Δ::Tn*903* G418^R *epa1*Δ::*URA3* *ne*Δ::*cat* *sil*Δ::FRT *hdf2*Δ::FRT	This work
CGM2930	BG1124	*ura3*Δ::Tn*903* G418^R *epa1*Δ::*URA3* *URA3* under the control of the *EPA1* promoter *ne*Δ::NAT	This work
***ne*Δ (pop-in)**			
CGM1919	BG14	*ura3*Δ::Tn*903* G418^R *ne*Δ::pLF1 (*Bln*I, integrative plasmid)	This work
CGM1921	CGM742	*ura3*Δ::Tn*903* G418^R *sil*Δ *ne*Δ::pLF1 (*Bln*I, integrative plasmid)	This work
CGM2438	BG14	*ura3*Δ::Tn*903* G418^R *ne*Δ::pLF1 (*Bln*I, integrative plasmid)_2	This work
CGM2440	CGM742	*ura3*Δ::Tn*903* G418^R *sil*Δ *ne*Δ::pLF1 (*Bln*I, integrative plasmid)_2	This work
***EPA6* and *EPA7* promoter activity assays**			
CGM1973	BG14	*ura3*Δ::Tn*903* G418^R pYC177	(Yáñez-Carrillo *et al.* 2015)
CGM3085	BG14	*ura3*Δ::Tn*903* G418^R pLF50	This work
CGM3087	BG14	*ura3*Δ::Tn*903* G418^R pLF52	This work
CGM3089	BG14	*ura3*Δ::Tn*903* G418^R pLF14	This work
CGM3091	BG14	*ura3*Δ::Tn*903* G418^R pLF55	This work
CGM3093	BG14	*ura3*Δ::Tn*903* G418^R pLF40	This work
CGM3095	BG14	*ura3*Δ::Tn*903* G418^R pLF42	This work
CGM3097	BG14	*ura3*Δ::Tn*903* G418^R pLF49	This work
CGM3101	BG14	*ura3*Δ::Tn*903* G418^R pLF44	This work
Reconstruction of the BG1132 strain			
CGM2309	BG14	*ura3*Δ::Tn*903* G418^R *epa1*Δ::*URA3* *ne*Δ::*cat* / pAP658 (*Bsg*I) *URA3* under the control of the *EPA1* promoter Note: There are seven strains more and their phenotype is the same.	This work
Sil-*URA3* integrated at -50kb ChrE$_{-R}$			
CGM1027	BG14	*ura3*Δ::Tn*903* G418^R pAJ34 *Cla*I integrated at -50kb of telomere E-$_R$	(Juárez-Reyes *et al.* 2012)
CGM3586	CGM1027	*ura3*Δ::Tn*903* G418^R pAJ34 *Cla*I integrated at -50kb of telomere E-$_R$ *sil*Δ::hph (pAJ25-*Bcg*I)	This work

CGM3590	CGM3586	*ura3*Δ::Tn*903* G418^R pAJ34 *Cla*I integrated at -50kb of telomere E-$_R$ *sil*Δ::FRT	This work

11.3. Table S2. Plasmids used in this study

Plasmid	Relevant genotype	Reference
Cloning vectors		
pYIp*lac*211	Cloning, integrative vector URA3 Amp^R	(Gietz and Sugino 1988)
pLS9	Replicative vector expressing Sc*FLP1* (recombinase gene) for removing selection marker, P$_{EPA1}$::*FLP1*::(3' UTR of *HIS3*) Cg *CEN ARS*, Amp^R, *nat1*	Lab collection
pMZ21	Replicative vector expressing Sc*FLP1* (recombinase gene) for removing the hygromycin marker, P$_{EPA1}$::*FLP1*::(3' UTR of *HIS3*) Cg *CEN ARS*, Amp^R, *URA3*	Lab collection
pAP599	Cloning, integrative vector with 2 FRT direct repeats flanking a hygromycin resistance cassette [FRT-P$_{PGK1}$::*hph*::3'UTR$_{HIS3}$-FRT], Amp^R, Hyg^R, *URA3*	(Domergue *et al.* 2005)
pYC44	Initial Integrative Vector pYC40::3UTR$_{CTA}$::FRT Amp^R NAT^R *URA3*	(Yáñez-Carrillo *et al.* 2015)
pYC46	Recipient FLAG integrative Vector pYC44:FLAG Amp^R NAT^R *URA3*	(Yáñez-Carrillo *et al.* 2015)
pYC55	Recipient YFP replicative vector pMJ22::YFP Amp^R, NAT^R	(Yáñez-Carrillo *et al.* 2015)
pYC177	Recipient YFP replicative vector pMJ22::YFP::3'UTR$_{HIS3}$ Amp^R, NAT^R	(Yáñez-Carrillo *et al.* 2015)
pBC176	Replicative plasmid to cloned N-terminal of cell wall proteins (P$_{TEF}$::C-terminal *CWP2*::3'UTR$_{CYC1}$) Amp^R, *URA3*	(Frieman *et al.* 2002)
Plasmids integrated at -32kb from the telomere E$_{-R}$		
pAP430	Plasmid to integrate the protosilencer Sil2126 and *URA3* at the intergenic region between *C.g. ISC1* and *C.g.HYR1*. Cloned into pYIp*lac*211. Amp^R	(De las Peñas *et al.* 2003)
pAP509	Vector to integrate *URA3* at the intergenic region between *C.g. ISC1* and *C.g. HYR1*. A 0.686 kb *Pst* I-*Sal* I PCR fragment (Primers #962, #963) carrying the intergenic region between *C.g. ISC1* cloned into pYIp*lac*211. Amp^R	(Rosas-Hernández *et al.* 2008)
pAP571	A 1792pb deletion (nucleotide 334 to 2126) from the 3' end of Sil2126 in pAP430	(Juárez-Reyes *et al.* 2012)
pAP572	A 2020 deletion (nucleotide 106 to 2126) from the 3' end of	(Juárez-

	Sil2126 in pAP430	Reyes *et al.* 2012)
pAJ7	A 262pb deletion from the 5' end of Sil2126 (nucleotides 1-262) in pAP430	(Juárez-Reyes *et al.* 2012)
pAJ33	A 204pb deletion from the 5' end of Sil2126 (nucleotides 1-204) in pAP430	(Juárez-Reyes *et al.* 2012)
pAJ59	An internal deletion of 58pb from nucleotide 204 to 262 of Sil2126 in pAP430	(Juárez-Reyes *et al.* 2012)
pAJ51	Vector to integrate Sil2126-*URA3* at 26 kb from left telomere of chromosome C. A 587 pb *PstI-SalI* PCR fragment (Primers #867,#866) of a region of chromosome C, replacing *Pst I-Sal I* integration sequence of pAP430. Amp^R	(Juárez-Reyes *et al.* 2012)
pAJ53	Vector to integrate Sil2126-*URA3* at 23 kb from left telomere of chromosome I. A 475 pb *PstI-SalI* PCR fragment (Primers #871,#870) of a region of chromosome I, replacing *Pst I-Sal I* integration sequence of pAP430. Amp^R	(Juárez-Reyes *et al.* 2012)
pAJ55	Vector to integrate Sil2126-*URA3* at 19 kb from right telomere of chromosome K. A 658 pb *PstI-SalI* PCR fragment (Primers #874,#875) of a region of chromosome K, replacing *Pst I-Sal I* integration sequence of pAP430. Amp^R	(Juárez-Reyes *et al.* 2012)
Plasmids for deletion of *cis*-acting elements		
pAJ25	Sil2126 deletion vector Hph^R. A 1025pb *Kpn*I-*Xho*I fragment (Primers #339, #340) and a 935pb *Bam*HI-*Sac*I fragment (Primers #337, #338), cloned into pAP599 on either side of *hph* marker	(Juárez-Reyes *et al.* 2012)
pLF1	NE deletion integrative vector. A 2.34kb *Bam*HI-*Sac*I fragment from pAP658 cloned in the pYIplac211.	This work
pLF5	Sil2126 deletion vector Nat^R. A 1001bp *Kpn*I-*Xho*I fragment from pAJ25 and a 906pb *Bam*HI-*Sac*I fragment from pAJ25 cloned into pYC44 on either side of NAT cassette.	This work
pLF11	NE knock-out deletion vector. A 208pb *Bam*HI-*Spe*I fragment (Primers #1758, #1757) and a 950pb *Xho*I-*Kpn*I fragment (Primers #1759, #1795), cloned into pYC44 on either side of NAT cassette	This work
Plasmids for the replacement of the intergenics of *EPA* genes		
pLF60	Replacement of the intergenic region between *EPA1* and *EPA2*. A 631bp *Pst*I-*Eco*RV fragment (Primers #2303, #2304) and a 486bp *Xho*I-*Kpn*I fragment (Primers #2305, #2306) cloned into pYC44 on either side of NAT cassette	This work
pLF70	Replacement of the intergenic region between *EPA2* and *EPA3*. A 512bp SacI-SacII fragment (Primers #2307, #2308) and a 583bp SpeI-BamHI fragment (Primers #2309, #2310) cloned into pYC44 on either side of NAT cassette	This work
Plasmids used to tag Rap1 and Abf1 proteins		
pCI24	Vector to tag Rap1 protein in the C-terminal with Flag epitope. A 1254bp *Sac*I-*Bgl*II fragment of C-terminal of *RAP1* (Primers #1613, #1614) and a 455bp *Xho*I-*Kpn*I of 3'UTR of *RAP1* (Primers #1615, #1616) cloned into pYC46 on either side of	(Castanedo-Ibarra and Castaño 2015)

	NAT cassette	
pGH3	Replicative vector P_{MT1}::c-Myc-Linker::3'UTR_{HIS3}, Cg *CEN ARS*, NAT^R	Lab collection
pGH8	Vector to tag Abf1 in the N-terminal with c-Myc. A 1440bp *Cla*I *ABF1* ORF (Primers #2353, #2354) cloned into pGH3	(Hernandez-Hernandez and Castano 2017)
Plasmid used to construct *abf1-43* strain		
pCl32	A fragment of 940bp *BamH*I-*Sac*I corresponding to the *abf1-43* partial allele (Primers #1559, #1880) and a 750bp *Kpn*I-*Xho*I fragment corresponding to the 3'UTR of *ABF1* (Primers #1561, #1562) cloned into pYC44 on either side of NAT cassette	(Castanedo-Ibarra and Castaño 2015)
hdf1*Δ*::hph* and *hdf2*Δ*::hph		
pAJ27	*HDF1* deletion vector. A 804pb *KpnI HindIII HDF1 5'* fragment and a 826pb *SacI-BglII HDF1* 3' fragment, cloned into pAP599 at both sides of *hph* marker	(Juárez-Reyes *et al.* 2012)
pAJ28	*HDF2* deletion vector. A 905pb *KpnI HindIII* 5' *HDF1* fragment and a 813pb *SacI-BglII* 3' *HDF1* fragment, non-coding regions cloned into pAP599 on either side of *hph* marker	(Juárez-Reyes *et al.* 2012)
Construction of a replicative plasmid containing Sil2126		
pLF9	Sil2126 in a replicative plasmid. A 2126bp *Xho*I-*Kpn*I corresponding to Sil2126 (Primers #1749, #1750) clones into pGRB2.0.	This work
Analysis of the 5'UTR and 3'UTR of *EPA6* and *EPA7*		
pLF12	A 1767bp *Eco*RI-*Bam*HI fragment upstream to *EPA7* (Primers #1764, #1762) cloned into pYC55.	This work
pLF14	A 1767bp *Eco*RI-*Bam*HI fragment upstream to *EPA7* (Primers #1764, #1762) cloned into pYC177.	This work
pLF17	A 975bp *Eco*RI-*Bam*HI fragment upstream to *EPA6* (Primers #1761, #1762) cloned into pYC55.	This work
pLF33	A 3075bp *Eco*RI-*Bam*HI fragment upstream to *EPA6* (Primers #1760, #1762) cloned into pYC55.	This work
pLF36	A 2552bp *Eco*RI-*Bam*HI fragment upstream to *EPA7* (Primers #1763, #1762) cloned into pYC55.	This work
pLF40	A 1322bp *Sac*I-*Sac*II fragment downstream to *EPA6* amplified from *epa7*Δ (Primers #2219, #2220) cloned into pLF17.	This work
pLF42	A 1322bp *Sac*I-*Sac*II fragment downstream to *EPA6* amplified from *epa7*Δ (Primers #2219, #2220) cloned into pLF33.	This work
pLF44	A 1386bp *Sac*I-*Sac*II fragment downstream to *EPA7* amplified from *epa6*Δ (Primers #2219, #2220) cloned into pLF36.	This work
pLF49	A 1386bp *Sac*I-*Sac*II fragment downstream to *EPA7* amplified from *epa6*Δ (Primers #2219, #2220) cloned into pLF12.	This work
pLF50	A 975bp *Eco*RI-*Bam*HI fragment upstream to *EPA6* (Primers #1761, #1762) cloned into pYC177.	This work
pLF52	A 3075bp *Eco*RI-*Bam*HI fragment upstream to *EPA6* (Primers #1760, #1762) cloned into pYC177.	This work
pLF55	A 2552bp *Eco*RI-*Bam*HI fragment upstream to *EPA7* (Primers #1763, #1762) cloned into pYC177.	This work
N-terminal of PWPs cloned in pBC176		

pLF19	A 1275bp *Xba*I-*Eco*RI fragment of *PWP1* C-terminal (Primers #1939, #1940) cloned into pBC176.	This work
pLF21	A 843bp *Xba*I-*Eco*RI fragment of *PWP2* C-terminal (Primers #1941, #1942) cloned into pBC176.	This work
pLF23	A 1107bp *Xba*I-*Eco*RI fragment of *PWP3* C-terminal (Primers #1943, #1944) cloned into pBC176.	This work
pLF25	A 732bp *Xba*I-*Eco*RI fragment of *PWP4* C-terminal (Primers #1945, #1946) cloned into pBC176.	This work
pLF27	A 1593bp *Xba*I-*Eco*RI fragment of *PWP5* C-terminal (Primers #1947, #1948) cloned into pBC176.	This work
pLF29	A 693bp *Xba*I-*Eco*RI fragment of *PWP6* C-terminal (Primers #1949, #1950) cloned into pBC176.	This work
pLF31	A 1078bp *Xba*I-*Bam*HI fragment of *PWP7* C-terminal (Primers #1951, #1952) cloned into pBC176.	This work
pLF56	Flag epitope cloned into pBC176 (Primers #2237, #2238)	This work
pLF64	A 723bp *Sma*I-*Eco*RI fragment containing *EPA1* repeats (Primers #2239, #2240) cloned into pLF56	This work
Flipase in a plasmid with Hph^R		
pLF16	A 2131bp *Bam*HI-*Xho*I fragment from pAJ25 cloned into pMZ18 previously digested with *Sma*I.	This work
Constructions of Sil2125		
pLF71	Vector to integrate *URA3* adjacent to Sil2125 in ChrA. A 968bp *Pst*I-*Kpn*I fragment (Primers #2451, #2452) cloned into pAP509 (*Pst*I-*Kpn*I digested).	This work
pLF75	Intermediate vector to integrate Sil2125-*URA3* at -18kb in ChrA. A 605bp *Pst*I-*Kpn*I fragment (Primers #2457, #2458) cloned into pAP509 (*Pst*I-*Kpn*I digested).	This work
Analysis of *EPA1* promotor activity		
pMC14	A 0.717 kb BamHI/EcoRI fragment carrying the *GFP* and a 0.29 Kb EcoRI/XhoI fragment carrying the 3′UTR CTA1 were cloned in pGRB2.0. *URA3* CgCEN ARS Amp^R Promotorless GFP vector	(Juárez-Cepeda *et al.* 2015)
pAP354	A 2.5-kb *Bst*XI PCR fragment carrying the promoter region of *EPA1* was cloned into pAP353. *URA3* Amp^R P_{EPA1} :: *GFP*::3'UTR_{HIS3}	(Gallegos-García *et al.* 2012)
pAP385	A 3.1-kb XhoI PCR fragment carrying the 3'UTR_{EPA1} fragment cloned at *Xho*I site of pAP354. *URA3* Amp^R P_{EPA1}:: GFP::3'$UTR_{EPA1\text{-}3.1Kb}$	(Gallegos-García *et al.* 2012)
pAP658	Vector to construct the BG1132 strain.	(Gallegos-García *et al.* 2012)
Integration of Sil-URA3 at -50kb in Chr E_{-R}		
pAJ34	Vector to integrate Sil2126-*URA3* reporter system at 50Kb from telomere E_{-R}. A 742pb *Pst*I-*Sal*I PCR fragment replacing *Pst*I-*Sal*I integration sequence in pAP430	(Juárez-Reyes *et al.* 2012)

11.4. Table S3. Primers used in this work

Primer	Name	Sequence 5' to 3'	Site(s) added
Primers used to construct plasmid for Negative Element (NE)Δ (pLF11)			
1757	EPA1@+1 Fw	TGA**ACTAGT**GG**GTGCAG**AACCAGAAAATATAA TAACTTCTATAG	*Spe*I, *Bsg*I
1758	EPA1@+208 Rv	AGT**GGATCC**TAATATCTCTCATTTCAAGTGTG ACCAG	*BamH*I
1759	EPA1@+1238 Fw	TTA**CTCGAG**GAGAGTCTTGTTGCTCGAACAAC	*Xho*I
1795	EPA2@+34 Rv	CAT**GGTACC**TG**GTGCAG**GATCGATATGTCATA TACATG	*Kpn*I, *Bsg*I
Primers to diagnose the *ne*Δ			
36	EPA1@593	GGGCTCAAAAACAGCTAAAG	None
1097	NAT-FRT@+11 Fw	CAT**GTCGAC**CAGTACTGACAATAAAAAGATTC TTGTTTTC	*Sal*I
1098	NAT-FRT@+287 Rv	CAT**CTCGAG**GACGAAGTTCCTATTCTCTAGAA AGTATAG	*Xho*I
1988	EPA2@3848	GTGTGCAATCTGTACCATCG	None
Primers used to generate replacements of intergenic regions of Chr E_{-R} (pLF60 and pLF70)			
2303	EPA1@2788	CAC**CTGCAG**CAC**GTGCAG**GTTATGAGTCTTTA GGTGGAAC	*Pst*I, *Bsg*I
2304	EPA1@+315	GAA**GATATC**GGTCCCTGCTCAAAAGTTGAATT CTC	*EcoR*V
2305	EPA2@+315	GGT**CTCGAG**GCTCATTGTCACATCCACTC	*Xho*I
2306	EPA2@3811	AAC**GGTACC**CAC**GTGCAG**GGTAATTTATCAC CTTC	*Kpn*I, *Bsg*I
2307	EPA3@+359	CCA**GAGCTC**GGCATTGGATTGACTGTTTAAC	*Sac*I
2308	EPA3@3226	CAT**CCGCGG**CAC**GTGCAG**CCATCTCCAAGCA AAACAAC	*Sac*II, *Bsg*I
2309	EPA2@330	CGT**ACTAGT**CAC**GTGCAG**CTGTAATGTCAGC GAGTTTG	*Spe*I, *Bsg*I
2310	EPA2@-233	TAT**GGATCC**CAAAAGCTTCGAGACCCTC	*BamH*I
Primers to diagnose the replacement of the intergenic region between *EPA1* and *EPA2*			
979	EPA2@519 Fw	CGAATCAACTTTAGACAATTTTG	None
1097	NAT-FRT@+11 Fw	CAT**GTCGAC**CAGTACTGACAATAAAAAGATTC TTGTTTTC	*Sal*I
1098	NAT-FRT@+287 Rv	CAT**CTCGAG**GACGAAGTTCCTATTCTCTAGAA AGTATAG	*Xho*I
2059	EPA1@1459 Fw	CGACTTCAATGCATACTTCCTCCG	None
Primers to diagnose the replacement of the intergenic region between *EPA2* and *EPA3*			
14	Primer 14	TATGTTGTGTGGAATTGTGAGCGGA	None
1567	Ec cat@+230 Fw	CAGTTTGCTCAGGCTCTCCC	None
1989	EPA2@465	GTAAAGTTTGTGTAAGTTAATGTG	None
1992	EPA3@138	GACAATGGAACTTTACTCTTAC	None

Primers used to generate tagged versions of Rap1 and Abf1 proteins			
1613	RAP1@812 Fw	CATACAGGTAACTCAATTAGACACAG	None
1614	RAP1@2061 Rv	CTT**AGATCT**CTATCAGATTTCTCTCCAAAAACTTC	*Bgl*II
1615	RAP1@+1 Fw	GTT**CTCGAG**AGAATGAGTGGAGATATTCAGTTTAGATAAG	*Xho*I
1616	RAP1@+455 Rv	CAC**GGTACC**TTC**GTGCAG**CTCTATGTCACTAAGCTCGCTATC	*Kpn*I, *Bsg*I
2353	ABF1@1 Cla AAA Fw	TCT**ATCGAT**AAAATGGATGACGGTATGATTTCTG	*Cla*I
2354	ABF1@1440 Cla Rv	TCT**ATCGAT**TTATTGTCCTCTTAATTCAGG	*Cla*I
Primers to diagnose RAP1-Flag::NAT in the chromosome			
1617	Rap1@+687 Rv	TCTTTTGCTCGATATCCTCTCC	None
1618	Rap1@1751 Fw	CCCATGAGACGTACTACACACAC	None
Primers to construct the *abf1-43*Δ plasmid			
1559	ABF1@385 Fw	GTT**GAGCTC**TTGTGCAGACGATCCGCAGGTCACCG C	*Sac*I
1561	ABF1@+13 Fw	CTT**CTCGAG**GCTCCAATTATTAAAATGAATAAAAGG	*Xho*I
1562	ABF1@+755 Rv	CTT**GGTACC**TT**GTGCAG**TGCCGCCAACTTAAGCATA	*Kpn*I, *Bsg*I
1880	ABF1@1308 Rv	GTT**GGATCC**TTAGACTTCACGAGGAAGCTTGTCGTC GG	*BamH*I
Primers to clone Sil2126 in a replicative plasmid			
1749	Sil@1 Fw	GTTGCAGCAAGAACCATGTTG	*Xho*I
1750	Sil@2126 Rv	ATAGATGCATGTAGCCATATC	*KpnI*
Primers to clone 5'UTR and 3'UTR of *EPA6* and *EPA7*			
1760	EPA6@-3075 Fw	TGAGAATTCTCTGCTGGTAAGTTGCTGGAC	*EcoRI*
1761	EPA6@-975 Fw	AAAGAATTCATATACGTAATGTATCCTATG	*EcoRI*
1762	EPA6@-1 Rv	TAAGGATCCTGGTCTCTAATCTTTTTCAATC	*BamH*I
1763	EPA7@-2552 Fw	GGGGAATTCGAGGTATCTATGCACTAATTG	*EcoRI*
1764	EPA7@-1767 Fw	ATCGAATTCCTTAATGAAACTTGGTATCTC	*EcoRI*
2219	EPA6/7@+6 Fw	TAGCCGCGGGTGATACCACATTTCCTAAGATAG	SacI
2220	EPA6/7@+1328 Rv	CATGAGCTCATACCACTCATATTCGTGCCAC	SacII
Primers to clone the N-terminal of PWPs			
1939	PWP1 Fw	CCGTCTAGAAAAATGGTAAGGTTCGCAGCCGCC	*XbaI*
1940	PWP1 Rv	AGTTGGAATTCCTATCACGTCATACTCGGTCACCTG	*EcoRI*

1941	PWP2 Fw	CCGTCTAGAAAAATGCTAATTGACTGTATACT GAAATTATTTC	*XbaI*
1942	PWP2 Rv	AGTTGGAATTCCTATAGTAACTGTGGTAATTG GAGG	*EcoRI*
1943	PWP3 Fw	CCGTCTAGAAAAATGCTTTGGTCATTGTTGGT ATTTG	*XbaI*
1944	PWP3 Rv	AGTTGGAATTCCAACAGTACTACTCGTGGTGA TTATGCC	*EcoRI*
1945	PWP4 Fw	CCGTCTAGAAAAATGTGGATAATGAAATTTTT GACAG	*XbaI*
1946	PWP4 Rv	AGTTGGAATTCCTGGTGGTGGTACATAAGAAC ATGTATC	*EcoRI*
1947	PWP5 Fw	CCGTCTAGAAAAATGCCCCTCATAGGAAAATA TTTTC	*XbaI*
1948	PWP5 Rv	AGTTGGAATTCCCATAGTCCAATACGTTACAA CCTC	*EcoRI*
1949	PWP6 Fw	CCGTCTAGAAAAATGAATAAAAATATGAATGC TTTCAAATCC	*XbaI*
1950	PWP6 Rv	AGTTGGAATTCCTGCATCTGGGATTGGTTTAT AGTC	*EcoRI*
1951	PWP7 Fw	CCGTCTAGAAAAATGTTTTCAAACGTCATTAAC TTTTG	*XbaI*
1952	PWP7 Rv	CGCGGATCCCTCTTGTTAGTATAACTACTGG	*BamH*I
2237	Flag Fw	GATCCGGAGCAGACTACAAAGATGACGATGA CAAAGGAGCCGATTATAAGGACGATGACGAT AAAGGGGCTGACTACAAAGATGACGATGACA AGCCC	*BamH*I *Sma*I
2238	Flag Rv	GGGCTTGTCATCGTCATCTTTGTAGTCAGCCC CTTTATCGTCATCGTCCTTATAATCGGCTCCTT TGTCATCGTCATCTTTGTAGTCTGCTCCG	*Sma*I *BamH*I
2239	EPA1@1017 Fw	GGGGTGACAAAAACAACTTCACATACAAC	*Sma*I
2240	EPA1@1740 Rv	ATTGAATTCGCGTTGTGCTGTTGAATTTTAGG AC	*EcoRI*
Primers to construct Sil2125 integrative plasmids			
2451	Sil2125@+150 Fw	CGTCTGCAGGTAATACCTAAAGGATTAGATG	*PstI*
2452	Sil2125@+1118 Rv	GCTGGTACCCAATGGTAGAAAACTTATTCAC	*KpnI*
2457	Int_Chr_A_-18kb Fw	GACCTGCAGGTCCAGCCGTCCTCATATTG	*PstI*
2458	Int_Chr_A_-18kb Rv	TTAGGTACCCGCTACAGAGATCAATAAC	*KpnI*
Primers used for the ChIP assays			
246	EPA1@+524	CGCTCATACAGGCACAGAAG	
245	EPA1@+848	GTGGAGTAGTTAGTTCTTGTGTCCAG	
1741	EPA2@-2442 Rv	CAAAAGTAAGGGTTAAACCATGATGAAC	
1742	EPA2@-2227 Fw	CCTTGTCCATGGTAACGTATATTG	
2222	EPA2@-1471 Rv	CTCAGGGCTAGCTAACAG	
2223	EPA3@-1360 Fw	GTTGCAGCAAGAACCATGTTG	

2224	EPA3@-1637 Rv	CTCTTGAGAGGAAAGCTGTC
2225	EPA3@-1617 Fw	GACAGCTTTCCTCTCAAGAG
2226	EPA3@-1887 Rv	GTTGAGGGTTCTTTCAGC
2229	ISC1@+1003 Fw	CATAAACGAAGTCCTAGCC
2230	EPA3@-5802 Fw	GAAACTTCTGAACAGACTACG
2231	EPA3@-6034 Rv	GACCCCACAGTACCCAGACC
2503	ISC1@1137 Fw	GTAGCTGGGTGGTCATCG
2504	ISC1@+71 Rv	GACTAGCTTGCTGCGGACTC
Primers and probes used for the 3C assay		
Probe_H*	AGACCCAAATATACACAGCATTAGCCCA	
Anchor_H	TCAACCGATCTCCGATAATTT	
H1	CAGGCTTTACACTTTATGCTTC	
H2	ACTACCGCTGTCTCTATCTC	
H3	GATAACTCGCGAACACACTTA	
H4	CGATATCGCTGATACAAACAAT	
H5	CAGCACCAATTATAGGCTACAT	
H6	TCAGATTATTGCACCCGATATG	
H7	AGCATGGTATCTTCAAGGTATTC	
H8	TGGTATGGAAAGCCATGAAA	
H9	GTTGTTTGAGCCTTGAAGTAAC	

11.5. Table S4. Data analysis for interaction between Sil2126 in its original position and Chr E$_{-R}$

	CGM1				*****			
	Parental strain (Sil2126)				***rap1-21***		***sir3*Δ**	
Primer	**Standard curve parameters**							
	a (slope)	**b (intercept)**	**CT Mean**	**Quantity Mean**	**CT Mean**	**Quantity Mean**	**CT Mean**	**Quantity Mean**
H2	-3.34	40.125	33.16	125.31	32.02	268.05	33.20	104.28
H3	-3.45	38.319	31.24	92.93	31.24	189.79	31.25	82.23
H4	-3.45	38.287	30.24	190.23	29.93	238.35	30.24	222.98
H5	-3.35	37.177	29.98	140.58	29.73	276.52	29.73	135.72
H6	-3.34	37.05	29.19	187.24	29.19	273.93	29.19	238.22
H7	-3.41	37.211	28.87	256.35	28.10	438.23	29.25	202.89
H8	-3.37	37.686	28.28	583.91	28.35	782.79	28.35	356.59
H9	-3.39	36.771	27.57	525.14	26.93	800.97	27.54	390.26

* The standard curve parameters used in the *rap1-21* and *sir3*Δ strains were the same than the CGM1.

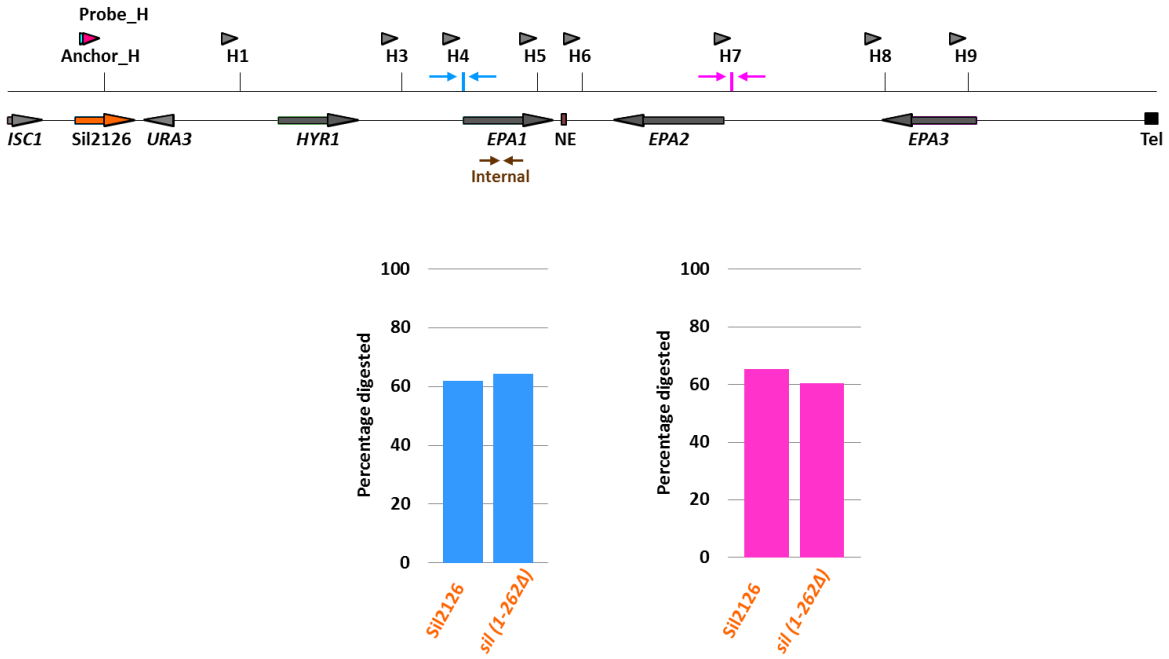

11.6. Figure S1. Evaluation of the chromatin digestion in the 3C assay.

(**Top**) Schematic representation of the Chr E_R drawn at scale. The primers, the anchor primer and the probe used in the 3C assay are indicated. The primers to test the digestion with the restriction enzyme (HindIII) are indicated in blue (cut site close to H4) and pink (cut site close to H7). The internal primers align in the ORF of EPA1, they are indicated in brown. (**Bottom**) The percentage of chromatin digestion is indicated for two strains used in the 3C assay (CGM817 and CGM3559). The genotype for each strain is indicated in each graph. The percentage was calculated by qPCR (Sybr Green) with the following equation: % restriction = 100 – 100 / 2^((Ct_{Across} – $Ct_{Internal}$)D – (Ct_{Across} – $Ct_{Internal}$)UND). (D: digested; UND: Undigested).

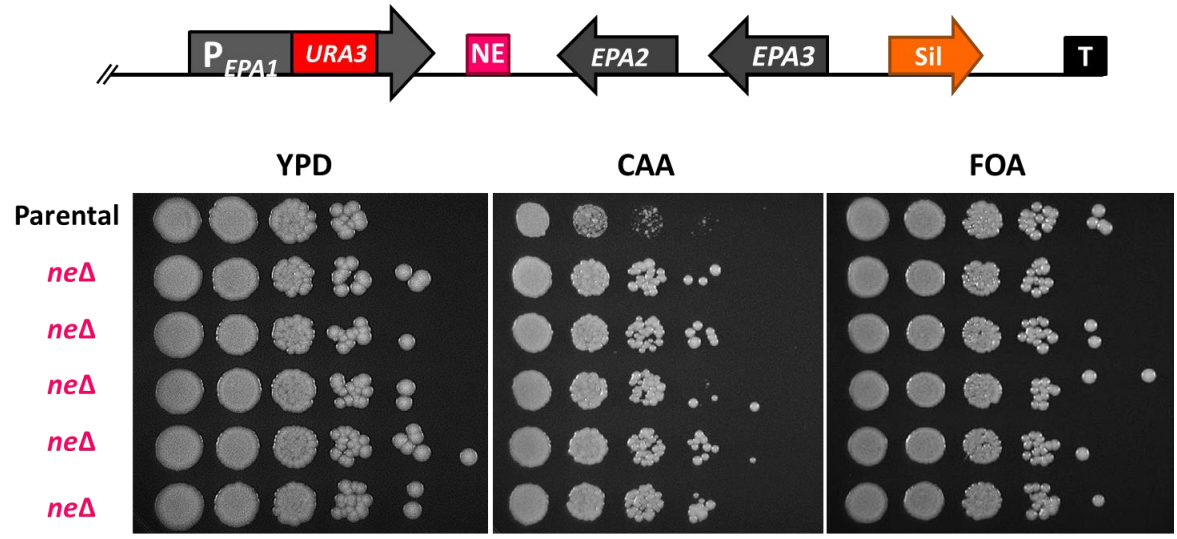

11.7. Figure S2. Independent colonies from the reconstruction of the *ne*Δ strain display the same level of expression of *EPA1*.

(**Top**) Map of the Chr E$_{-R}$ representing the *URA3* reporter under control of the *EPA1* promoter in its chromosomal location. (**Bottom**) Plate growth assay of five different mutants from independent colonies.

REFERENCES (Supplemental Material)

Calvin N. M., Hanawalt P. C., 1988 High-efficiency transformation of bacterial cells by electroporation. J. Bacteriol. 170: 2796–801.

Castanedo-Ibarra L., Castaño I., 2015 Análisis de la interacción entre las proteínas Abf1 y Rap1 de Candida glabrata con los elementos de regulación en cis del telómero E derecho.

Cormack B. P., Ghori N., Falkow S., 1999 An adhesin of the yeast pathogen Candida glabrata mediating adherence to human epithelial cells. Science 285: 578–82.

De Las Peñas A., Pan S., Castaño I., Alder J., Cregg R., Cormack B. P., 2003 Virulence-related surface glycoproteins in the yeast pathogen Candida glabrata are encoded in subtelomeric clusters and subject to RAP1- and SIR-dependent transcriptional silencing. Genes Dev. 17: 2245–2258.

Domergue R., Castaño I., Las Peñas A. De, Zupancic M., Lockatell V., Hebel J. R., Johnson D., Cormack B. P., 2005 Nicotinic acid limitation regulates silencing of Candida adhesins during UTI. Science 308: 866–70.

Fidel P. L., Cutright J. L., Tait L., Sobel J. D., 1996 A murine model of Candida glabrata vaginitis. J. Infect. Dis. 173: 425–31.

Frieman M. B., McCaffery J. M., Cormack B. P., 2002 Modular domain structure in the Candida glabrata adhesin Epa1p, a beta1,6 glucan-cross-linked cell wall protein. Mol. Microbiol. 46: 479–492.

Gallegos-García V., Pan S.-J., Juárez-Cepeda J., Ramírez-Zavaleta C. Y., Martin-del-Campo M. B., Martínez-Jiménez V., Castaño I., Cormack B., Las Peñas A. De, 2012 A novel downstream regulatory element cooperates with the silencing machinery to repress EPA1 expression in Candida glabrata. Genetics 190: 1285–97.

Gietz R. D., Sugino A., 1988 New yeast-Escherichia coli shuttle vectors constructed with in vitro mutagenized yeast genes lacking six-base pair restriction sites. Gene 74: 527–34.

Hernandez-Hernandez G., Castano I., 2017 Abf1 es una proteína esencial y participa en el silenciamiento subtelomérico en Candida glabrata.

Juárez-Cepeda J., Orta-Zavalza E., Cañas-Villamar I., Arreola-Gómez J., Pérez-Cornejo G. P., Hernández-Carballo C. Y., Gutiérrez-Escobedo G., Castaño I., Las Peñas A. De, 2015 The EPA2 adhesin encoding gene is responsive to oxidative stress in the opportunistic fungal pathogen Candida glabrata. Curr. Genet. 61: 529–544.

Juárez-Reyes A., Ramírez-Zavaleta C. Y., Medina-Sánchez L., Las Peñas A. De, Castaño I., 2012 A protosilencer of subtelomeric gene expression in Candida glabrata with unique properties. Genetics 190: 101–11.

Juárez-Vega G., Castaño I., 2010 " Diseño de herramientas moleculares para la caracterización de las proteínas Sir3 y Sir4 en.

Mathelier A., Fornes O., Arenillas D. J., Chen C. Y., Denay G., Lee J., Shi W., Shyr C., Tan G., Worsley-Hunt R., Zhang A. W., Parcy F., Lenhard B., Sandelin A., Wasserman W. W., 2016 JASPAR 2016: A major expansion and update of the open-access database of transcription factor binding profiles. Nucleic Acids Res. 44: D110–D115.

Rosas-Hernández L. L., Juárez-Reyes A., Arroyo-Helguera O. E., Las Peñas A. De, Pan S.-J., Cormack B. P., Castaño I., 2008 yKu70/yKu80 and Rif1 regulate silencing differentially at telomeres in Candida glabrata. Eukaryot. Cell 7: 2168–78.

Yáñez-Carrillo P., Orta-Zavalza E., Gutiérrez-Escobedo G., Patrón-Soberano A., Las Peñas A. De, Castaño I., 2015 Expression vectors for C-terminal fusions with fluorescent proteins and epitope tags in Candida glabrata. Fungal Genet. Biol. 80: 43–52.